April 2020

Analyzing Climate Risk to Maritime Cypress Swamps and Pine Savannas of the Gulf of Mexico Coastal Plain

Clay Stephens Tucker
Louisiana State University and Agricultural and Mechanical College

ANALYZING CLIMATE RISK TO MARITIME CYPRESS SWAMPS AND PINE SAVANNAS OF THE GULF OF MEXICO COASTAL PLAIN

A Dissertation

Submitted to the Graduate Faculty of the
Louisiana State University and
Agricultural and Mechanical College
in partial fulfillment of the
requirements for the degree of
Doctor of Philosophy

in

The Department of Geography and Anthropology

by
Clay Stephens Tucker
B.S., Geography, Louisiana State University, 2013
M.S., Louisiana State University, 2015
May 2020

For Louisiana.

Acknowledgements

No science is done in a silo. The contents of this Dissertation are the result of help, advice, and guidance of no fewer than four dozen people. From field work to editing, the following people made this work better. The reader should recognize that these acknowledgements do not merely show gratitude to those mentioned, but rather they show a list of people who have actively participated in this project in some way.

Certainly the first person to be mentioned here is the person who has spent more than seven years teaching me geography, showing me how science is done, and keeping me on my toes. No other person has participated more in this Dissertation than Jill Trepanier, and she embodies the ideal academic. She consistently teaches 400 undergraduate students per semester, undertakes countless service duties, researches and communicates high-level science, and she has somehow had time to see the completion of eight graduate degrees in five years. She has also taught me that life is not only work. Life is family; life is fun; life is good. Thank you, Jill.

The initial idea of the research in this Dissertation was inspired by a conversation with Kristine DeLong many years ago. She made me realize that trees could tell us about past hurricanes, that the research could be done on the Gulf Coast, and that the resources to complete the research were at LSU. There are not many subjects more interesting to me than past changes in Earth's climate and landscape, and Kristine fostered that passion. Her knowledge and teaching of paleoecology are largely evidenced in the background knowledge of this Dissertation.

Full-time dendrochronologists do not exist at LSU, so I was required to find one elsewhere. Luckily, the nearby University of Southern Mississippi faculty had Grant Harley on staff at the time. He had completed research on subtropical pine trees, and he understood Southeast U.S. climate-tree growth relationships as much as anybody else, but even more so, he had a distinct aptitude for tree-ring science. I have not met another scientist who wants to do his science more than Grant does, and though he has moved further away, every conversation with him makes me want to be a better scientist.

The three people above could have made the perfect committee for a dendrotempestologist, but a gap presented itself. Much of the research of this Dissertation was founded on principles in coastal plant ecology. Andy Nyman has forgotten more about Louisiana coastal plant ecology than most people will ever know, so he was an excellent representative to fill the gap. Little did I know that Andy would provide much more than a section in the Introduction. For starters, he drove an airboat through a cypress swamp for my field work; that is no small feat. More importantly though, he understands that research and education are the result of their failures as much as their successes, that interpretation of results should be based on facts and data, and that management goals should have a basis in science. Andy is the kind of scientist we should all want to be. Oh, and he can deep-fry a mean turkey.

Before acknowledging other participates of the work in this Dissertation, I must acknowledge the staff and administration of the LSU Department of Geography and Anthropology. Fahui Wang and David Chicoine, Department Chair and Graduate Director respectively, work tirelessly to streamline the student experience. Their efficiency makes my job all that less stressful, and that efficiency translates to the office staff. A combined experience of more than eight decades exists among Linda Strain, Nedda Taylor, Erika DeLeon, and Lauren Evans. Every time I approach them with a question, I get an answer. Every time I need a signature, they get one. Every time I want a snack, they have a king cake. Somehow, they fix every problem, every time.

Every scientist should find another with whom they can share ideas, provide and receive assistance, and laugh about the failures. I first met Thomas Patterson at the North American Dendroecological Fieldweek (NADEF) in 2015, and since then we have vowed to conquer the world of Southeast U.S. tree-ring research. Tommy never ceases to have the latest idea or research question, and he can talk about geographical theory for hours. I look forward to participating in a long career alongside him.

Field work is a necessary component to the research in this Dissertation. Bill Platt introduced me to my first study site, and he has also been a beacon of knowledge in pine savanna ecology. Ashley Booth, Gilman Ouellette, Kory Konsoer, Tommy Patterson, Jill Trepanier, and Alyssa Crowell all provided valuable skills in the field work for this Dissertation. Additionally, the Doyle's Bayou data were collected as part of a larger citizen science project. Nessie Galliano's eighth-grade students from Our Lady of Mercy School in Baton Rouge, LA collected the Doyle's Bayou data in conjunction with the LSU Coastal Roots program. The leaders of Coastal Roots, Pam Blanchard and Ed Bush, have brought more than 25,000 students in nearly 20 years to plant 180,000+ trees in an effort to restore Louisiana's coast. The entire state is indebted to them. I was lucky enough to participate in the same program with Mrs. Galliano when I was in middle school, and my passion for natural sciences was fostered by her and the Coastal Roots program at that young age.

Another necessary component to research is funding. On my journey through graduate school, I first received a stipend in the form of an undergraduate assistantship from the LSU Coastal Sustainability Studio followed by a teaching assistantship from the LSU Department of Geography and Anthropology and LSU College of Humanities and Social Sciences. The majority of this Dissertation was funded thrrough research assistantships from the South Central-Climate Adaptation Science Center, the National Academy of Sciences Gulf Research Program, and Louisiana Sea Grant. I also received valuable funds for field work, laboratory work, and conference travel from the Southwest Division of the American Association of Geographers, the LSU Graduate School, the Coastal Studies Institute at LSU, Kam-biu Liu, and a National Science Foundation NADEF Fellowship.

The background knowledge for this Dissertation stands upon the teachings of giants. Few scientists study changes in growth of coastal wetland trees. Those few include Matthew

Therrell, Jessie Pearl, David Stahle, Lauren Stachowiak, Paul Knapp, Thomas Doyle, Ken Krausse, and Richard Keim. Conversations with these scientists are embedded in the research questions, introductory knowledge, and methodology in this Dissertation. Additionally, though we spent little time together, I have thought frequently about Niranjan Baisakh's (my Dean's Representative) comments on my research. Simply knowing that other plant ecologists care deeply about abiotic stressors encourages tree-ring scientists like myself to continue exploring past environments.

Jim Speer and the entire NADEF team work tirelessly to teach tree-ring science to new generations. Each of my three visits to a NADEF changed my research for the better. My own group leaders taught me stand dynamics (Shawn Fraver), intense climate reconstructions (Bryan Black and Justin DeRose), and tree-ring isotopes (Adam Csank). Additionally, with the careful editing of computer programs, NADEF leaders Chris Gentry and Stockton Maxwell have provided hundreds of scientists with the ability to properly assess trends in tree growth.

I would also like to acknowledge those who work tirelessly to communicate science. The LSU Communications Across the Curriculum and TEDxLSU teams and their leaders (Annemarie Galeucia, Morgan Kastner, Rebecca Burdette, Becky Carmichael, and Melissa Thompson) create the ultimate stage for science communication. I would also like to acknowledge my fellow editorial board members of the Early Career Climate Forum for editing my own personal science communication online (Adrienne Wooten, Toni Klemm, Lindsay Middleton, and Cait Rottler). Lastly, the team from Louisiana Sea Grant, especially Dani Dilullo, bring science to the public on a full-time basis. Their work has become synonymous with the trust of the people.

The final section of these acknowledgements serves to thank those who provided intangible, though arguably the most important support for this Dissertation. Without a well-lived life, a Dissertation holds no importance, and the first of these thanks must go to Taylor Rowley.

She was the first to hear my complaints, the first to address and expunge my bad ideas, and the first to support my good ones. As a fellow doctoral student at LSU, she understood my own struggles more than anyone, and together we made it through the highs and the lows. Other graduate students in the Geography and Anthropology Department provided much needed fun times and invaluable support. I would also like to thank the few coastal plant ecology graduate students at LSU for listening to and answering my unending questions: Ashley Booth, Aimee Beaudette, Scott Graham, and Gina Groseclose.

Those outside my academic life created room in my mind for a life of science. My best friend since high school, Stephen Peltier, edited my graduate school application letter, and I still follow many of the guidelines he helped me set for myself those many years ago. Stephen, thank you for being a friend. My coworkers at the LSU University Recreation Center kept me fit physically and mentally, while my oldest friends reminded me of loyalty. Finally, to the "Baws" who set up tailgates, organized summer beach trips, screamed at the television during football games, and provided general revelry at almost any time, Geaux Tigers!

If a Dissertation ends and begins with an Introduction and a Conclusion, life begins and ends at parenthood. Through failure and success, my parents have never faltered to stand by my side. Susan and Rusty taught me the value of family, the importance of hard work, and the caliber of a person's word. They provided me with a home, they fed me weekly, and they even helped sand a tree core or two. They raised me in a place I will never stop loving, and they did it all without wanting anything in return. No one person has earned more of my respect than the two of them.

Table of Contents

List of Tables

List of Figures

Abbreviations

The following short abbreviations are used throughout this Dissertation.

COOP — NOAA Cooperative Observer Program

CPFP — Coastal Plain Floristic Province

CRMS — Coastwide Reference Monitoring System

CRU TS — Climate Research Unit Time Series

ENSO — El Niño-Southern Oscillation

GOM — Gulf of Mexico

GPS — Global Positioning System

HURDAT — NOAA Hurricane Database

IADF — Inter-Annual Density Fluctuations

ITRDB — International Tree-Ring Data Bank

LSU — Louisiana State University

MRGO — Mississippi River Gulf Outlet

NACP — North American Coastal Plain

NADEF — North American Dendroecological Fieldweek

NERR — National Estuarine Research Reserve

NOAA — National Oceanic and Atmospheric Administration

PCP — Precipitation

PDSI — Palmer Drought Severity Index

ppt — Parts per thousand

PRISM — Parameter-Elevation Regressions on Independent Slopes Model

SEA — Superposed Epoch Analysis

SOI — Southern Oscillation Index

SPEI — Standardized Precipitation-Evapotranspiration Index

SS — Storm Surge

SURGEDAT — LSU Storm Surge Database

TC — Tropical Cyclone

TC_{10} — Top-ten Tropical Cyclone

TMAX — Average maximum monthly temperature

TMIN — Average minimum monthly temperature

VPDB — Vienna Pee Dee Belemnite

WS — Wind Speed

Abstract

As sea levels rise, coastal trees are increasingly stressed by saltwater inundation, and stressed trees are ideal for studying changes in the environment through time. Dendrochronology has been used for more than a century to explain changes in past environments using tree rings. Using ring widths and stable isotopes from coastal trees, the effects of tropical cyclones and freshwater moisture availability are shown in regard to tree growth and ultimately are discussed in terms of change to the environment as a whole. Changes in tree growth as they relate to various climate parameters are measured using superposed epoch analysis, moving-window correlations, and spatial correlations.

Results show that tropical cyclones cause rapid declines in tree growth. In the first two years following large storm surges (>2.0 m), trees reduce growth in the stem as much as 15%, whereas inland urban trees only show major growth declines in years following tropical cyclones with hurricane-force wind speeds (>33 ms^{-1}). For coastal trees that do not show strong tropical cyclone signals, drought conditions play a key role in growth declines. For example, tree-ring carbon isotopes show strongest spatial correlations ($r>0.5$, $p<0.05$) with precipitation and maximum average monthly temperatures in the early growing season (January–July). Evidence for anthropogenic causes can also be seen in tree rings. Trees near New Orleans, Louisiana declined in growth following the opening of a canal that brought increased saltwater into the region in 1965, and some trees never recovered. Patterns of tree growth, precipitation, and tropical cyclones also match closely with shifts in the El Niño-Southern Oscillation.

Coastal trees inundated by saltwater experience declines in growth following pulses such as drought, tropical cyclones, and anthropogenic disturbances. Future land management of coastal forests should consider changes in freshwater soil moisture availability when project-

ing changes in the environment. In summary, with accelerating sea-level rise and increasing tropical cyclone intensity, coastal areas can expect to see declines in tree growth.

Introduction

Since the last glacial maximum, global sea level has risen approximately 125 m Clark and Mix [2002]; Spratt and Lisiecki [2016]; Donoghue [2011]; Bocanegra-Ramírez et al. [2019]. Landscapes have been reclaimed by the sea, and coastal habitats have migrated inland as a result. As the Laurentide ice sheet over North America retreated, many plant communities moved pole-ward Delcourt et al. [1984]. New coastal land formed in the past 7,500 years when sea-level rise slowed and rivers dropped sediment atop the northern Gulf of Mexico (GOM) continental shelf Coleman et al. [1998]. As a biodiversity hotspot, the ecosystem of the North American Coastal Plain (NACP; Figure 1.1) stands to lose hundreds of plant and animal species in the face of any future sea-level rise Noss et al. [2015]. Some studies have assessed future changes of GOM landscapes in South Florida Doyle et al. [2003]; Berger et al. [2008], but changes in the northern GOM are lacking and a previous study recommends more research in the area Doyle et al. [2010].

Researchers have uncovered relationships of the growth of GOM coastal trees to global climate patterns Stahle et al. [1998], destruction from hurricane occurrences Tucker et al. [2017], and relationship to saltwater intrusion Pezeshki et al. [1990]. Storm surges associated with tropical cyclones (TCs) in the GOM can cause coastal waters to rise as much as 10 m in height and travel inland Turner et al. [2006]; Needham and Keim [2012]. Many coastal trees have been susceptible to lack of freshwater availability from resulting saltwater intrusion from the storm surge Pezeshki et al. [1990]; Conner and Askew [1992]; Conner [1994]. Trees reduced growth in years following a TC event and the stress was recorded in the rings Tucker et al. [2017]. Tree-ring records can (1) tell us when a TC likely occurred, and (2) how that TC affected tree growth. Understanding coastal processes and their interaction with trees is key in discovering the full suite of knowledge in the growth rings of coastal trees. The purpose of this Dissertation is to define how TCs, moisture stress, and saltwater intrusion

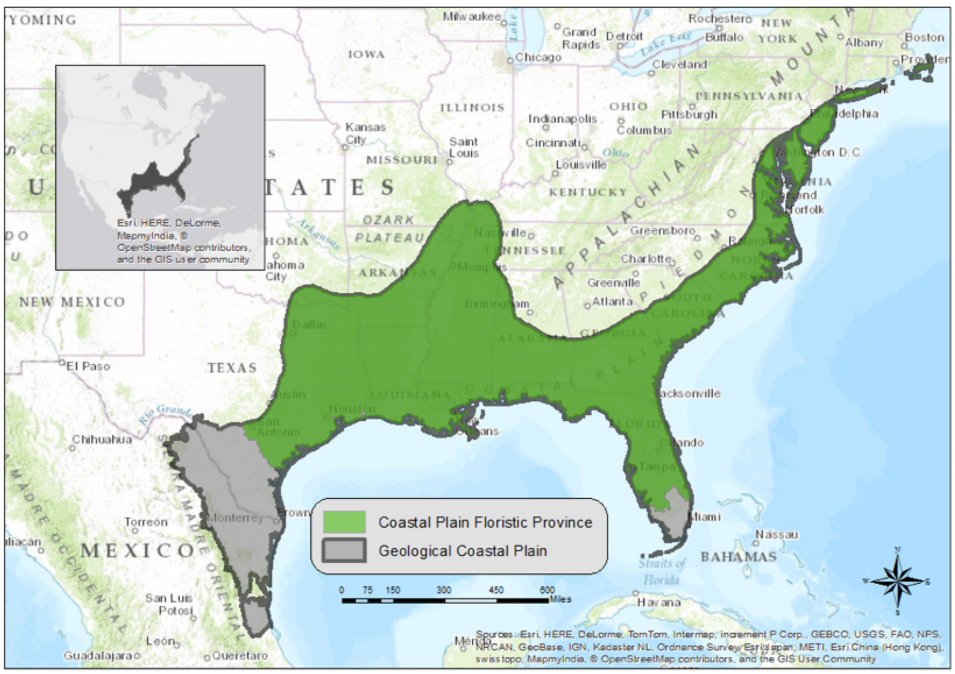

FIGURE 1.1: The North American Coastal Plain (NACP). The area represented in this figure marks the extent of the region of concern in this Dissertation. The pine savannas and cypress swamps contained within its reaches contain high biodiversity, maintain a myriad of flora and fauna habitat, and support international fisheries, agriculture, and tourism dollars. It is based on a figure from Noss et al. [2015].

affect coastal tree growth and to quantify the occurrence of TCs and sea-level rise using tree-ring data.

1.1 Tree Rings

Dendrochronology, or the science of tree rings, dates back more than a century in the U.S. when A. E. Douglass attempted to correlate tree growth with sunspot activity in arid Arizona Douglass [1909]. For trees to record their environment, they must be stressed in some way, otherwise growth reaches its maximum potential each year, and no environmentally-driven pattern can be discerned from the tree's rings Speer [2010]; Fritts [2012]. With better technology and persistent scientists, tree-ring researchers have reached all corners of the globe: tree rings of vineyard grape bushes in northern California Maxwell et al. [2016], tropical locations in the Andes Mountains of South America where trees usually do not produce annually-separated rings Villalba et al. [1998], and even ancient underwater forests in the GOM Reese et al. [2018].

Florence Hawley was the first American dendrochronologist to bring tree-ring methods east of the Mississippi River to showcase that tree-ring science could work in many different areas Hawley [1937]; Barnes [2010]. Various tree species have been useful in dendrochronological studies in the eastern U.S. since the 1940s when Hawley began research: the growth rings of *Pinus* species have been applied to fire history Lafon and Kutac [2003], climate relationships Harley et al. [2011], archaelogical dating Harley et al. [2017], and disease-spreading insects Patterson and Knapp [2018] among others, and those studies range from the mesic mountains of Virginia to the rocky shores of the Florida Keys. *Taxodium* species are longer-lived than *Pinus* species, but their climate proxy capability has been difficult to analyze for tree-ring scientists Stahle et al. [2012]. *T. distichum* is now the oldest dated species in the eastern U.S. and among the oldest organisms in the world, and they frequently occur in coastal areas Brown [1996]; Stahle et al. [2019].

However, tree-ring studies of the coastal zone are few, because climate is often ideal for growing conditions and does not provide the stress necessary for producing patterns in tree rings. Other tree-ring studies in the coastal zone, including many baldcypress studies, occurred in freshwater wetlands far from saltwater inundation Stahle et al. [1998]; Miller et al. [2006]. A small group of studies have addressed the relationship between saltwater inundation and long-term tree growth Atwater and Yamaguchi [1991]; Yanosky et al. [1995]; Rodgers III et al. [2006]; Doyle et al. [2007]; Trouet et al. [2016]; Tucker et al. [2017]; Pearl et al. [2020].

The first study to analyze TC occurrences using tree-ring analysis was conducted on the barrier islands of Mississippi Stoneburner [1978]. That study showed tree growth and regeneration of barrier island pine forests was driven by the disturbance of TCs, similarly to the growth and reproduction around their inland neighbors to the north. Another study showed similar results: tree growth on the Alabama coast increased following TCs Rodgers III et al. [2006]. However, those studies analyzed only those trees that survived hurricanes and were able to take competitive advantage over the trees destroyed during the TC. Additionally, those studies found spurious lags of growth following TCs, which may have resulted from the stand-wide tree growth average in their analyses.

Methods vary for other early studies in dendrotempestology (*i.e.*, the effects of hurricanes on trees Grissino-Mayer et al. [2010]). For example, Johnson and Young [1992] analyzed tree-ring widths using non-standard dendrochronological techniques. In Puerto Rico, mangrove trees provided researchers with annual growth rings, but due to their high tolerance to TC damage, the tree-ring widths did not correlate to TC occurrences Drew [1998]. Another study focused on heavy metals in baldcypress tree rings, and simply noted that tree growth was lower following hurricanes in 1947 and 1965 Latimer et al. [1996].

Saltwater inundation often leads to reduced tree growth overall, reduced tree regeneration, and eventual loss of coastal forests Pezeshki et al. [1990]; Yanosky et al. [1995]; Conner [1998]; Doyle et al. [2007]. More recent dendrotempestology researchers show that, at the individual level, tree growth was suppressed following TCs for up to six years after saltwater inundation Doyle and Gorham [1996]; Trouet et al. [2016]; Tucker et al. [2017]. Sites for those studies were all in areas where mature trees survived wind damage, and storm surge for each TC inundated the site with saltwater. Thus, saltwater inundation from a storm surge was hypothesized as the reason for growth declines following TCs in those studies.

Though tree growth is affected by changes in water salinity, different types of trees vary in their response to TC characteristics. *Pinus* species are often more resistant to high winds but not resistant to increased flooding from storm surge and rainfall Platt et al. [2000], while hardwood trees respond oppositely to those characteristics Gresham et al. [1991]. *Taxodium* species often respond well to multiple effects of hurricanes, consistent with its high-density, high-flexibility wood structure Doyle et al. [1995]. In this Dissertation, I aim to parse out the complex TC factors affecting coastal tree growth in the northern GOM.

Isotopic analysis of the cellulose in tree rings has also added value to dendrotempestology. Two studies note that a depletion in tree-ring oxygen-18 isotope matched TC precipitation records in inland Georgia and coastal sites in South Carolina and Florida Miller et al. [2006]; Nelson [2008]. Two other chronologies have also successfully shown evidence of TCs in tree-ring oxygen isotopic ratios (personal conversation, Grant Harley and Jessie Pearl). However, the isotopic values of water within a TC have been shown to differ spatially in multiple TCs Good et al. [2014]; Sánchez-Murillo et al. [2019]. Chapter 3 of this Dissertation discusses the results of previous studies in tree-ring carbon isotopic analysis, the processes of carbon isotope fractionation, and how tree-ring carbon isotopic data used in this Dissertation compare to previous research.

1.2 Sea-Level Rise

Long-term research is important for explaining the impacts, consequences, and projections of accelerating sea-level rise. Eustatic (*i.e.*, global) sea-level rise through the past century has approached 1.7 mm per year Church and White [2006]. In coastal Louisiana, that rise is accelerated by natural deltaic plain evolution and anthropogenic modifications, and it often exceeds 11 mm per year in that same time interval Penland and Ramsey [1990]; Blum and Roberts [2009]. A rapid pace of sea-level rise provides an analog laboratory to study how future sea-level rise may affect other coastlines around the globe.

Sea-level changes before the Pleistocene Epoch were due mostly to tectonic activity. However, roughly 3 million years ago, large ice sheets began to form atop continental land in the northern hemisphere that grew and collapsed concurrent with changes in Earth's movement known as Milankovitch Cycles Milankovitch [1920]; Berger [1980, 1988]. Three separate cycles form the basics of Milankovitch cycles: Earth's orbital eccentricity (100,000 year cycle), tilt (41,000 years), and precession (23,000 years). Continental ice sheets expand and contract as a result of high-latitude temperature changes during Milankovitch cycles, and global sea-level rise and temperatures respond to that ice loss/gain Rohling et al. [2009]. In the current interglacial, sea levels have risen about 125 m from approximately 20,000 years ago until 6,000 years ago when sea-level rise slowed Clark and Mix [2002]; Spratt and Lisiecki [2016]; Donoghue [2011]; Bocanegra-Ramírez et al. [2019].

However, in the past 150 years, sea-level rise rates have increased, not due to tectonic or solar forcing, but to the greenhouse gas effect Church and White [2006]. Carbon dioxide and methane, produced by burning fossil fuels, are molecules that efficiently trap longwave radiation and ultimately allow the atmosphere to trap more heat. This effect is seen in the last 50 years of CO_2 data in Hawaii Keeling and Keeling [2017]. A climate reconstruction of Earth's temperatures shows the drastic increase in global temperatures through that period as well (Figure 1.2) Mann et al. [1999].

Modern sea-level rise is concerning because of both the uncertainty of what might come from such rapid warming and the unprecedented nature of its acceleration in the past century. Though plants are responsible for offsetting some elevation loss from sea-level rise, other non-halophytic plants suffer in the face of saltwater intrusion, including most tree species.

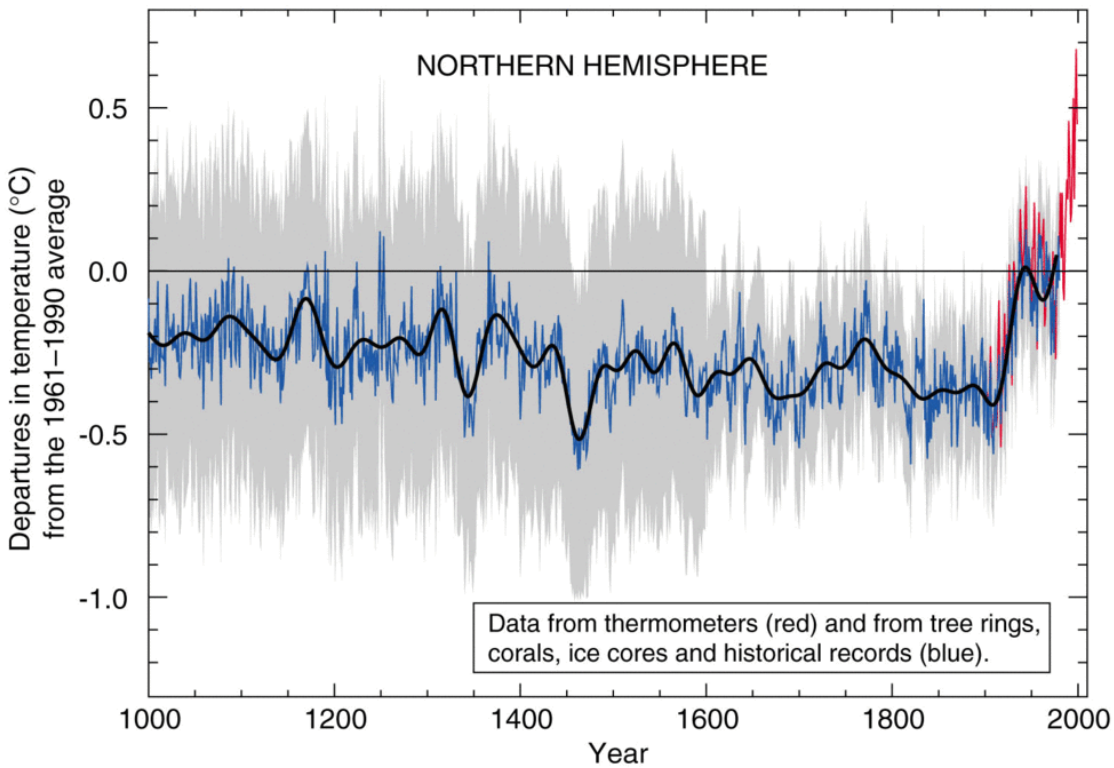

FIGURE 1.2: Temperature reconstruction for the last 1,000 years, also known as the "hockey stick figure" because of the rapid acceleration of temperatures at the end of the millennium Mann et al. [1999].

Mangrove trees thrive in saltwater environments by using mechanisms to exclude, exude, and concentrate salts Liang et al. [2008]. Some other non-halophytic tree species can uptake saltwater (*e.g.*, *Taxodium distichum*), and their offspring can germinate in small amounts, but most trees have dramatic reductions in sapflow and water use under increased saltwater conditions Pezeshki [1990]; Conner and Askew [1992]; Yanosky et al. [1995]; Krauss and Duberstein [2010].

As a result of sea-level rise, coastal plant communities will be forced to move inland because of land erosion and, more importantly, because of a lack of adaptations to flooding and saltwater intrusion. Those organisms best adapted to saltwater (*e.g.*, *Spartina alterniflora*) will continue to thrive along the coast and their populations may not be reduced dramatically Nyman et al. [1993]. However, the range of non-halophytic organisms (*e.g.*, *Taxodium distichum*, *Pinus elliottii*, *Quercus* spp.) will be squeezed as the coastline migrates inland in the face of sea-level rise Doody [2004]; Pontee [2013]; Torio and Chmura [2013]. Sea-level rise is an important component to changes of future coastal forests, and few studies address the long-term impacts of saltwater intrusion on trees using their growth rings.

1.3 Climate

Climate plays a key role in the environmental factors controlling tree growth. For coastal forested wetlands, the amounts of salt in available soil water can be driven by both TCs and drought conditions.

1.3.1 Tropical Cyclones

Tropical cyclones are large storm systems with violent wind and heavy rainfall circulating around a center of low pressure, and they occur in tropical and subtropical locations on Earth. In the 21st century alone, and only including the top 10 costliest hurricanes within the GOM, TCs have caused more than $400 billion in damage in the U.S. Hebert et al. [1996]; Grinsted et al. [2019]. They are known by different names in each of five ocean basins: hurricanes (Atlantic and Eastern Pacific), typhoons (Western Pacific), and cyclones

(Indian and South Pacific). TCs are frequently defined by their wind speeds, as is true for the categories associated with the Saffir-Simpson Hurricane Wind Scale used for Atlantic hurricanes Simpson and Saffir [1974].

Previous studies suggest that the most intense TCs will become more intense with warming temperatures Elsner et al. [2000, 2008]; Trepanier et al. [2017]. Storm surges from TCs in the future will be higher, and as a result, saltwater will stay on coastal landscapes for longer periods of time. Additionally, low-lying, deltaic coastlines will be much more susceptible to increasing TCs than other areas Woodruff et al. [2013]. Both human and ecological landscapes will be affected by future TCs, but our record of those past events is limited. Proxy evidence of TCs will be necessary to explain the ecological ramifications of more intense TCs and to increase our confidence of future TC projections.

Data for Atlantic hurricanes are kept in the HURDAT2 (HURricane DATa) system of the National Oceanic and Atmospheric Administration Landsea et al. [2015]. For each hurricane, HURDAT2 contains location, maximum sustained wind speed, landfall location, and minimum central pressure for 1851–present. Rainfall for Atlantic hurricanes can be gathered from any one of dozens of COOP weather stations. Storm surge data are available in Louisiana State University's SURGEDAT (SURGE DATa) system for most landfalling Atlantic hurricanes for 1900–present Needham et al. [2013].

1.3.2 El Niño-Southern Oscillation

Global weather patterns have been correlated to changes in the Walker Circulation and the El Niño-Southern Oscillation (ENSO) of the Pacific Ocean Julian and Chervin [1978]; Andrade Jr and Sellers [1988]; Bove et al. [1998]; Wang et al. [2014]. The Walker Circulation describes the general pattern of Pacific Ocean surface winds traveling from east to west across the basin. As the Walker Circulation reverses (*i.e.*, the 'warm' phase of ENSO, or "El Niño") in the central Pacific Ocean, El Niño conditions in the Pacific shift major atmospheric circulations around the globe, including that of the subtropical jet stream in North America

(Figure 1.3). As the North American subtropical jet stream shifts southward during El Niño, winter storms increased and drought conditions improved in the following year for the Southeast U.S. Noel and Changnon [1998]; Mo and Schemm [2008]. If the general Walker Circulation pattern strengthens, the 'cold' phase of ENSO begins, known as a "La Niña." Results from previous researchers show that strong La Niña events have been linked with declines in tree growth in the Southeast U.S. Stahle et al. [1998]; Brienen et al. [2012]. Additionally, some teleconnections of ENSO may not be as strong as others. For example, Mo and Schemm (2008) also noted that El Niño conditions are not as strongly associated with wet years in the southeastern U.S. as La Niña conditions are associated with dry years.

Each chapter of this Dissertation uses indices and measurements of climate data to correlate tree growth to water availability. The most common of those measurements are available through Divisional Climate Data available from the National Oceanic and Atmospheric Association (NOAA). An example of those data and where to find them is available in Appendix B. For all data used in this Dissertation, only significant correlations ($p<0.05$) with those climate data are discussed.

1.4 The Gulf Coast

The GOM has changed in size dramatically since the last glacial maximum. Rapid continental ice sheet melting beginning 20,000 years ago caused global sea levels to rise as fast as 40 mm per year Donoghue [2011]. After rapid melting stopped 6,000 years ago, sea level was relatively stagnant. During sea-level stagnation, rivers brought sediment to coasts around the world where they formed river deltas Stanley and Warne [1994]; Milliken et al. [2008]. River systems play an important role in coastal development because they are natural builders of land, and their deltas often sink in the face of sea-level rise Swift [1973]; Kindinger et al. [1994]. Evidence of those changes exists for major river deltas around the world, including northeastern South America Vital and Stattegger [2000], the Indian subcontinent Allison [1998], and northern Africa Milliman et al. [1989] among many others.

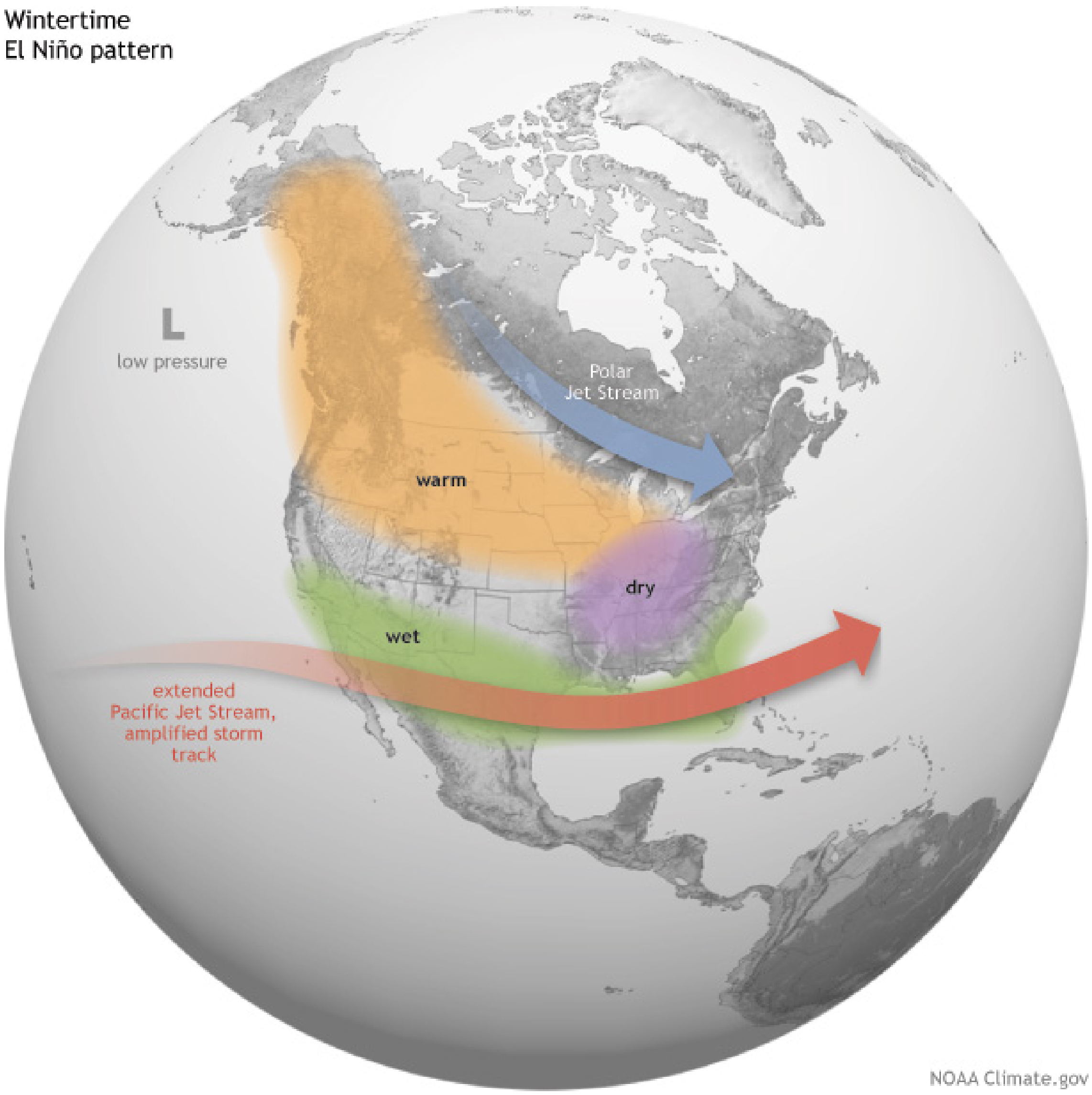

FIGURE 1.3: El Niño teleconnections in the U.S. The effects on North American atmospheric circulation and corresponding climate effects from a wintertime El Niño in the Pacific Ocean. This image is available through the website `climate.gov` available from NOAA.

Deltaic plain formation relies on two important factors: (1) steady sediment supply and (2) stagnant or slow sea-level changes Roberts [1997]; Coleman et al. [1998]. Those previous studies on deltaic developments concentrated on geologic formation, wherein the delta would switch among various lobes as each delta prograded into the sea. Eventually, the river would switch to a new delta. Old deltas, starved of sediment, would sink into the sea under their own weight. In the 1980s, scientists began to discover that some marshes kept up with slow sea-level rise because plants grew as fast as the sea was rising McCaffrey and Thomson [1980]; Nyman et al. [1993]. Both ecology and geology were necessary for explaining coastal landscape change Nyman [2014].

Forty percent of the world's population lives within 60 miles of a coast, and large cities are often located near the mouth of major rivers similar to those described above Small and Nicholls [2003]. The Mississippi River has now experienced centuries of human modification to reduce flood impacts while enhancing the river's capacity for navigation and irrigation Twilley et al. [2016]. In a time of accelerating sea-level rise, resource extraction, and marsh degradation, deltaic coasts around the world are sinking into the sea faster than any other landscape Day Jr and Templet [1989]; Syvitski et al. [2009]. Research providing analogs of past sea-level rise effects will increase confidence of projections for future coastal habitats, and deltaic plains offer a unique natural laboratory where coastal processes are hastened.

Future plans to combat sea-level rise are important to long-term plans like Louisiana's Coastal Master Plan, which intends to invest as much as $50 billion over the next 50 years through various projects such as marsh creation, structural protection, and river diversions, among others Peyronnin et al. [2013]; Knox [2017]. Field and laboratory studies are essential for determining the right projects in the right places. Louisiana currently has a coast-wide reference monitoring system (CRMS) with nearly 400 CRMS sites that measure a multitude of environmental variables from vertical marsh accretion to changes in plant species Steyer et al. [2003]. CRMS sites were placed spatially in Louisiana to cover the landscape as much as possible. However, the CRMS data are no older than 15 years. Environmental proxies can help fill in the time gap, and in the form of tree rings, the NACP is not at a loss for data.

From Brownsville, Texas to Key West, Florida, the coastline of the northren GOM remains floristically and geologically similar Noss et al. [2015]. The vast majority of the Coastal Plain Floristic Province (CPFP; Figure 1.1) is comprised of various bottomland habitats that largely include pine savannas interwoven with hardwood/cypress swamps within north-south running rivers. Cypress trees are the oldest living organisms that live within the CPFP, some of which live for more than 2,500 years Stahle et al. [2019]. Though the oldest *Taxodium* exist in backswamps of major rivers, *Taxodium* in coastal areas can live for more than 500 years (personal observation). While *Taxodium* inhabit river valleys and cutoff swamps with frequent flooding and clay soils, *Pinus* take root in flatter, savanna-like landscapes with sandy, nutrient-poor soils. Those two genera (*i.e.*, *Taxodium* and *Pinus*) are the two most common canopy tree genera in the Southeast U.S. Sorrie and Weakley [2001].

Common plant communities of the northern GOM coast occurring frequently throughout the field work completed for this Dissertation include:

- Pine savanna-brackish marsh at Grand Bay National Estuarine Research Reserve (NERR), Mississippi (Figure 1.4).
- Pondcypress domes at Grand Bay NERR, Mississippi (Figure 1.5).
- Pine forest-beach hummocks at Gulf State Park, Alabama (Figure 1.6).
- Baldcypress swamp at LaBranche Wetlands, Louisiana. (Figure 1.7).
- Degraded baldcypress swamp at LaBranche Wetlands, Louisiana (Figure 1.8).

FIGURE 1.4: Slash pine savanna abutting *Juncus* salt marshes in Grand Bay NERR, Pascagoula, MS. Trees decrease in height as they approach the marsh. Data used in Tucker et al. [2017] and in Chapter 3.

FIGURE 1.5: Pondcypress 'dome' within pine savannas of Grand Bay NERR, Pascagoula, MS. Pondcypress trees often inhabit stagnant-water areas within vast pine savanna ecosystems and provide an important refuge for animals that cannot outrun wildfires. Data used in Chapter 2.

FIGURE 1.6: Slash pine forest near the beach at Lake Shelby, Alabama. Note the proximity of these trees to the human landscape in the form of a multi-level condominium complex – the ultimate connection of data and purpose. Data used in Chapter 4.

FIGURE 1.7: Cypress swamp in the LaBranche Wetlands west of New Orleans. Notice the abundance of freshwater plants: red maple, blue iris, and water hyacinth. Data used in Chapter 4.

FIGURE 1.8: Cypress swamp approximately two miles from Figure 1.7. Note the addition of an important saltmarsh plant, *Spartina patens* indicating higher saltwater inundation at this site. Data used in Chapter 4.

1.5 Objectives, Merit, and Impacts

Tucker et al. [2017] confirmed the first step in assessing environmental impacts to the coastal GOM: coastal trees do record TC activity. That result created a suite of new questions including

- Do all tree species tell the same story?
- Can we use advanced methods to provide more information than ring-widths alone?
- What signal remains in different geographic locations?

1.5.1 Intellectual Merit

The research in this Dissertation aims to increase knowledge related to the long-term changes in the environment of GOM coastal forested wetlands using tree growth parameters. As described in detail above, little dendrochronological research has analyzed changes in coastal regions, and coastal regions will change most in the face of sea-level rise. The GOM coastline has some of the highest rates of sea-level rise in the world, making it the "canary in the coalmine" for global coastal change. Ghost forests around the world indicate that saltwater intrusion from sea-level rise is changing the face of coastal ecosystems. Prior to widespread mortality, coastal forests hold knowledge of slow saltwater intrusion in their growth rings.

Finding trees affected by saltwater inundation is key for studying the effects of sea-level rise on tree growth. Coastal forested wetland research requires that the scientist find locations where tidal seawater enters coastal forests. The study sites within this Dissertation are denoted with specific GPS points, descriptions of the landscape, and lists of halophytic plant species in the understory. In addition to careful field methods, less common laboratory methods proved to enhance the signal of coastal processes. For example, trees in this Dissertation were frequently cored more than twice to eliminate problems from rot, and visual crossdating was frequently verified using non-quantitative measures (*e.g.*, ring color).

Advanced tree-ring analysis methods aid coastal research by adding value to traditional techniques. The development of suppression chronologies and superposed epoch analysis reveal TC occurrences better than traditional dendrochronological detrending and correlation methods. Isotopic ratios tend to agree with tree-ring width data, but their correlations with climate data are stronger and more widespread. Finally, new computer programs for dendrochronological analysis (*e.g.*, *dplr*, *TreeClim*) allow the researcher to explore their data more quickly and efficiently. These methods and results are described in detail in the individual research chapters of this Dissertation.

1.5.2 Broader Impacts

Global changes in sea level and temperatures will cause coastal flora and fauna to adapt, move, or perish. Human population in those locations will also suffer at the loss of land and habitat concurrent with sea-level rise. Predicting the future of coastal landscapes will require long-term data from the past as an analog for future predictions. Tree-ring research can provide centuries of data of coastal change evidenced in growth rings of trees.

Engineered coasts will require management intervention as sea levels rise. Understanding the effects of surface water changes and soil moisture stress on coastal plants will provide managers with best practices for managing coastal systems. For example, increasing freshwater resources in coastal forested wetlands provides plants respite from saltwater inundation and the ability to migrate upslope during flood events.

Wetlands provide numerous benefits to society, and losing wetlands means losing those benefits. Wetlands store carbon at high rates, they filter and assimilate nutrients in surface waters, they are home to species from nearly all animal phyla, they store flood waters, and they provide free recreation and beauty to humans. Studying coastal wetland history through the lens of tree-rings provides a basis for land management, predictions for future change, and increases their inherent benefits through increased knowledge.

All three studies within this Dissertation explore the effect of saltwater, moisture stress, and TCs on tree growth, with a future goal of finding trees old enough to add temporal data to the North American TC record. Chapter 2 explains how *Taxodium ascendens* growth compares to that of their neighboring *Pinus elliottii*. Chapter 3 uses methods in tree-ring isotopes to further explore how trees are affected by moisture stress in coastal locations. Finally, Chapter 4 expands the research on how moisture stress and past TCs are recorded in various tree species in different coastal plant communities.

Assessing the Use of Maritime Trees for Dendrochronological Analysis

2.1 Introduction

Tree-ring research explores the fundamentals of how trees respond to various environmental factors (*e.g.*, precipitation, temperature, disease, insects, wildfire), and crossdating is possible where trees experience a common stressor Speer [2010]. However, few dendrochronological studies have explored how non-halophytic trees (*i.e.*, trees not adapted to saltwater) are affected by saltwater inundation Ross et al. [1994]; Harley et al. [2015]; Tucker et al. [2017]. Saltwater inundation can affect tree growth by supplanting freshwater in the soil Pezeshki et al. [1990]; Krauss and Duberstein [2010]. Most tree species must then exclude the salt from the water before uptake in the roots Allen et al. [1994]. This process results in less water being consumed by the tree to be later used during photosynthesis, thus creating a stressed tree due to lack of freshwater. The tree cannot grow at normal rates, and the change in growth is recorded in its annual growth rings. Therefore, crossdating should be possible on trees in areas where trees are stressed by saltwater inundation.

Coastal areas experience saltwater inundation from high tides, storm surges, and saltwater intrusion in groundwater as well as aerosolized salt from breaking waves. Most trees occupying those areas are those adapted to saltwater environments (*e.g.*, mangroves). However, many areas around the world are experiencing sea-level rise rates in which inland habitats are inundated by saltwater more than they were previously Church and White [2006]; Hay et al. [2015]. The northern Gulf of Mexico (GOM) coast is experiencing higher-than-average rates of sea-level rise, and in some cases 10 times faster than the global rate (10.4 mm yr^{-1} versus 1.2 mm yr^{-1}) Penland and Ramsey [1990]; Hay et al. [2015]. As a result, coastal pine savannas and cypress swamps are rapidly changing to coastal marshes and tidal flats, especially in river deltas Blum and Roberts [2009]. Trees in coastal areas show similar growth signals and thus are sensitive to various climate parameters, such as precipitation, temperature, and tropical cyclone (TC) occurrences Harley et al. [2011]; Tucker et al. [2017].

2.1.1 Tree-Ring Research and Site Conditions

The Principle of Site Selection in dendrochronology states it is important for selecting trees that are sensitive to specific climate variables, such as high altitude trees that are temperature sensitive and trees in arid regions that are moisture sensitive Speer [2010]. Trees in areas with long growing seasons and high precipitation often produce complacent growth that does not correlate well with climate variables. The Southeast U.S. has long summers, mild winters, and precipitation in excess of 150 cm. Trees produce wide rings each year in this region because they have ample resources available to them. However, some localized regions, especially in the Southeast U.S. do have conditions that allow for climate-sensitive trees.

Common locations for dendrochronology in the Southeast U.S. include high-elevation Appalachian mountain outcrops Saladyga and Maxwell [2015]; Copenheaver et al. [2017], xeric pine savannas Ford and Brooks [2003]; Knapp et al. [2016]; Patterson and Knapp [2016]; Rother et al. [2018], and fluvial baldcypress swamps Stahle et al. [1985]; Doyle and Gorham [1996]; Stahle et al. [2012]. Appalachian outcrops at high elevations have shorter growing seasons associated with colder annual temperatures. Pine savannas have well-drained soils, and trees in well-drained soils are susceptible to drought conditions because the soil does not store water. Fluvial swamps are directly connected to nearby trees on natural river levees, and streamflow levels drive water availability to riverine trees.

Previous studies have assessed the growth of various pine (*i.e., Pinus*) and cypress (*i.e., Taxodium*) tree species near the GOM and Atlantic Ocean coastlines Rodgers III et al. [2006]; Harley et al. [2011]; Day et al. [2012]. *T. ascendens* and *T. distichum* growing on the northern GOM coast in areas not associated with high riverine input are often located in cypress domes Kurz and Wagner [1953]; Ewel and Mitsch [1978]. Cypress domes are areas of monocultured stands of *Taxodium* spp. in poorly drained sites that hold water for long periods of time and exclude fire. Fire exclusion and ample water allows trees in the center to grow higher, ultimately producing a domed appearance Ewel [1995]. Poorly drained sites cause trees to produce less biomass and produce smaller stem growth than trees in better drained sites Mitsch and Ewel [1979]. Trees growing in those stressful environments produce micro-rings, numerous locally absent rings, and inconsistent ring growth within one tree, all of which makes visual crossdating difficult. However, some *T. ascendens* sites occur without a dome and without standing water. My previous research at the site used in this study showed that TCs are associated with *Pinus elliottii* growth, whereas this study explores similar techniques on a new species Tucker et al. [2017].

2.1.2 Tree Rings and Tropical Cyclones

The northern GOM coastline is home to both a mix of estuarine environments that can support tree growth and to numerous TCs, often making landfall annually Keim et al. [2007]; Trepanier et al. [2015], which makes this region ideal for studying the effects of past TCs on trees. The GOM region is also home to some of the only dendrotempestological studies Rodgers III et al. [2006]; Grissino-Mayer et al. [2010]; Trouet et al. [2016]; Tucker et al. [2017]; Mitchell et al. [2019].

Some studies have shown correlations with tree-ring isotope chemistry and TCs Miller et al. [2006]; Mora et al. [2006], but studies of actual TC rainfall oxygen isotopic ratios show that the rain from different parts of the storm can have different isotopic values Good et al. [2014]; Sánchez-Murillo et al. [2019]. Other studies analyze TCs in tree rings using ring-width chronologies, yet discrete events such as TCs may be clouded by other variables in an averaged growth of many trees [*e.g.*, Rodgers III et al., 2006]. My recent research using trees directly on the coast, analyzed with individual suppression chronologies shows that tree growth decreases following TC events, and the most intense TCs correspond with the largest declines in tree growth Tucker et al. [2017].

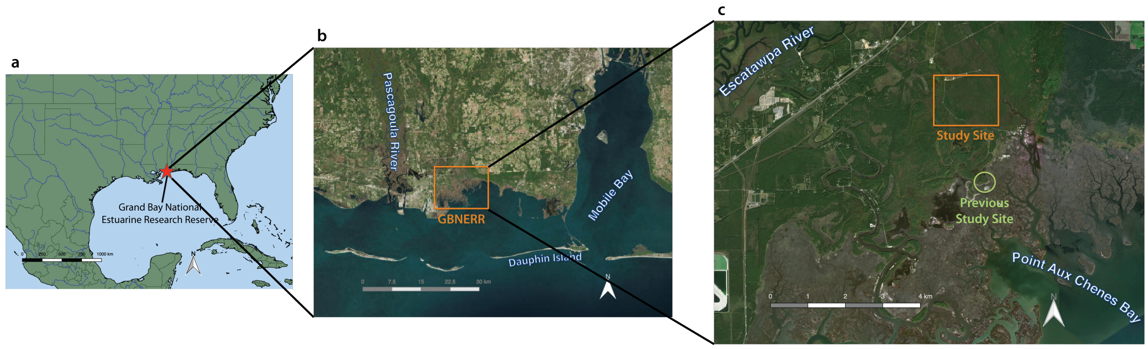

FIGURE 2.1: Study area. Red star indicates location of Grand Bay National Estuarine Research Reserve (Grand Bay NERR) along the GOM coast. (b) A zoomed-in view shows Grand Bay NERR proximity to both riverine input and GOM influence. (c) The study site area and a previous study site at Grand Bay NERR are included to show proximity of the site to tidal inlets and coastal marshes.

2.1.3 Study Area

Grand Bay National Estuarine Research Reserve (Grand Bay NERR; 30.42°N, 88.42°W) is located adjacent to a major GOM river (Pascagoula River via the Escatawpa River) and is also adjacent to GOM waters via Point Aux Chenes Bay (Figure 2.1). Subtropical climate with hot, wet summers, and cool, dry winters characterize this region. According to the Southern Regional Climate Center (1940–2016), precipitation here exceeds 150 cm and average temperatures in July are 27°C and 10°C in January.

Grand Bay NERR is proximal to both riverine input and tidal influence (Figure 2.1b). Grand Bay NERR is buffered from TC high winds and storm surge by nearby barrier islands, where the inland bays provide a mix of saltwater that enters Grand Bay NERR through tidal inlets (Figure 2.1c). The occurrence of *T. ascendens* in Grand Bay NERR is associated with depressional wetlands, and multiple plant communities comprise the savanna ecosystem at Grand Bay NERR (Figure 2.2). Nearest to the coast, only brackish and salt marshes exist. Further inland the landscape contains pine savannas, cypress swamps, oak groves, and open ponds. Common tree species within Grand Bay NERR include *P. elliottii*, *P. palustris*,

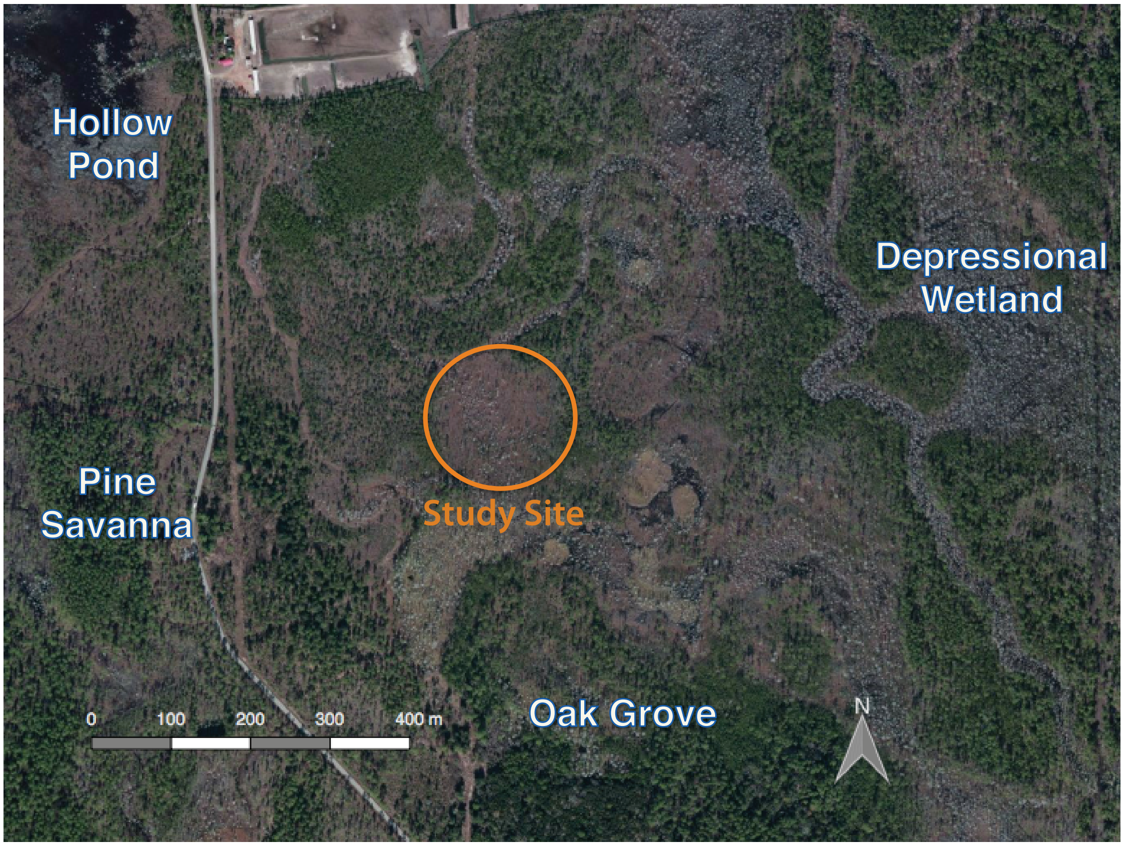

FIGURE 2.2: General map of the area within the orange square of Figure 2.1c. Trees for this study can be found in the orange circle denoted as "Study Site", which is a depressional wetland of *Taxodium ascendens* trees.

Quercus virginiana, and *T. ascendens*, with common co-habiting coastal marsh vegetation that includes *Juncus roemarianus*, *Spartina patens*, and *Cladium jamaicense*.

Water collects in low-lying areas to form open ponds and depressional wetlands. *T. ascendens* trees dominate the lowest areas, *Pinus* spp. occupy flat, well drained areas, while *Quercus* spp. grow on ridges (Figure 2.2). Those ecosystem features are consistent with the seepage slope swamps of the northern GOM coast from Big Branch Marsh in Louisiana (30.28°N, 89.94°W) to the Suwannee River in Florida (29.30°N, 83.14°W), and those wetlands support a wide range of niches for some of the highest biodiversity in North America Keddy [2009]; Noss et al. [2015].

In the following sections, I describe the viability of maritime *T. ascendens* for dendrochronology. The tree-ring data in this study are analyzed against summer temperatures,

TABLE 2.1: *Taxodium ascendens* trees sampled for this study with their number assigned during sampling, diameter at breast height (DBH) in inches, and the first reliable year of growth for visual crossdating.

No.	DBH	First Year
7	35.3	1930
9	28.2	1969
13	37.3	1934
22	24.9	1935
26	36.6	1991
28	30.2	1930
29	28.4	1949
31	29.7	1921
33	32.0	1934
34	29.7	1944
35	24.9	1970

growing-season precipitation, and TC occurrences. I conclude with suggestions for future maritime dendrochronological studies especially as they relate to site selection.

2.2 Materials and Methods

Tree-ring data for this Chapter were collected similarly to the data in Tucker et al [2017].

2.2.1 Tree Ring Data

On 10–12 March 2018, a total of 37 *T. ascendens* greater than 10 cm in diameter at breast height were selected for sampling. *T. ascendens* grow in mono-stands within flooded areas (*i.e.*, depressional wetlands) surrounded by higher, drier areas with *P. elliottii*. This study site is located 3 km from an open saltwater bay. All trees used in this study had at least some standing freshwater present at the base during fieldwork, and some trees had as much as 10 cm of water present on the ground. All trees sampled were alive at sampling, and green needles were just becoming visible on stems of all trees at the time of fieldwork.

Trees were given a sample number in the field corresponding to the order of sampling, and GPS coordinates and diameter at breast height (DBH) measurements were recorded for each tree (Table 2.1). Two 5.15 mm-diameter samples were taken from each tree using a Haglöf increment borer using traditional sampling techniques Stokes and Smiley [1968], and each core sample was transported back to the lab using paper straws and a large map storage tube. Tree cores were secured to pre-routed wooden mounts made specifically for tree cores using water-based glue and binder clips, and the glue was allowed to dry for 48 hours before cores were sanded using a succession of finer grit sizes to reveal clear tree-ring boundaries (ANSI 120, 220, 320, 400 grit) Speer [2010]. Tree cores were visually crossdated using the list method Yamaguchi [1991], and total ring widths were scanned at 2400 dpi and measured to the nearest 0.01 mm using the CooRecorder and CDendro softwares Larsson [2014].

To ensure visual crossdating was robust, the computer program COFECHA was used to find any discrepancies in crossdating Holmes et al. [1986]. The number of series needed to produce acceptable signal-to-noise ratio was calculated using the expressed population signal (EPS) method, which is commonly used to assess statistical quality of the mean chronology versus a theoretical noise-free chronology Wigley et al. [1984]. Following crossdating verification, two tree-ring index chronologies were created for further analysis: indexed tree-ring width chronology and a suppression chronology (described below). The computer program ARSTAN was used to create the ring-width index with a 67% spline for the length of each individual series to remove the growth-related trend Cook and Peters [1981]. Three existing tree-ring chronologies were accessed from the International Tree-Ring Data Bank (ITRDB). Those three additional chronologies were selected based on their similarity to the dataset in this study. They are all *Taxodium* chronologies from swamps in the Southeast U.S.

2.2.2 Climate Data

To assess any outstanding climatological factors possibly contained in the tree growth chronologies, three climate variables were used to assess temporal and spatial correlation of the tree-ring data from this study: (1) El Nino Southern Oscillation (ENSO) represented as the Southern Oscillation Index (SOI) NOAA [2018], (2) monthly averaged precipitation, and (3) monthly average temperatures. SOI is the difference in sea-level pressure between Tahiti and Darwin, Australia, and they reflect ENSO variability in Pacific Ocean temperatures known to have global teleconnections. SOI data are available on the National Centers for Environmental Information website via their teleconnections page NOAA [2018]. Precipitation values were accessed for 0.5° grid size from the Climate Research Unit (CRU) Time Series (TS) version 4.01 provided by the UK National Center for Atmospheric Science and University of East Anglia Harris et al. [2014]. Temperature values were accessed for 4 km grid size from the PRISM (Parameter-elevation Regressions on Independent Slopes Model) Climate Group at Oregon State University Daly et al. [1997].

Spatially gridded data sets were preferred for this study because they span the time interval of the chronology used in this study, and the data sets are already fixed for quality control and used in previous studies Salzer et al. [2009]; Preechamart et al. [2018]. Additionally, gridded data products are useful in exploratory studies, because they allow the user to test numerous climate parameters on a single chronology easily. The CRU TS v4.01 data span years 1901–2017 at 0.5° resolution. They are derived from monthly observations of weather stations in land areas across the world. CRU TS v4.01 measurements are used frequently to show large spatial patterns between tree-ring chronologies and regional climate Preechamart et al. [2018]; Huang et al. [2019]; George and Esper [2019]. The PRISM Climate data (4 km resolution; 1895–2017) are also a gridded product, and have been used in numerous tree-ring studies Salzer et al. [2009]; McCullough et al. [2017].

2.2.3 Tropical Cyclones

A tropical cyclone impacting Grand Bay NERR is defined for this study as one with a storm surge recorded no more than 45 km away from the study site, and with wind speeds exceeding 33 ms^{-1} within 120 km of the study site. Those values are consistent with previous studies of the size and the widespread effects of TCs Keim et al. [2007]; Needham et al. [2013]; Trepanier and Scheitlin [2014]. Tropical cyclone storm surge data were acquired from the storm surge database SURGEDAT available from the Southern Climate Impacts Planning Program at Louisiana State University Needham and Keim [2012]. Tropical cyclone

TABLE 2.2: Tropical cyclone storm surge data used in this study. Surges in meters are listed as the highest recording for that storm within 45-km radius of Grand Bay NERR.

Name	**Year**	**Surge Height**	**Rank**
Unnamed	1947	3.66	3
Unnamed	1948	1.81	11
Unnamed	1949	1.33	16
Brenda	1955	1.83	10
TS no. 1	1956	1.42	13
Hilda	1964	1.40	15
Betsy	1965	2.24	8
Camille	1969	4.70	2
Frederic	1979	3.20	4
Danny	1985	0.50	19
Beryl	1988	1.10	17
Chantal	1989	0.75	18
Georges	1998	2.90	5
Isidore	2002	2.08	8
Bill	2003	1.41	14
Ivan	2004	2.05	9
Katrina	2005	7.90	1
Gustav	2008	2.49	6
Lee	2011	1.50	12

wind speeds were acquired from the National Hurricane Center HURDAT2 "Best Track" database Jarvinen et al. [1984]; Landsea et al. [2004]; Landsea and Franklin [2013]. Storm surge measurements larger than 2.0 m (19 events) and wind speeds higher than 50 ms^{-1} (21 events) were included in the analyses for the period 1928–2014 (Tables 2.2 and 2.3). The TC data are truncated because the statistical analysis used to correlate tree growth and TC occurrence uses a moving window analysis that cannot account for the first three and last three years of tree-ring data. These methods are described in the next section.

A simple ranking system was also created to determine the top 10 most detrimental TCs impacting the study site (Table 2.4). The ranking system aimed to combine the risk of storm surge and high winds from TCs together to determine if tree growth responds to the entirety of a TC differently than just to specific parameters (*i.e.*, surge and wind). TCs from Tables 2.2 and 2.3 are ranked in order of magnitude, with one (1) being the most detrimental. This

TABLE 2.3: Tropical cyclone maximum wind speeds used in this study. Maximum wind speeds in ms^{-1} are listed as the highest recording for that storm within a 120-km radius of Grand Bay NERR.

Name	**Year**	**Wind Speed (ms^{-1})**	**Rank**
Unnamed	1947	48.87	11
Unnamed	1948	35.57	20
Baker	1950	38.58	17
Florence	1953	46.30	14
Flossy	1956	41.15	15
Ethel	1960	41.15	15
Betsy	1965	63.72	4
Camille	1969	72.02	1
Agnes	1972	38.58	17
Carmen	1974	66.87	2
Eloise	1975	58.77	6
Frederic	1979	59.16	5
Andrew	1992	65.48	3
Opal	1995	56.58	7
Danny	1997	36.01	19
Georges	1998	48.87	11
Barry	2001	33.64	22
Ivan	2004	56.58	7
Katrina	2005	56.58	7
Gustav	2008	48.87	11
Ida	2009	33.98	21

ranking was created by adding a ranking of the storm surges and wind speeds for each TC impacting Grand Bay NERR. The lowest rank is considered the most impactful storm for this study.

2.2.4 Statistical Analyses

Gridded data products are already tested for quality control and used by previous studies. SOI data were tested for normality using the Shapiro-Wilk test, because it represents n<50 well Wilk and Shapiro [1965]; Razali et al. [2011]. Pearson's product-moment correlation was used to test for relationships between the climate data and the tree-ring chronology because both data sets are n>30 and are normally distributed. As described previously, the tree-ring

TABLE 2.4: Ranking of the top 10 tropical cyclones (TC_{10}) affecting trees at Grand Bay NERR with their associated storm surge (SS) and wind speed (WS) ranks from Tables 2.2 and 2.3. This ranking is based on the combined ranking of the most detrimental tropical cyclones from Tables 2.2 and 2.3.

Name	**Year**	**SS Rank**	**WS Rank**	**Combined Rank**	**TC_{10} Rank**
Unnamed	1947	3	11	14	5
Flossy	1956	13	15	28	9
Betsy	1965	8	4	12	4
Camille	1969	2	1	3	1
Frederic	1979	4	5	9	3
Danny	1985	19	10	29	10
Georges	1998	5	11	16	6
Ivan	2004	9	7	16	6
Katrina	2005	1	7	8	2
Gustav	2008	6	11	17	8

data introduced in this study were standardized and averaged to compare to climate data sets.

Additionally, I created a suppression chronology for event-based analysis. Previous researchers have found that superposed epoch analysis (SEA) using suppression chronologies produced better results than simple correlations with a master indexed chronology of all tree-ring series Baisan and Swetnam [1990]; Swetnam [1993]; Tucker et al. [2017]. Suppression chronologies note the number or percentage of trees exhibiting a user-defined reduction in growth Trouet et al. [2016]; Tucker et al. [2017]. For this study, the computer program JOLTS, designed at the Lamont-Doherty Earth Observatory, was used to produce suppression chronologies. When creating a suppression chronology, the user defines what a suppression is in terms of a percentage reduction in width of subsequent tree-ring years. Then, the user defines the epoch through which the calculation should be run. Tucker et al. [2017] used a conservative value of 15% reduction in growth within a 7-year running mean. Previous researchers have also used the more liberal values of 25% reduction in growth within a 10-year running average Trouet et al. [2016]. This study compares the two different methods (conservative *vs.* liberal) to determine which method is most indicative of physical processes impacting the tree growth.

SEA reveals temporal relationships among time series by comparing statistical windows, or *epochs*, of one variable onto the other. Event years are selected within the range of the original time series. Event years for this study were defined for three different impacts from TCs: (1) storm surge above 2.0 m, (2) wind speeds above 50 ms^{-1}, or (3) a compilation of the top ten TCs (TC_{10}) in Grand Bay NERR determined from storm surge and wind speed. These values were selected to represent the top 50% ranked storms for 1928–2014. Randomly selected, user-defined epochs are compared to the list of event years through 1000 bootstrapped Monte Carlo simulations. The model also compares these simulations to a series of lag years before and after the event year. Lag years allow the user to see how the event might have changed tree growth through the epoch.

2.3 Results

Taxodium ascendens tree-ring widths for this study were difficult to crossdate, especially in years prior to 2000. However, in an effort to expand the usefulness of this species in the future, the following results show examples and goals of *T. ascendens* tree-ring research. Though the results here are from a low number of tree cores and from tree-ring data that do not crossdate well, they represent exploratory measures that can be performed on coastal trees in the future.

2.3.1 Comparing *Taxodium ascendens* to Other Tree-Ring Records

Tree-ring data for this study extend from 1921–2016 with a maximum of 21 tree-ring series contributing to master chronologies (Figure 2.3). Not all trees sampled for this study were used for final analysis. Twenty-eight percent of cores sampled in the field were able to be visually crossdated and verified. The remaining 72% were not included in the master chronology due to young age (less than 30 years), damaged cores, high presence of locally absent rings, complacency in growth, and/or poor correlation with the master chronology.

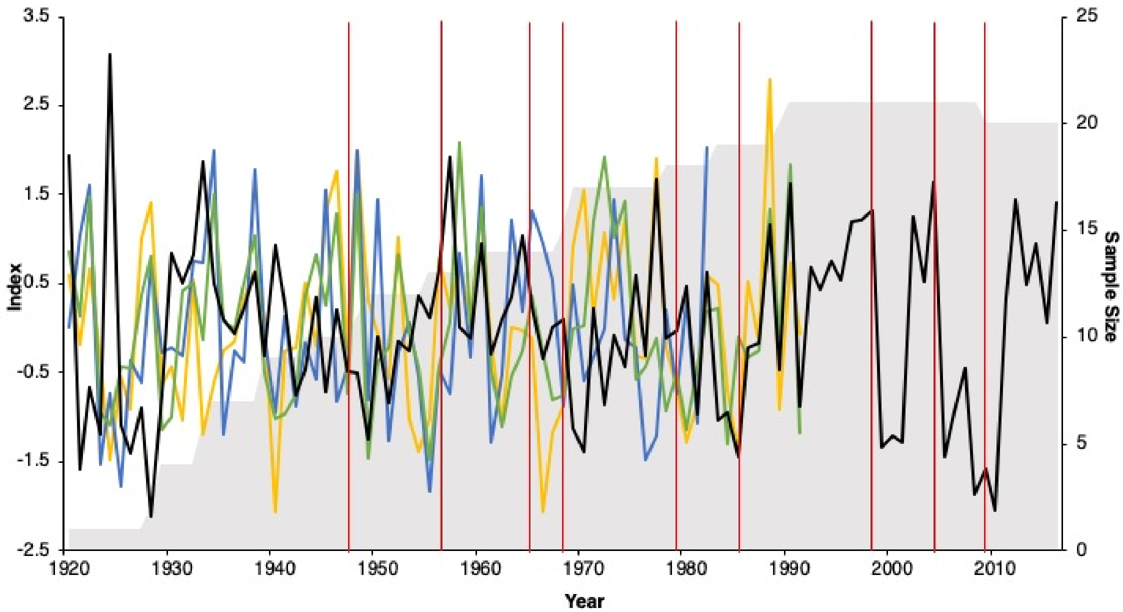

FIGURE 2.3: Comparison of time series of indexed tree-ring data in this study. Ring-width indices are included for Grand Bay NERR *Taxodium ascendens* (black line) and *T. distichum* from the Choctowatchee (yellow), Pearl (blue), and Pascagoula (green) Rivers. Vertical red bars indicate years of top-ten hurricane occurrence. The gray box indicates the sample size of *T. ascendens* tree-ring series used in this study.

Sample size increases as the year increases because not all trees are the same age and tree recruitment has not occurred in total in one year. Interseries correlations and average mean sensitivities for *T. ascendens* used in this study are r=0.45 and r=0.52 respectively. All individual series contribute positive correlations with the master chronology and the mean sensitivity is above r=0.50.

The individual series crossdate with co-existing species (*P. elliottii*) at Grand Bay NERR Tucker et al. [2017], but they do not correlate with nearby *T. distichum* chronologies from the Choctowatchee, Pearl, and Pascagoula, Rivers accessed via the ITRDB Stahle and Cleaveland [1992] (Figure 2.3). Agreement among all chronologies is the similarity in growth variability from 1980–1992, during which period, growth changes in the same direction each year for the four series, and the magnitude of indexed change is similar. Peaks in growth among series are matched at years 1938, 1960, and 1982. However, reductions in growth never match among all series, and only occasionally between two or three series (*e.g.*, 1985, Figure 2.3).

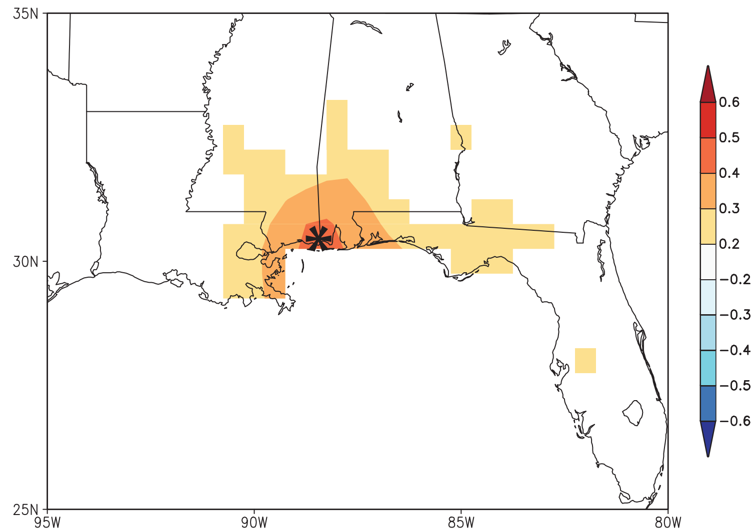

FIGURE 2.4: Spatial correlation of tree-ring width and average precipitation during the growing season. Precipitation data are averaged over the period April–July for each year. Tree-ring and climate data overlap through the period 1921–2016. The study site is denoted by the black asterisk.

2.3.2 *Taxodium ascendens* Tree Rings and Climate

Taxodium ascendens growth at Grand Bay NERR shows little correlation with ENSO. Only the month of April shows a significant, negative correlation with SOI ($r \geq$-0.23, $p<0.05$). However, *T. ascendens* tree growth at Grand Bay NERR correlates with growing season precipitation (Figure 2.4). Directly over the study site, averaged April–July rainfall positively correlates with tree growth for the period 1921–2016 ($r>0.4$, $p<0.05$). Other individual monthly averaged temperatures do not significantly correlate to tree growth at Grand Bay NERR. Therefore, as growing season precipitation increases, tree growth increases. This pattern decreases with distance away from Grand Bay NERR.

Some temperature correlations also exist with *T. ascendens* tree growth at Grand Bay NERR (Figure 2.5). Temperature correlations with *T. ascendens* growth at Grand Bay NERR are not similar throughout the year. For averaged monthly maximum temperatures, two months within the growing season show opposite correlations with tree growth: July (negative) and September (positive). When July maximum temperatures are high, *T. ascendens* tree growth at Grand Bay NERR is more likely to be lower (Figure 2.5a), and when

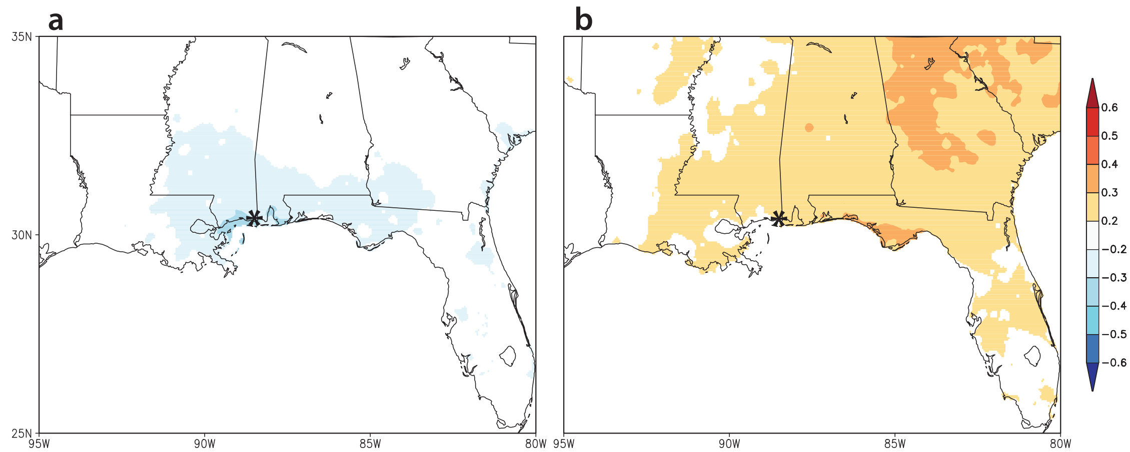

FIGURE 2.5: Spatial correlation of tree-ring width and maximum temperatures averaged for July (a) and September (b) using data from 1921–2016. The study site is denoted by the black asterisk.

September maximum temperatures are high, *T. ascendens* tree growth at Grand Bay NERR is more likely to be higher (Figure 2.5b). No other correlations between *T. ascendens* tree growth at Grand Bay NERR and average temperatures exist.

2.3.3 *Taxodium ascendens* Tree Rings and Tropical Cyclones

T. ascendens tree growth at Grand Bay NERR shows similar correlations with TC occurrences to a previous study of the co-existing *P. elliottii* at Grand Bay NERR Tucker et al. [2017]. Following years with TCs producing wind speeds greater than 50 ms^{-1} and storm surges greater than 2.0 m, *T. ascendens* tree growth is suppressed in subsequent years (Figure 2.6). As described in Section 2.2.4, two different thresholds were used in the superposed epoch analysis for this study: a conservative 15% reduction in growth within a 7-year window (Figure 2.6a) and a more liberal 25% reduction in growth within a 10-year window (Figure 2.6b). Both analyses show significant suppressions in tree growth in lag year 1 (the year following one of the top ten TCs). Additionally, both analyses show a suppression in growth in lag year 2, but only the more conservative analysis (a) is significant. Analyses were also conducted for TC wind speeds, but no results were significant similar to results found in Tucker et al. [2017].

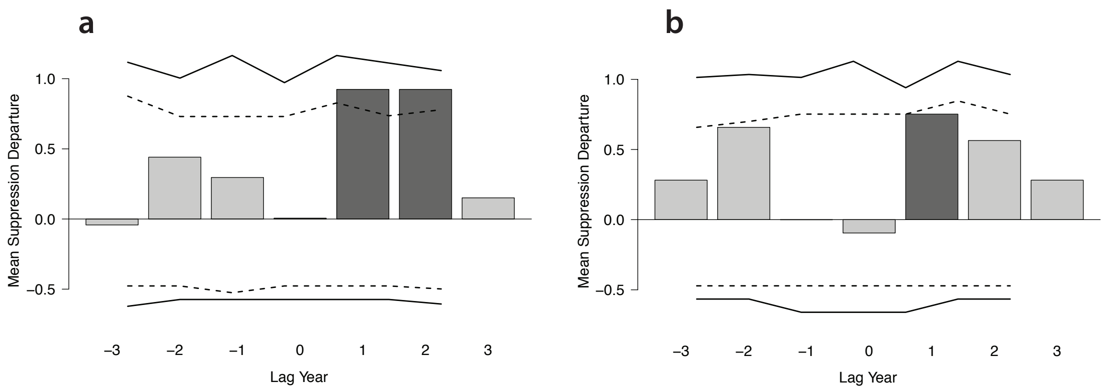

FIGURE 2.6: Results for superposed epoch analysis for growth suppressions of *Taxodium ascendens* following the top ten most intense TCs affecting the study site. Lag year 0 represents the exact year of TC occurrence. Vertical bars represent the likelihood of suppression for any given lag year, and the horizontal lines represent confidence intervals of 0.95 (dashed) and 0.99 (solid). Results for two user-defined settings are shown here: (a) 15% reduction in growth within a 7-year window and (b) 25% reduction in growth within a 10-year window.

2.4 Discussion

Taxodium ascendens at Grand Bay NERR show significant correlations to other nearby tree-ring chronologies, TCs, and summer temperature and precipitation.

2.4.1 *Taxodium ascendens* Dating Potential

For a tree species to be crossdated, the tree must produce clearly defined growth rings that are sensitive to some environmental forcing. After visually crossdating the tree cores for this study and validating that crossdating with COFECHA, 28% of the total cores taken in the field were used in final analysis. As mentioned in the introduction, *T. ascendens* often exists in poor growing conditions (*e.g.*, standing water, low nutrients). Tree cores for this study frequently displayed rot, and rings for numerous ring-width series could not be dated because of physical damage to the tree prior to core collection. Additionally, some trees at Grand Bay NERR are relatively young (less than 30 years old), and trees younger than 30 years did not crossdate with trees older than 50 years because their growth patterns did not match growth patterns in the older trees. However, the final master chronology for this study produced an acceptable interseries correlation (r=0.45).

This study site at Grand Bay NERR may allow for climate sensitivity in *T. ascendens* rings because of its relatively new change in geomorphology and geology. Neither the Pascagoula River, nor its more proximal tributary the Escatawpa River, currently flow directly through Grand Bay NERR, but prior to the diversion of the Escatawpa River in 1854, riverbeds did wind through the landscape and evidence of rivers are still present in aerial photographs today Kramer [1990]; Schmid [2000]; Hilbert [2006]. An introduction of riverine processes onto this landscape would allow for flowing water and a change in sediment supply, both of which may have made for better growing conditions. Though no trees used in this study extend prior to 1854, the landscape is likely still affected by the riverine processes once dominating its geology. For example, a previous researcher has shown that submarine groundwater discharge is important for controlling localized hydrology that can ultimately control the ecology of a site Kolker et al. [2013]. The trees at Grand Bay NERR may benefit from better drained soils and higher nutrient availability based on submarine groundwater discharge at the site. Grand Bay NERR is not unique in this way, however. Numerous rivers transect the northern GOM coastal landscape, and their deltas may produce similar areas for future dendrochronological research (*e.g.*, Pearl, Mobile-Tensas, Perdido, Escambia, Yellow, Choctowatchee, and Apalachicola Rivers).

2.4.2 Climate-Tree Growth Relationships

Climate-growth relationships are an established resource for dendrochronologists. However, no single climate variable can explain a total year of growth for a tree. Thus, when exploring the dendrochronological viability of a new species, tree growth must be compared to multiple variables to ensure that a tree growth chronology is suitable for analysis. For example, more than 100 years of researchers have shown that at least some tree growth is correlated to rainfall Douglass [1914]; Granato-Souza et al. [2018]. The physical mechanism to explain the relationship is solid: when trees have less moisture available, they produce less growth. Results from this study show a similar process: as precipitation increases, Grand Bay NERR tree growth also increases (Figure 2.4). Though the signal for this trend extends more than 200 km, the strongest signal is seen directly over the study site at Grand Bay NERR. Furthermore, the correlation between tree growth and precipitation is during its growing season (April–July), during which the tree would be actively using water. A lack of correlation to precipitation for other months of the year alludes to annual precipitation dependency as well.

Temperature also plays a role in tree growth. In non-tropical areas where annual temperatures fluctuate, temperature may be one of the factors (others might include daily photoperiod and/or water availability) causing trees to go dormant and stop growing until the following growing season. Higher fall and winter temperatures may allow for the growing season to extend, thus allowing a tree to produce a larger ring for that year. For this study, high maximum temperatures in September (likely near the end of the growing season) correlate with larger ring widths for that given year. Conversely, the average high summer temperatures may cause ring width to be smaller. During respiration when trees are producing biomass, trees must keep themselves cool through evapotranspiration. When temperatures are high, more energy is used for evapotranspiration than for new tissue creation. Additionally, high temperatures mean that any surface or soil moisture normally used by a tree will evaporate more quickly. For this study, high maximum temperatures in July correlate to narrow rings for that given year (Figure 2.5a).

2.4.3 Effects of Tropical Cyclones

Similarly to previous studies Doyle et al. [1995]; Conner [1998]; Harley et al. [2012]; Tucker et al. [2017], this study finds that major TC occurrences cause suppression of tree growth. In the first year after a TC, *T. ascendens* reduce growth in the stem by a least 25% (Figure 2.6b). Significant suppressions of at least 15% may also occur for the second year following an event (Figure 2.6a), and previous studies show that trees affected by TCs frequently do not recover to average growth for 2–7 years Doyle and Gorham [1996]; Tucker et al.

[2017]. Lack of correlation to TCs with high winds may lead to the conclusion that some coastal trees are more disturbed by storm surge than the entire TC event. *T. ascendens* have shown that freshwater availability is an important factor of growth. Storm surge disrupts the availability of freshwater by adding salts to the surface water, and the salts eventually leach into the ground. Though high winds may remove leaves and damage branches, trees may repair themselves before the growing season ends for that year, or at the latest, the following year.

2.4.4 Potential for Future Coastal Tree-Ring Research

This study is the first of its kind to use *T. ascendens* in tree-ring-based climate analysis. However, the methods used in this study are not unique to the study locale or the study species. Methods used for analysis are traditional for dendrochronology, but future studies may find the field methods of this study useful. Future coastal dendrochronology should consider the following suggestions:

(1) "Coastal", or "maritime" locations, as defined in this study, pertain to those landscapes located at the interface of land, sea, and air. Without the interaction of all three of those components, trees may not be stressed enough to be climate-sensitive along coastline ecotones. Talking to landowners or accessing tide gauge data is essential in finding locations regularly inundated by saltwater. Additionally, landscapes with higher sea-level rise rates relative to the global rate will contain trees rapidly inundated by saltwater. Those places are often located by or within river deltas, where sediment is compacting and subsiding quickly, thus increasing local sea-level rise rates Blum and Roberts [2009].

(2) A proper knowledge of halophytic flora help to identify the likely commonality of saltwater inundation. Though the majority of plants in a site may not be adapted to saltwater intrusion, the presence of one species may allude to a regular presence of saltwater in the soil. For example, the common understory grass at Grand Bay NERR is *Spartina patens*, a common brackish marsh grass.

(3) Trees growing in coastal wetlands often experience increased rot from various infections aided by hot, humid conditions. Special care should be taken to avoid using core segments when rot is present. In many cases, three cores should be obtained from each tree to account for field errors. Only 28% of tree cores from the field were used in the final analysis of this study, so accessing as many trees as possible is necessary for future analysis.

(4) First-time analysis of new sites and new species should include some obvious correlations if they exist (*e.g.*, precipitation, temperature). KNMI Climate Explorer can be a good first tool for exploring climatological factors of growth at a site Trouet and Van Oldenborgh [2013]. Finding other sources of growth changes can also be useful, and discrete events can be used to explain rapid changes in growth (*e.g.*, tropical cyclones).

2.5 Conclusions

The Southeast U.S. and coastal areas have previously been criticized for their ability to produce non-climate-sensitive trees. This study shows that a previously unused species in tree-ring research is useful for climate analyses likely because of its proximity to the coast and interaction with saltwater. Though temperatures on the northern GOM coast are moderated by maritime air and precipitation is plentiful, tree growth is stressed in extreme coastal locations because saltwater inhibits recharge of freshwater in the soil. *T. ascendens* at Grand Bay NERR are sensitive to hot, mid-summer temperatures likely causing increased transpiraton by the plant and thus less growth. Conversely, Grand Bay NERR tree growth is enhanced when high autumn temperatures allow for longer growing seasons. Tree growth at Grand Bay NERR decreases following TC storm surge events when freshwater availability decreases. Site selection is vital when choosing coastal trees for tree-ring research. Incorporating rarely assumed stressors such as saltwater intrusion and inundation may assist in finding new species and new areas of research for tree-ring climate proxy studies.

Evidence of Moisture Stress from Coastal Tree Rings Using Carbon Isotopes

3.1 Introduction

Sea-level rise causes changes in coastal plant communities, and for coastal forests the change is largely occurring due to saltwater inundation Couvillion and Beck [2013]; Steyer et al. [2013]. The term "ghost forests" refers to coastal forests that die as a result of high soil salinity, and those locations increase in frequency with an increase in sea levels Senter [2003]; Kirwan and Gedan [2019]; Taillie et al. [2019]. Tree growth studies indicate that during periods of saltwater intrusion, growth is stunted in subsequent years, possibly leading to heavy mortality Doyle and Gorham [1996]; Kirwan et al. [2007]; Tucker et al. [2017].

In coastal locations, the definition of soil moisture must also include "freshwater" resources, and freshwater soil moisture resources can change based on two factors: (1) freshwater input (*e.g.*, precipitation, river flow, shallow groundwater fluxes) and (2) presence/absence of seawater salts (*e.g.*, tidal flows, storm surges). The presence of salts in coastal soils forces plants to exclude, exude, or compartmentalize the salt in order to acquire water Liang et al. [2008]. Some plants adapt well to saltwater environments (*e.g.*, mangroves) while many others suffer loss in biomass, height, and/or regeneration Pezeshki et al. [1990]; Pezeshki [1990]; Conner and Askew [1992]; DeLaune et al. [1994]. The long-term effects of saltwater intrusion to maritime forests is important for projections of the effects of sea-level rise and for properly managing coastal systems Doyle et al. [2010]. Tree-ring carbon isotopic analysis provides researchers the ability to further analyze relationships between tree growth and moisture stress Evans and Schrag [2004].

Carbon isotope ratios in tree-ring cellulose are controlled by stomatal conductance between the plant and the source (*e.g.*, atmospheric) CO_2 Francey and Farquhar [1982]; Saurer et al. [1995]; McCarroll and Loader [2004]. Carbon exists as two stable isotopes and one radioactive isotope in the atmosphere (^{12}C, ^{13}C, and ^{14}C), and trees naturally uptake CO_2 molecules freely and non-discriminantly. When leaf stomata are open to allow free gas exchange, plants prefer to photosynthesize molecules with the lightest isotopes (*i.e.*, ^{12}C). However, the stomata close to prevent evaporative loss of water in response to moisture stress. When the stomata close, the free gas exchange is lost and the plant must process any available CO_2 within the leaf. Therefore, the plant is enriched with ^{13}C during times of moisture stress because it does not have the freedom to photosynthesize with only the lightest isotopes. Numerous studies have shown that moisture stress is strongly correlated to tree-ring carbon stable isotopes Leavitt and Lone [1991]; Csank et al. [2016]; Nicklen et al. [2019]. However, few studies have assessed changes in tree-ring carbon stable isotopes in coastal locations.

The majority of coastal studies assessing changes in tree-ring carbon stable isotopes occurred on the Pacific coast of the U.S. Coastal *Sequoia sempervirens* relies on heavy fog throughout the year for sufficient moisture, and their tree-ring carbon isotopes followed fog patterns of the past Roden et al. [2009]; Johnstone et al. [2013]. Coastal trees in those studies showed correlation to growing season fog and drought patterns especially in spring and early summer. Additional researchers have assessed changes in tree-ring carbon isotopes for trees along a transect running inland from the coast in Oregon Roden et al. [2005]. For that study, changes in tree-ring carbon stable isotopes followed precipitation patterns, and in the area of highest precipitation (*i.e.*, the site closest to the coast), ^{13}C depletion occurred.

Other sites demonstrated that moisture availability is not the sole reason for changes in tree-ring carbon isotopes. *Pseudotsuga menziesii* in coastal Oregon showed that artificial fertilization can also change patterns of tree-ring carbon isotopes, because as the tree receives more nutrients, it requires more water to process those additional nutrients Cornejo-Oviedo et al. [2017]. In Italy, tree-rings with intra-annual density fluctuations (IADFs) within a tree ring caused changes in carbon isotopic ratios De Micco et al. [2007]. Specifically, IADFs were associated with enriched ^{13}C indicating periods of water stress during the production of the IADF.

Following an extensive literature review, I found only one study that explored changes in North American subtropical coastal wetlands Anderson et al. [2005]. That study showed that *Taxodium ascendens* tree-ring carbon isotopes followed different patterns than nearby *T. distichum*. Precipitation patterns were negatively correlated to *T. ascendens* tree-ring carbon isotopic values, indicating more stress at times of high water levels, whereas tree-ring carbon isotopes in *T. distichum* changed depending on levels of salinity in the soil. Trees at the site with higher saltwater intrusion show enrichment of ^{13}C perhaps explaining that an increase in salts is causing direct moisture stress to trees.

Methods for tree-ring carbon isotopic analysis differ for the aforementioned studies. Due to high cost, additional time for analysis, and destructive sampling, the added value of tree-ring isotopic analysis can become expensive. Therefore, tree-ring isotopic analysis often sacrifices sample resolution for increased knowledge as defined by the researcher. For example, to find isotopic changes within a year, a researcher might choose to limit the number of trees used and the number of years through time to instead concentrate time and money spent on multiple samples within a year Roden et al. [2005]; De Micco et al. [2007]. Other isotopic tree-ring studies rely on pooling multiple years to produce long-term chronologies of environmental proxy data Anderson et al. [2005]; Johnstone et al. [2013].

3.2 Materials and Methods

Because the tree-ring width data for this study have been published in Tucker et al. [2017] and due to small physical samples, I chose to sample whole rings for tree-ring carbon isotopic analysis through a 20-year period that was climatologically heterogeneous (*i.e.*, a period containing drought years, tropical cyclones (TCs), and increased saltwater intrusion) so that differences in tree-ring carbon isotopic values would emerge clearly.

3.2.1 Study Area

Grand Bay National Estuarine Research Reserve (Grand Bay NERR) is comprised of salt marsh and pine savanna plant communities and covers 7,284 hectares near Pascagoula, Mississippi Hilbert [2006]. Southern Mississippi has a subtropical climate with hot, wet summers and cool, dry winters. According to the data archived by the Southern Regional Climate Center (1940–2019) for Pascagoula, Mississippi, mean annual precipitation exceeds 150 cm, with more than 500 mm occurring during June–August. Mean January and July temperatures are 10°C and 27°C, respectively.

The most common canopy tree species, *Pinus elliottii* var. *elliottii*, grows as close as one kilometer from open saltwater bays that connect to the Gulf of Mexico (GOM; Figure 3.1). Nearest to the coast, *P. elliotti* grow on slightly elevated lands surrounded by salt marshes and tidal creeks. Other canopy trees at Grand Bay NERR include *Quercus virginiana*, *Magnolia virginiana*, and *Taxodium ascendens*. The most common understory grass nearest to the coast is the halophytic grass *Spartina patens*.

The tree-ring width data for this study were used in a previous study, and four tree cores from that study were used to sample for tree-ring isotopic analysis Tucker et al. [2017]. Three 5.15 mm cores were taken from each tree during summer 2016 using a lubricated Haglöf increment borer (*i.e.*, using beeswax and WD-40), and they were mounted and sanded with progressively finer grit sizes (ANSI 120, 220, 320, 400) to reveal clear ring boundaries in the wood Stokes and Smiley [1968]. The tree cores were visually crossdated that was assessed for quality using the computer program *dplr* (Appendix B) Bunn [2008]. Each of the final tree cores was measured to produce ring-width series for total, latewood, and earlywood ring widths.

3.2.2 Sampling for Isotopic Analysis

Tree-ring carbon isotope chronologies were formed for four trees (Figure 3.1, numbers 9, 20, 23, and 25). Tree cores were sampled for years 1996–2015 (n=20) because during that period, three hurricanes brought substantial storm surge (>2.5 m) to Grand Bay NERR: Hurricanes Georges (1998), Katrina (2005), and Gustav (2008) Needham and Keim [2012].

FIGURE 3.1: Aerial photo of the study site on a salt panne island and location of trees sampled. Photo colors are exaggerated to discern the different ecosystems present near the coast. Green area depicts the mostly freshwater ecosystem similar to inland pine savannas bordered closely by a fringe of sandy, unvegetated land (grayish-white), all of which is surrounded by salt marsh (unmodified gray color). Numbers indicate the tree number recorded chronologically in the field. Color scale of points denotes age of the tree. Image taken from Tucker et al. [2017].

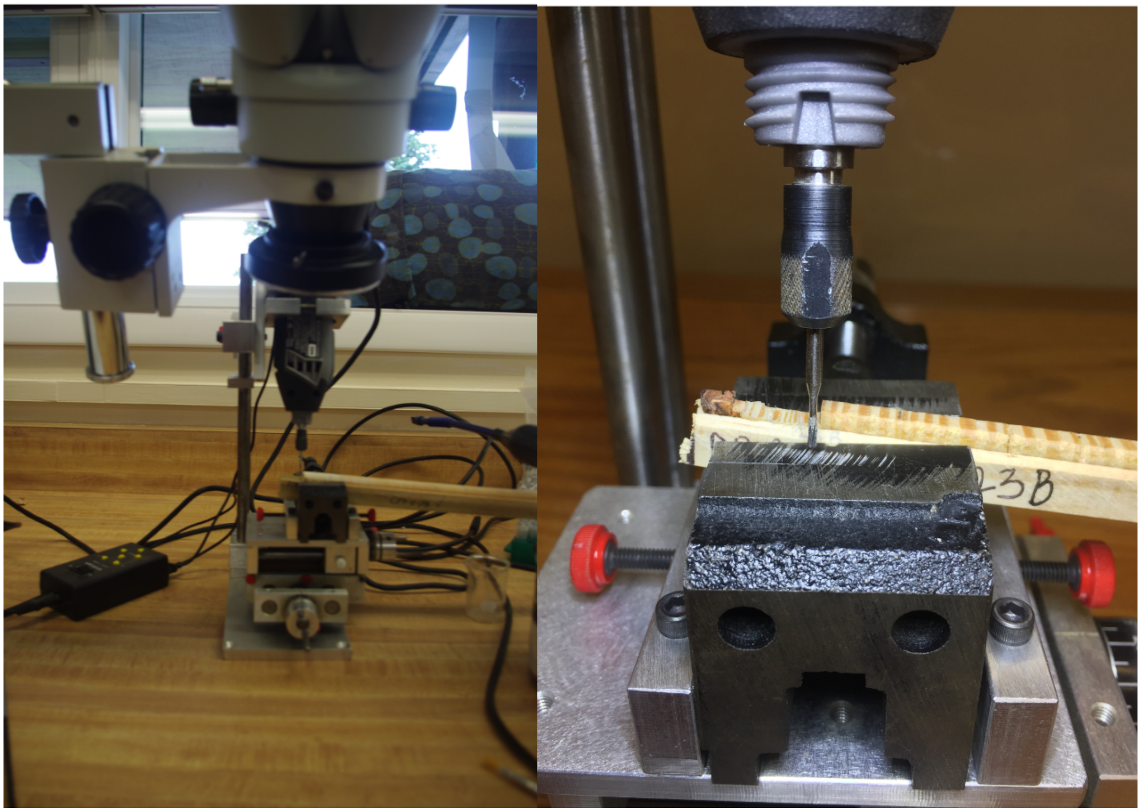

FIGURE 3.2: Micromill setup used in this study. The larger-scale image (left) shows the general setup with a stereoscope, Dremel tool, and manual sliding stage holding a tree core. Zooming into a similar image (right) shows the milling bit, core holder, and the milled section of tree core 23B used in this study. Note that the tree core is held at an angle because the tree rings within the core are not at a right angle to the core.

For the samples in this study, a manual micromill was used to obtain wood powder from each ring (Figure 3.2). A manual micromill was preferred because ring boundaries were often curved and irregular. The Dremel milling tool was mounted below a stereoscope so the user could see each individual ring to be drilled. The core was mounted into a manual slide stage that allows the core to move in four cardinal directions. The drill bit was often wider than individual tree rings (>1.0 mm), so each ring was milled at 5,000 RPM, not drilled, into a fine powder that was collected into 1.5 mL microcentrifuge tubes. If the ring was larger than the drill bit, the ring was milled using multiple passes parallel to the next ring boundary. After each individual ring was drilled and stored, the work space was cleaned with pressurized air before sampling the next ring.

Whole wood stable isotopes have shown to differ from wood cellulose in response to climate parameters, so each sample was processed to obtain α-cellulose Loader et al. [2003]; McCarroll and Loader [2004]; Gori et al. [2013]. The chemical processing used in this study is a modified version of the Brendel method combined with holocellulose extraction Brendel et al. [2000]; Anchukaitis et al. [2008]. The final chemical processing method used in this study was designed by Adam Csank at the University of Nevada, Reno, and it is described here in more detail.

To first remove lignin from the cellulose, the samples were soaked in a bleaching solution formed from a dilute mixture of sodium chlorite and acetic acid. After a rinse of ethanol and deionized water, sodium hydroxide was added for a limited time to remove holocellulose, and then hydrochloric acid was added quickly to neutralize the matrix before the entire cellulose sample could be consumed. Between each step, samples were centrifuged, and the liquid matrix was removed from the sample before the next chemical addition. A final ethanol rinse was applied to the sample to hasten the drying process prior to weighing.

The remaining α-cellulose powder was weighed on a microbalance to the nearest μ-gram and packed into tin capsules. Samples were sent to the Stable Isotope Facility at the University of California, Davis for δ^{13}C using a PDZ Europa 20-20 isotope ratio mass spectrometer coupled with a PDZ Europa ANCA-GSL elemental analyzer (Sercon, Cheshire, UK). Analytical precision was based on repeat analysis of seven internal lab reference materials that were previously calibrated against international reference materials. The mean standard deviation of the lab reference materials replicates (n=49) in this project was 0.06‰ for δ^{13}C. The long term lab standard deviation is 0.2‰ for ^{13}C. Mean absolute accuracy for calibrated reference materials was within 0.05‰ for δ^{13}C.

Each tree-ring carbon isotope series normalized because the average δ^{13}C varied among trees. Differences in has been noted previouslyMcCarroll and Loader [2004]. The normalized data were averaged to form one averaged δ^{13}C chronology to account for any aberrations that one tree may hold. Averaged isotope chronologies created from four trees was common for previous studies Leavitt [2010]; Loader et al. [2013]; Csank et al. [2016].

To ensure that the tree-ring carbon isotopic data were not biased by the Suess Effect, they were also detrended for atmospheric changes in carbon isotopes. The Suess Effect describes the change in atmospheric CO_2 carbon isotopic ratios due to the increase in fossil fuel burning during the past two centuries Revelle and Suess [1957]; Cain and Suess [1976]; Keeling [1979]. McCarroll and Loader [2004] suggest that when removing the Suess Effect, it is also useful to represent the tree-ring carbon isotopic values as they are related to processes during photosynthesis. $\Delta^{13}C_{plant}$ represents carbon isotope discrimination, such that

$$\Delta^{13}C_{plant} = \frac{\delta^{13}C_{atmosphere} - \delta^{13}C_{plant}}{1-(\delta^{13}C_{plant}/1000)}$$

in which $\delta^{13}C_{atmosphere}$ is the carbon isotopic composition of the atmosphere for that year, and $\delta^{13}C_{plant}$ is the carbon isotope ratio of the plant measured from the tree rings. Values for $\delta^{13}C_{atmosphere}$ were obtained from McCarroll and Loader [2004] up until 2004 and from White and Vaughn [2011] up to 2011 White et al. [2011]. Values for 2012–2015 were obtained by extending the curve fitted to the 1950–2011 atmospheric δ^{13}C values forward in time.

3.2.3 Climate-Isotope Analyses

SOI data are available on the National Centers for Environmental Information website via their teleconnections page NOAA [2018]. Precipitation values were accessed for 0.5° grid size from the Climate Research Unit (CRU) Time Series (TS) version 4.01 provided by the UK National Center for Atmospheric Science and University of East Anglia Harris et al. [2014]. Temperature and precipitation values were accessed for 4 km grid size from the PRISM Climate Group at Oregon State University Daly et al. [1997]. Additional divisional climate data were downloaded from NOAA for analyses with local monthly averaged data (Appendix A).

Tree-ring carbon isotopic values were correlated with various monthly climate data variables using the online program KNMI Climate Explorer and a package from the R statistical programming environment (*TreeClim*) Bunn [2008]; Trouet and Van Oldenborgh [2013]; Team [2014]; Zang and Biondi [2015]. *TreeClim* allows the user to test the stability of any monthly climatic correlation through time using Pearson's product moment correlation (Appendix C). Correlation significance was tested at the 5% level, and response coefficients were bootstrapped 1000 times using random replacements of the initial data. Previous researchers show that the amount of water availability early in the growing season can be an important driver of tree growth Cleaveland et al. [2003]; Stahle et al. [2009]; Tucker et al. [2017]. Therefore, the tree-ring carbon isotopic values were compared to the monthly temporal window of the early growing season (January–June). This time interval also proved to contain the strongest correlations to the tree-ring carbon isotopic data.

KNMI Climate Explorer allows the user to input column-format data and compare those values to various climate indices and parameters. The user can also select the time interval for the analysis and the location of display for the spatial correlation. The CRU TS v4.01 data span years 1901–2017 at 0.5° resolution. They are derived from monthly observations of weather stations in land areas across the world. CRU TS v4.01 measurements are used frequently to show large spatial patterns between tree-ring studies and regional climate Preechamart et al. [2018]; Huang et al. [2019]; George and Esper [2019]. The PRISM (*i.e.*, Parameter-elevation Regressions on Independent Slopes Model) Climate data (4 km resolution; 1895–2017) are also a gridded product, and have been used in previous tree-ring analyses Salzer et al. [2009]; McCullough et al. [2017].

3.3 Results

Four Grand Bay NERR *Pinus elliotti* tree cores were analyzed for δ^{13}C differences and converted to Δ^{13}C data to show patterns of moisture stress for years 1996–2015 (Figure 3.3). Raw data for this study have an average of -24.8‰(σ=0.7), and they are similar to

δ^{13}C values in previous studies of carbon isotopic analysis (Appendix D; *e.g.*, Roden et al., [2005]), so it is assumed that hydrocarbons with similar carbon isotopic values used during field work (*i.e.*, beeswax and WD-40 White et al. [1998]; Kropf et al. [2010]; Schwartz et al. [2013]) and any heat generated by micromilling did not have a substantial effect on carbon isotopes in this study. Each analysis herein includes results for both δ^{13}C and Δ^{13}C values.

The δ^{13}C data trend negatively through time, while the Δ^{13}C trend positively (Figure 3.3). This opposite trend is expected because the Δ^{13}C formula creates positive values for Δ^{13}C. Additionally, the Δ^{13}C values appear smoothed because the Suess Effect has been removed.

For the two data sets, each individual series agrees with other series in the set. Average interseries correlations are r=0.64 (p<0.05) for δ^{13}C values and r=0.43 (p<0.05) for Δ^{13}C values. Marked decreases depicting higher moisture stress occur in 1999, 2006, and 2011, while peaks in the data indicating low moisture stress occur in years 2001, 2007, 2010, and 2014. Tree 25 has an average of 1‰ higher Δ^{13}C than the other three trees at the site. Three missing data points (Tree 09, years 2006 and 2007; Tree 20, year 2015) occur due to lack of enough physical sample necessary for chemical processing.

Due to the low number of values in the data sets (n=20), Spearman's rank correlation was used to compare tree-ring carbon isotopic values with the Southern Oscillation Index (SOI). Only SOI values for the month of March are significantly related to tree-ring carbon isotope values (r=−0.47, p=0.04; Figure 3.4). This r value is the same for both δ^{13}C values and Δ^{13}C values because Spearman's rank correlation ranked each value the same throughout the two series. High SOI values indicate years of strong La Niña conditions, thus this negative correlation means that when Δ^{13}C values are low (high moisture stress), La Niña conditions exist. Visual analysis of the short time series shows that the three lowest Δ^{13}C values correspond with strong La Niña years (1999, 2006, and 2011). Additionally, weak La

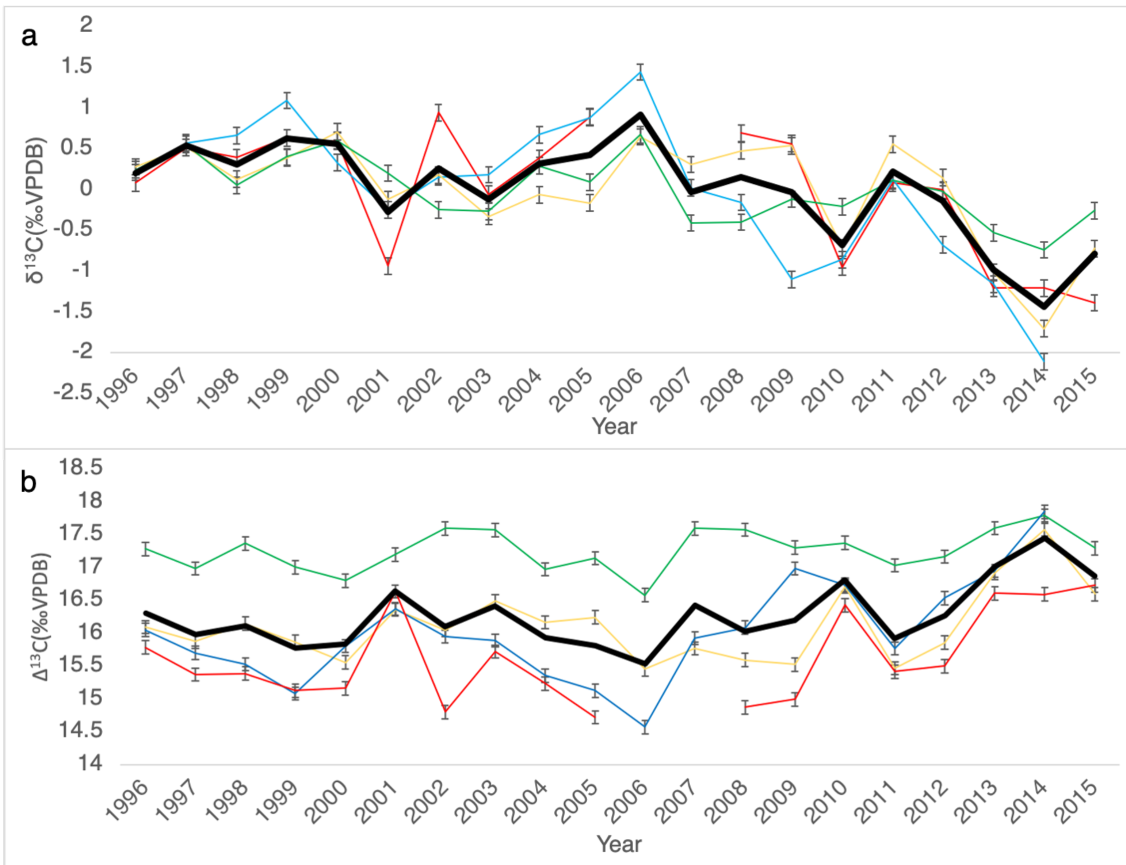

FIGURE 3.3: Time series of carbon isotopes for *Pinus elliotti* 1996–2015. $\delta^{13}C$ values (a) are included as well as $\Delta^{13}C$ values (b), which have the Seuss Effect removed. Each tree-ring carbon isotope series is included (red=09, blue=20, yellow=23, and green=25) and the average of all series is plotted in black. Standard error bars are included for analytical precision.

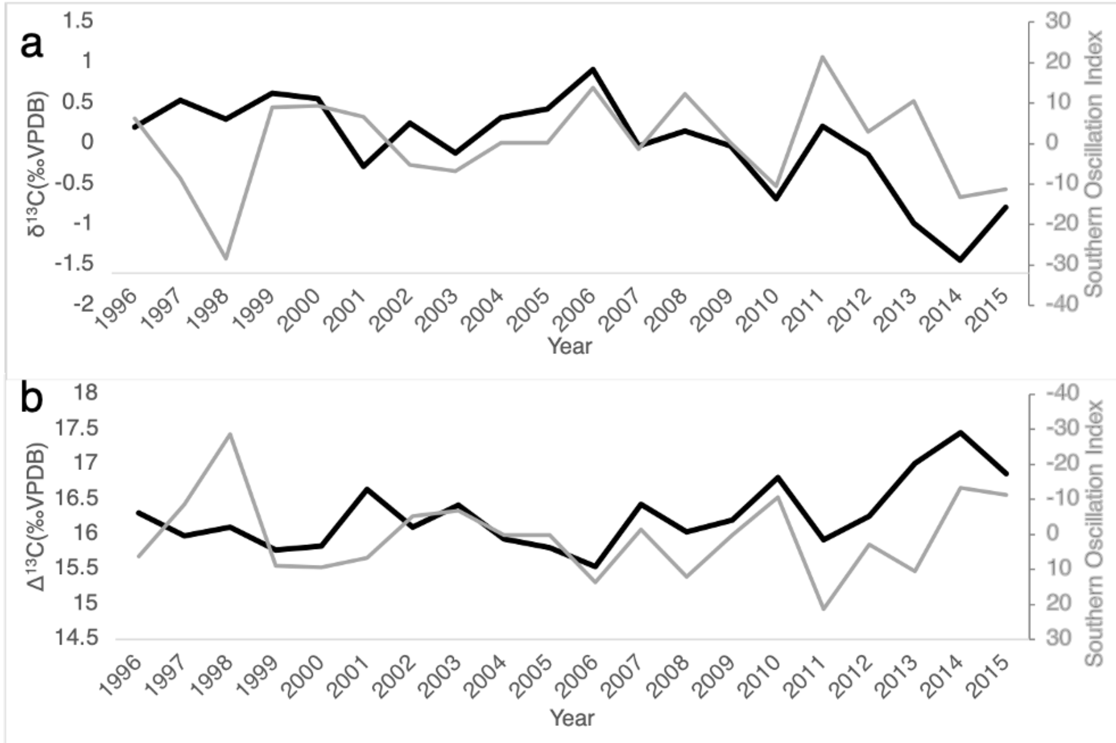

FIGURE 3.4: Time series of Southern Oscillation Index (SOI) and tree-ring carbon isotopes for this study. These values of SOI are for the month of March (gray) compared to δ^{13}C (a) and Δ^{13}C (b) values (black). Note that the SOI axis in plot b is flipped for ease of comparison with Δ^{13}C values.

Niña, normal, and El Niño conditions do not have an associated visual pattern of response with Δ^{13}C values.

Tree-ring carbon isotopic values are correlated to CRU TS v4.01 averaged precipitation data for the months February–May at the 0.5° scale (Figure 3.5). Correlation values directly on the location of the site are greater than r=0.5 (p<0.05), and they are opposite but identical for both δ^{13}C and Δ^{13}C values. The months of January and June were also significantly correlated to tree-ring carbon isotopic values, but when including them as additional months in this analysis, the area of correlation decreased slightly. Correlation remains significant throughout the northern GOM coast from the Mississippi River to the Florida panhandle, and the pattern extends further south through the state of Florida.

As an exploratory measure to determine their climate response through time, tree-ring carbon isotopic values for Grand Bay NERR were compared to nearby divisional climate

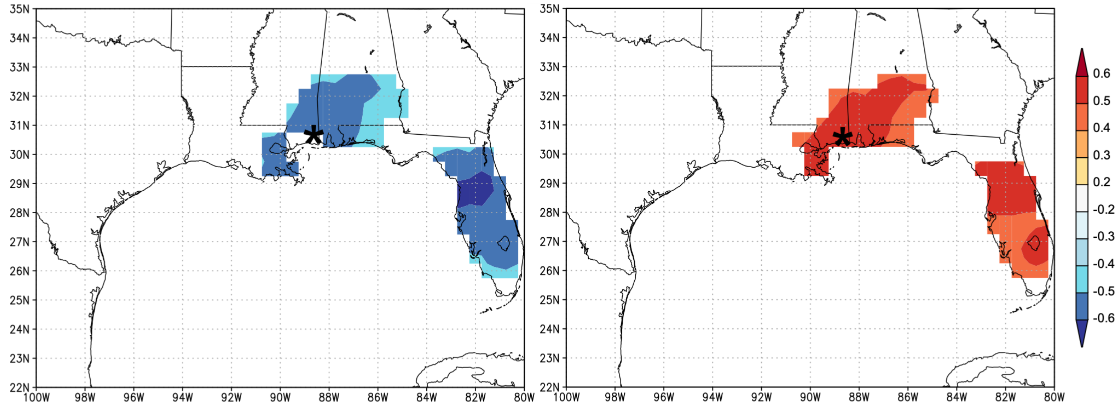

FIGURE 3.5: Spatial correlation of tree-ring carbon isotope values and precipitation (February–May) 1996–2015. Correlations with both $\delta^{13}C$ (a) and $\Delta^{13}C$ (b) values are shown. Red colors indicate positive correlations. The location of the study site is indicated by the black asterisk.

data to determine the relationship between isotopic values and climate parameters through time (Figure 3.6). $\delta^{13}C$ and $\Delta^{13}C$ values were compared to the annual time interval that was found to be significant in spatial analyses (January–June), and both forms of tree-ring carbon isotope data show similar results. Relationships that were significant include precipitation, maximum average monthly temperature (TMAX), and minimum average monthly temperature (TMIN), the latter two being most stable through time. Precipitation is only significantly stable through the last decade of tree-ring carbon isotopic values (2006–2015) in which the relationship was positive for $\Delta^{13}C$, similarly to previous spatial analyses.

Relationships with TMIN were stronger than TMAX, and both variables are negatively correlated to $\Delta^{13}C$ values. For all moving correlation analyses, correlation weakens and becomes non-significant in the middle of the record. Other annual time intervals were tested, but no other intervals showed stronger relationships than those discussed here. Additionally, no other climate variables tested (see Appendix A) showed stronger relationships than those depicted in Figures 3.5 and 3.6.

3.4 Discussion

Previous researchers suggest that tree growth declines at coastal sites because of moisture stress and lack of freshwater resources Doyle et al. [2007]; Raddi et al. [2009]; Tucker

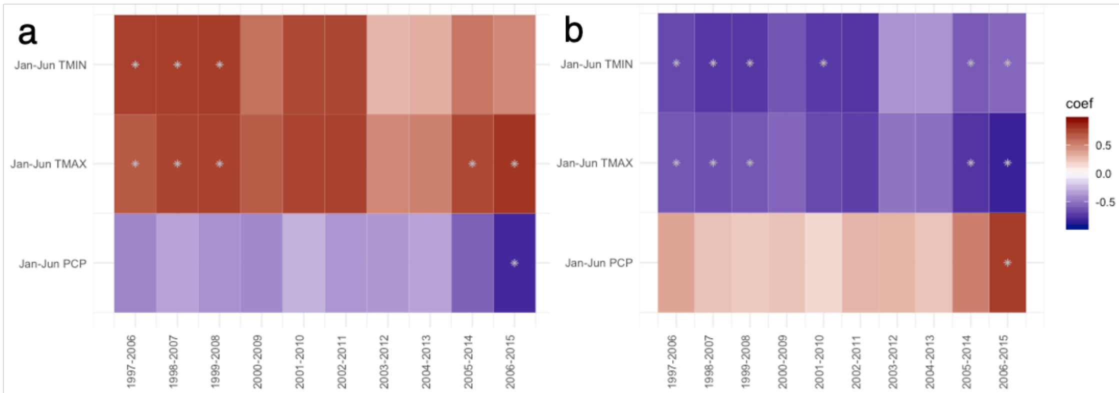

FIGURE 3.6: Moving window correlation of tree-ring carbon isotope values and climate variables 1996–2015. Correlations with both δ^{13}C (a) and Δ^{13}C (b) values are shown. Each square represents the correlation coefficient for that window of time. The vertical axis represents the monthly window of correlation for each climate variable: total precipitation (PCP), maximum average monthly temperature (TMAX), and minimum average monthly temperature (TMIN). The horizontal axis shows the interval for the window through which the correlation analysis was conducted. Red colors indicate positive correlations, and blue colors indicate negative correlations. A white asterisk indicates statistical significance at $p<0.05$.

et al. [2017]. Tree-ring carbon isotopic values are inherently linked to changes in stomatal conductance, which can be affected by moisture stress from soil moisture, precipitation, and high respiration. Results were produced for both δ^{13}C and Δ^{13}C values. However, results are nearly identical for all analyses. Therefore, the discussion of the results will concentrate on Δ^{13}C values, because they have been detrended to remove the Suess Effect, and they better represent processes within the tree as noted in Section 3.2.2.

Except for tree 25, Δ^{13}C values are consistent among trees used in this study. Additionally, McCarroll and Loader [2004] noote that results of previous studies indicate mean shifts in tree-ring carbon stable isotopic ratios are not uncommon. Local site conditions that may have changed the assimilation of carbon isotopes in tree 25 include exogenous stress other than saltwater intrusion, higher availability of freshwater, or lower competition from other plants. Tree-ring Δ^{13}C values for this study follow climatic changes at the site, particularly those climate variables associated with soil moisture (Figure 3.6). Additionally, isotopic values presented here are similar to values seen in other studies (*i.e.*, 15–18‰) Loader et al. [2003];

Nicklen et al. [2019], and the range of values is within normal carbon isotope ranges (1–3‰) as presented in Leavitt [2010].

Tree-ring $\Delta^{13}C$ values have been linked to teleconnections with ENSO globally, and these results agree with those studies Leavitt et al. [2002]; Schöngart et al. [2004]; Brienen et al. [2012]. The results of this study show that strong La Niña events are linked with declines in $\Delta^{13}C$ values indicating increased moisture stress in the tree. Additionally, little relationship exists with neutral and El Niño conditions. As the Walker Circulation reverses in the central Pacific Ocean, winter storms increase and drought conditions improve in the following year Noel and Changnon [1998]; Mo and Schemm [2008]. More specifically, Mo and Schemm (2008) note that El Niño conditions are not as strongly associated with wet years as La Niña conditions are associated with dry years. Results of this study agree that La Niña years can be an important driver of moisture stress in drought years, while other phases of ENSO may not play as strong of a role in the wetness of the Southeast U.S. The large spatial signal also alludes to the fact that the $\Delta^{13}C$ values are responding to a larger signal than simply localized precipitation (Figure 3.5).

Results of this study indicate a strong positive relationship between tree-ring $\Delta^{13}C$ and precipitation at the site and extend into South Florida (Figure 3.5). During the monthly analysis period (February–May), frontal systems are responsible for bringing the majority of the rain occurring in this region during that time of the year Powell and Keim [2015]. A lack of correlation exists during the summer when convective systems dominate rain patterns in the region Mitchell et al. [2019]. Frontal rain early in the growing season is likely an important source of freshwater for these trees. Additionally, this correlation is likely driven by the past 10 years of analysis (2006–2015; Figure 3.6).

Previous work suggests that increased levels of precipitation in South Florida result in increased moisture stress in vegetation due to high water levels Ewe and Sternberg [2002, 2003]. Additionally, *Taxodium ascendens* $\delta^{13}C$ at a nearby site in South Florida show negative correlations with precipitation Anderson et al. [2005]. *Taxodium ascendens* and *Pinus elliottii*, like those used in this study, typically grow together in similar habitats and environmental conditions Ewel [1995]. The two species may be physiologically responding to similar environmental conditions in different ways. Sandy soils prevalent in pine savanna-cypress dome environments allow water to percolate quickly, so trees are reliant on frequent precipitation in those systems Ford and Brooks [2003]. Additionally, the hydroperiodicity of flooding may be driving site differences rather than species differences. Trees for this study respond more similarly to the high salinity site in Anderson et al. [2005].

Tree-ring $\Delta^{13}C$ values in this study also correlate with early growing season temperatures (Figure 3.6). These temperature correlations are likely representative of soil moisture conditions, because temperatures can regulate the loss of water through evaporation from the soil surface and can increase respiration of trees, especially at night Lloyd and Farquhar [2008]. Correlations with TMAX show that high daily temperatures likely cause moisture stress through rapid evapotranspiration, especially during dry spells. Correlations with TMIN show that high nighttime temperatures are likely associated with high respiration rates at night, suggesting that the tree is using more water than usual.

Finally, an increase in evaporation increases the concentration of macro- and micronutrients in the soil. Previous work shows that trees with increased fertilization saw reductions in $\Delta^{13}C$ Cornejo-Oviedo et al. [2017]. Increased fertilization means the plant can respire more and will ultimately require more water. Recent researchers have shown that hurricane storm surge can increase phosphorous levels in the soil Castañeda-Moya et al. [2020], so the low value of $\Delta^{13}C$ in 2006 for this study may also suggest that storm surge from an intense 2005 Atlantic Hurricane season ($>$7.0 m) may have increased nutrients before the drought conditions set in for 2006. Though Hurricane Katrina in 2005 was the largest storm surge on record for this region (Table 2.2), other years of storm surges $>$2.0 m at this site do not correspond to any substantial spikes in the $\Delta^{13}C$ (*e.g.*, 1998, 2002, 2008).

3.5 Conclusions

Isotopic analysis of coastal tree rings is rare but useful for adding value to coastal dendrochronology. Tree-ring $\Delta^{13}C$ values in this study show correlations to moisture stress through years 1996–2015. ^{13}C is most enriched in years following TC storm surges accompanied by drought conditions (*e.g.*, 2006), especially as they relate to ENSO. Spatial correlations for tree-ring $\Delta^{13}C$ values exist for precipitation directly over the site. The combination of precipitation and high evaporation from higher-than-normal temperatures are both factors of moisture stress at the site.

Tree-ring width of the trees used in this study showed strong correlation to TC occurrences, but $\Delta^{13}C$ values did not. Additionally, spatial correlations with temperature and $\Delta^{13}C$ show that tree-ring carbon isotopic analysis can produce a wider spatial signal than ring widths. Tree-ring widths and tree-ring carbon isotopic values for this study and others show connections with ENSO, specifically that La Niña years correlate with moisture stress to trees in the northern GOM. Because TC storm surges may have affected the lowest $\Delta^{13}C$ value in this study, it is possible that sites with different saltwater intrusion rates may show different results.

Greenhouse studies on the effects of saltwater intrusion to sapling $\Delta^{13}C$ should be explored to best explain the dessicating effects of saltwater on tree-ring isotopic values. Additionally, future studies in colder coastal regions and in tropical coastal regions should focus on teleconnections from ENSO and also focus on varying drivers of moisture stress (*e.g.*, temperature versus precipitation). Future work should also confirm any intra-annual isotopic fluctuations, and sites with longer-living trees should be prioritized.

Comparing Growth of Three Tree Species in Relation to Their Distance from the Coastline

4.1 Introduction

Long-term loss of coastal wetlands in Louisiana has converted 1,800 mi^2 of land to water for the period 1932–2010 Couvillion et al. [2011]. Since 2006, nearly 400 sites of the the Coastwide Reference Monitoring System (CRMS) have recorded soil, hydrology, and vegetation changes in coastal Louisiana Steyer et al. [2003]; Steyer [2010]. However, other than aerial imagery and niche study sites, little long-term information exists for the effects of northern GOM land loss, tropical cyclones (TCs), and salinity changes on coastal plant flora. However, tree-ring records can provide researchers with long-term proxy data of past environmental changes.

Coastal wetland trees are useful for dendrochronological applications, especially *Taxodium distichum* and *Pinus elliottii*, which can live for hundreds of years Brown [1996]; Stahle et al. [2012]. Previous studies have analyzed the effects of precipitation, temperature, saltwater inundation, and TCs on tree growth of coastal sites Ewel and Parendes [1984]; Doyle et al. [2007]; Harley et al. [2012]; Tucker et al. [2017]. Environmental and climatic factors are important not only to the trees at each site, but also to other mid- and understory vegetation crucial to providing habitat and holding together soils in the face of sea-level rise Atwater and Yamaguchi [1991]; Nyman et al. [2006]. Tree rings can be an important long-term footprint of the environmental conditions affecting an entire habitat Speer [2010].

Moisture stress in coastal trees comes as a result of lack of precipitation, high evapotranspiration, and the influx of salts from seawater. The Palmer Drought Severity Index (PDSI) was developed in 1965 to measure moisture stress, and it has been used extensively to describe patterns in moisture stress (according to Google Scholar, Palmer [1965] has been cited over 5,300 times). Drought indices like PDSI are important to tree growth because they represent the incoming and outgoing water in an ecosystem necessary for plant photosynthesis and respiration Palmer [1965]. Effects of drought have been explored in previous coastal and wetland dendrochronological studies Stahle et al. [1988]; Henderson and Grissino-Mayer [2009]; Harley et al. [2011].

40% of people in the U.S. live in counties or parishes adjacent to coastal systems, and those areas are frequently abound with anthropogenic modification Small and Nicholls [2003]. Some efforts aim to keep the sea at bay while others allow a natural flow of tidal waters. Past researchers have identified numerous anthropogenic sources of tree growth changes in near-coastal environments Ragsdale and Berish [1988]; Rakowski et al. [2008]. Future change of coastal landcapes relies on past environmental data as an analog for future predictions, and tree-ring data can produce long-term chronologies linked to changes in their environment Doyle et al. [2010]. To assess long-term changes in coastal environments of the northern GOM, I compare tree-ring chronologies of three study sites with differing distance to the coastline.

4.1.1 Study Sites

Study site characteristics have proved to be important factors to finding trees that were sensitive to environmental parameters (see Chapters 2 and 3). Therefore, each study site used in this Chapter is mapped and described in detail (Figure 4.1). General climate data were gathered online from the Southern Regional Climate Center (`srcc.lsu.edu`).

Doyle's Bayou (30.68°N, 91.11°W; Figure 4.2) is a public park in northern East Baton Rouge Parish, Louisiana, more than 80 km from any saline bodies of water. Doyle's Bayou is currently the site of an urban forest restoration initiative to convert local open fields to closed-canopy forest. The tree cores collected at this site were collected through a Louisiana Sea Grant collaborative project (LSU Coastal Roots) initially designed to bring middle- and high-school students into their local environment in hopes of restoring the site Somers [2005]; Karsh et al. [2009]; Coker et al. [2010]. Average summer high (winter low) temperatures are 32.5°C (4.5°C), and average annual total precipitation is 160 cm.

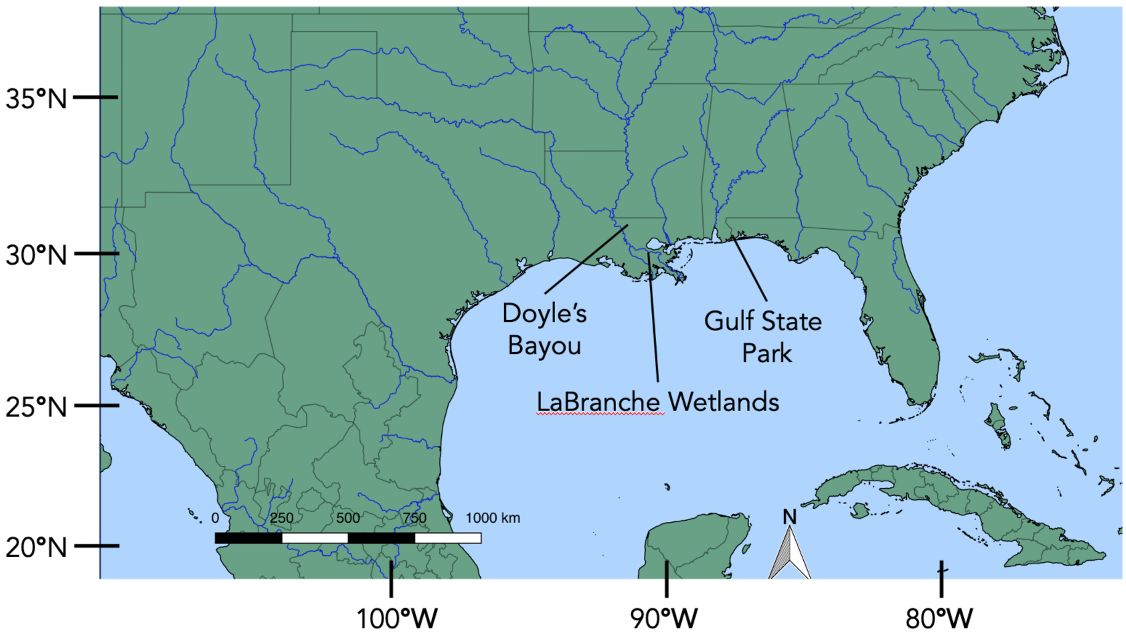

FIGURE 4.1: Location of study sites used in this chapter.

FIGURE 4.2: Location of Doyle's Bayou trees. Numbers indicate the order of tree cores taken in the field.

FIGURE 4.3: Forest structure at Doyle's Bayou. Note the dense midstory blocking light from allowing ground cover to grow.

The bottomland hardwood forest at Doyle's Bayou (Figure 4.3) shades the ground heavily during the growing season when the broadleaf deciduous trees produce leaves. Dominant canopy species include *Quercus nigra*, *Liquidambar styraciflua*, and *Celtis occidentalis*. Common midstory plants include *Carpinus caroliniana* and *Ligustrum sinense* among numerous unidentified vine species.

Gulf State Park (GSP; 30.26°N, 87.64°W; Figure 4.4) covers 6,000 acres located near Orange Beach, Alabama, where three freshwater lakes are surrounded by pine savanna and freshwater wetland plants. At this site, *Pinus elliottii* grow less than 500 meters from the open GOM. Between the trees and the GOM is a beach-dune system often accompanied by large condominium buildings. The nearby freshwater lakes have been used to reconstruct hurricane storm surge for the past 6,000 years using sedimentary records Liu and Fearn [1993]. Liu and Fearn (1993) found that large storm surges producing overwash into the freshwater lakes occurs at least once every 600 years. Modern instrumental records show that, other

FIGURE 4.4: Location of Gulf State Park trees. Numbers indicate the order of tree cores taken in the field.

than southern Florida, nearby Pensacola Beach is the most active landfalling location for major hurricanes in the 20th century in the U.S. Keim et al. [2007]. Average summer high (winter low) temperatures are 32°C (5°C), and average annual total precipitation is 165 cm.

In lines running parallel to the beach, hummocks of higher ground rise above hollow wetlands as relict beach dunes. Pine trees frequently occur on raised hummocks above flooded wetlands (Figure 4.5). Ground cover plants beneath *P. elliottii* included *Morella cerifera*, *Baccharis halimifolia*, *Sabal minor*, *Thelypteris palustris*, and the lichen *Usnea florida*. Flooded locations near the lakes also included *Cladium jamaicense* and *Typha* spp. Exposed soil surfaces often indicated the presence of white sand (Figure 4.5).

LaBranche Wetlands (30.00°N, 90.30°W; Figure 4.6) is a privately owned tract of land located west of New Orleans, Louisiana. It is also bordered by the Mississippi River to the south, brackish Lake Pontchartrain to the north, and Bonnet Carré Spillway to the west. The CRMS station number 2830 shows salinity during the mean growing season (May–October) is 0.26 parts per thousand (ppt), but salinity can be as high as 7.0 ppt during hurricane storm

FIGURE 4.5: The hummock-hollow topography at Gulf State Park. Note that the pine savanna plant community grows on higher ground (right), and surface soil is often white sand (foreground).

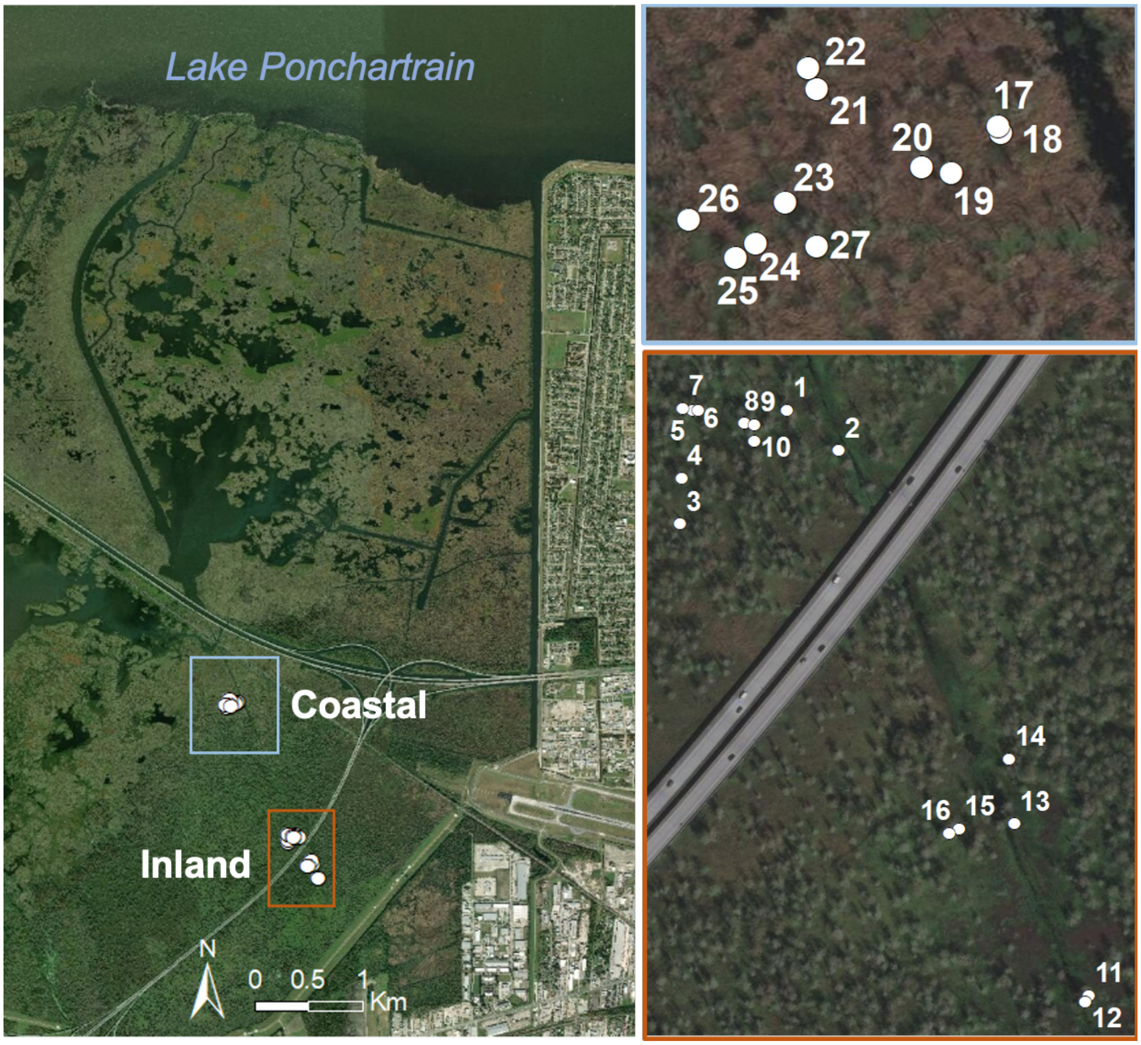

FIGURE 4.6: Location of LaBranche Wetlands trees. Numbers indicate the order of tree cores taken in the field.

surge inundation. *Taxodium distichum* tree rings at Bonnet Carré spillway nearby have been used to explore the effects of high water inputs during Mississippi River floods Day et al. [2012]. Average summer high (winter low) temperatures are 33°C (7°C), and average annual total precipitation is 163 cm.

Taxodium distichum grow in regions of LaBranche Wetlands furthest from Lake Pontchartrain, while halophytic plants grow near the lake indicating its brackish tendencies. Freshwater swamps and brackish marshes intersect and combine in one site used for this study, which is located near the intersection of Interstates 10 and 310 (29.99°N, 90.30°W). For the site labeled “coastal”, *T. distichum* trees show signs of growth stress including low stem density, low crown density, lack of regeneration, and low stem diameter (Figure 1.8). Understory vegetation at the coastal site is comprised almost entirely of *Spartina patens* and *Juncus roemarianus*. Plant species richness and diversity is higher in the “inland” site (Figure 1.7). Other tree species include *Nyssa aquatica*, *Acer rubrum* var. *drummondii*, and the non-native *Triadica sebifera*. Common understory species at the inland site include *Sagittaria lancifolia*, *Iris giganticaerulea*, *Hydrocotle* spp., and numerous undefined submerged aquatic vegetation species.

4.2 Materials and Methods

Tree-ring data for LaBranche Wetlands, Gulf State Park, and Doyles Bayou were collected in April 2018, May 2018, and January 2019, respectively. The Doyle’s Bayou tree cores were collected by citizen scientists from the Coastal Roots program at Louisiana State University Somers [2005]; Karsh et al. [2009]; Coker et al. [2010].

4.2.1 Tree-Ring Data

For all three sites, two cores per tree were obtained to reduce within-tree error. Tree cores were mounted to wooden mounts with tracheids in vertical growth position and sanded with successively finer grit sandpaper so that ring boundaries were clearly visible Stokes and Smiley [1968]; Speer [2010]. Each core was visually crossdated at 10X magnification, and cores were scanned and measured to the nearest 0.01 mm using the computer software CooRecorder. Cores that contained missing wood, did not visually crossdate, or were otherwise in poor condition were not included in final analysis. In combination, the computer programs CDendro, COFECHA, and the *dplr* package in R statistical programming environment were used to assess the quality of visual crossdating. To produce ring-width index chronologies, each tree-ring width series was detrended, and all series from a single site were averaged together. All chronologies used in this study were developed in *dplr* using interactive detrending. Doyle’s Bayou and Gulf State Park trees were individually detrended using a negative exponential spline (`method = "ModNegExp"` in *dplr*) because the raw ring widths at those sites exhibited a traditional age-related growth trend. Trees at LaBranche Wetlands were individually detrended using their mean growth value (`method = "Mean"` in *dplr*) because they did not express an age-related growth trend, and ultimately because those trees show a relationship with pulse-based river flooding and not long-term climate parameters.

4.2.2 Climate-Tree Growth Analyses

Ring-width index chronologies were correlated with various monthly climate data variables using the online program KNMI Climate Explorer and the *TreeClim* package from the R statistical programming environment Trouet and Van Oldenborgh [2013]; Team [2014]; Zang and Biondi [2015]. *TreeClim* allows the user to test the stability of any monthly climatic correlation through time using Pearson's product moment correlation. Correlation significance was tested at $p<0.05$ level, and response coefficients were bootstrapped 1000 times using random replacements of the initial data. KNMI Climate Explorer allows the user to input column-format data and compare those values to various climate indices and parameters. The user can also select the time interval for the analysis and the location of display for the spatial correlation.

The CRU TS v4.01 data used in KNMI Climate Explorer span years 1901–2018 at 0.5° resolution. CRU TS v4.01 data used in this chapter include average maximum monthly temperatures, average minimum monthly temperatures, monthly precipitation totals, and PDSI. They are derived from monthly observations of weather stations in land areas across the world. CRU TS v4.01 measurements have been used in previous research to show large spatial patterns between tree-ring chronologies and regional climate Preechamart et al. [2018]; Huang et al. [2019]; George and Esper [2019]. For use in *TreeClim*, divisional data were downloaded from a NOAA website (*e.g.*, Appendix A). Mississippi River monthly average discharge data for Tarbert Landing span the length of the tree-ring record used in this study, and they are complete for the entire time interval. These river discharge data are available from the U.S. Army Corps of Engineers website `rivergages.com`. Periods of analysis are described for each site in the Results section, and only statistically significant correlations (p<0.05) were reported.

4.3 Results

Results for this chapter include sites from two different coastal plant community characteristics: a beach pine savanna 500 meters from the GOM (Gulf State Park) and a cypress swamp located atop peat soils (LaBranche Wetlands). Additionally, an urban, inland site (Doyles Bayou, Baton Rouge, LA) is also included for comparison to the coastal sites.

4.3.1 Doyle's Bayou

Eight *Quercus nigra* tree cores of the available 18 (44%) were successfully crossdated for Doyle's Bayou for years 1973–2018 (Appendix E). Series intercorrelation and average mean sensitivity are r=0.52 and r=0.27, respectively. After detrending, *Q. nigra* at Doyle's Bayou show low variation in growth, except for a peak in 2002 (Figure 4.7). Visually, the 50% spline (red line) follows a 10–12 year pattern, and wavelet analysis confirms that this periodicity has a high power for the data set. However, the period of record for these data limits the statistical significance of this result.

The three lowest growth years occur in 1993, 2006, and 2009. Those years also represent the first year following the passage of three major hurricanes directly over the study site: Hurricanes Andrew (1992), Katrina (2005), and Gustav (2008). Those three hurricanes tracked from the southeastern Gulf of Mexico, and they recurved upon landfall. Two of them (Andrew and Katrina) made an initial landfall in South Florida, and their wind speeds near the site reached 54.0, 41.2, and 43.7 ms^{-1}, respectively (Figure 4.8). In nearby Lake Maurepas (25 miles to the east), each of those hurricanes also brought storm surge (1.5, 1.6, and 3.0 m, respectively) to the region indicating their power at the time of passage over Baton Rouge.

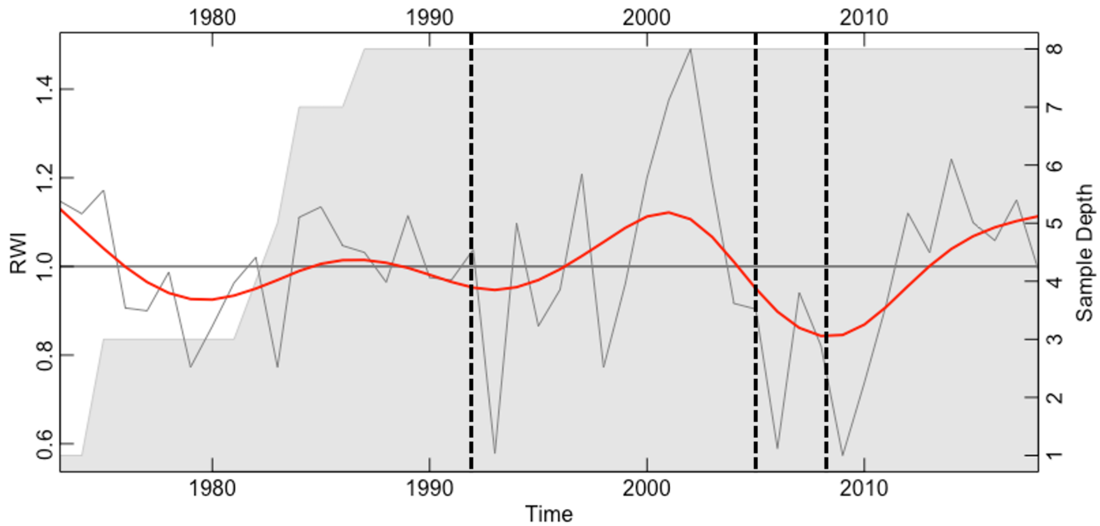

FIGURE 4.7: Ring-width index (RWI) of Doyle's Bayou *Quercus nigra* 1973–2018 (gray line). Red line is the 50% spline of the ring-width data within a 5-year moving window. The gray polygon in the background represents the sample depth for that given year. Vertical dashed lines indicate the three largest hurricanes impacting the site (Figure 4.8).

Aside from the three hurricanes corresponding to low growth in the tree-ring record, the Doyle's Bayou *Q. nigra* show little relationship to climate variables. Only one relationship had significantly strong relationships to growth: summer maximum temperatures. Spatial correlation of PRISM mean maximum monthly temperatures averaged for summer months (June–August) are negatively correlated to tree growth at Doyle's Bayou (Figure 4.9). This relationship is strongest (r>-0.5, p<0.05) near the study site, though the relationship shows correlation throughout the Southeast U.S.

4.3.2 Gulf State Park

Twenty *Pinus elliotti* var. *elliottii* tree cores of the available 34 (59%) were successfully crossdated for Gulf State Park (GSP) for years 1921–2017 (Appendix F). Series intercorrelation and average mean sensitivity are r=0.55 and r=0.38, respectively. Expressed population signal remains above 0.85 for years 1928–2017.

Following a peak of growth in the 1920s, tree-ring width is below average during the 1940s and 1950s (Figure 4.10). A twenty-year trend increases during the 1960s and 1970s,

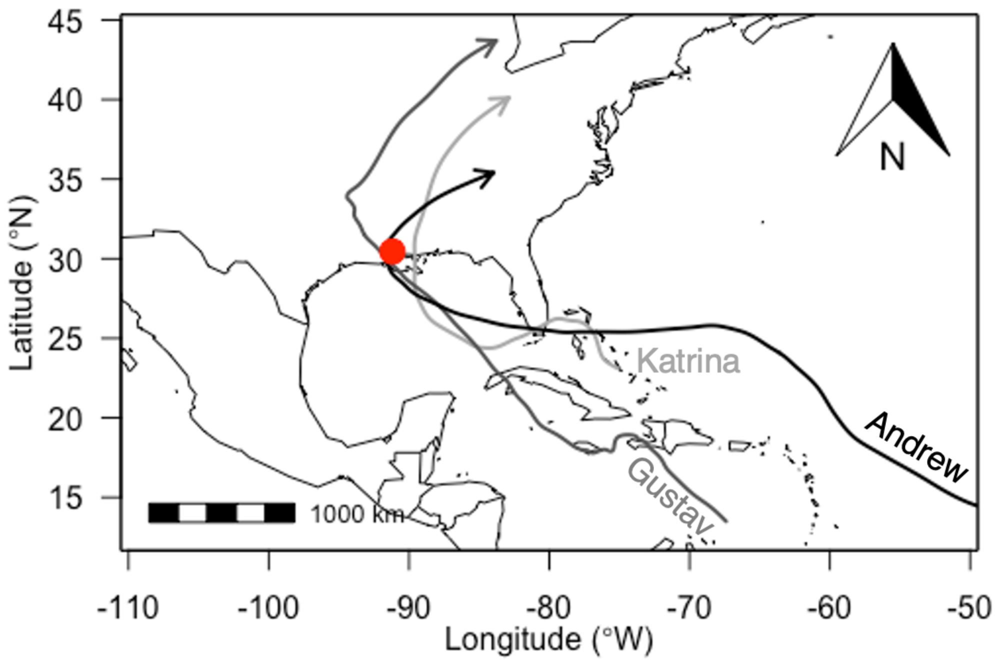

FIGURE 4.8: Tracks of hurricanes impacting Doyle's Bayou (red circle). Tracks are color coded to their wind speed intensity at time of passage over the study site (darkest = most intense). Note that the maximum wind speed at the study site does not match the maximum wind speed of the hurricane at landfall.

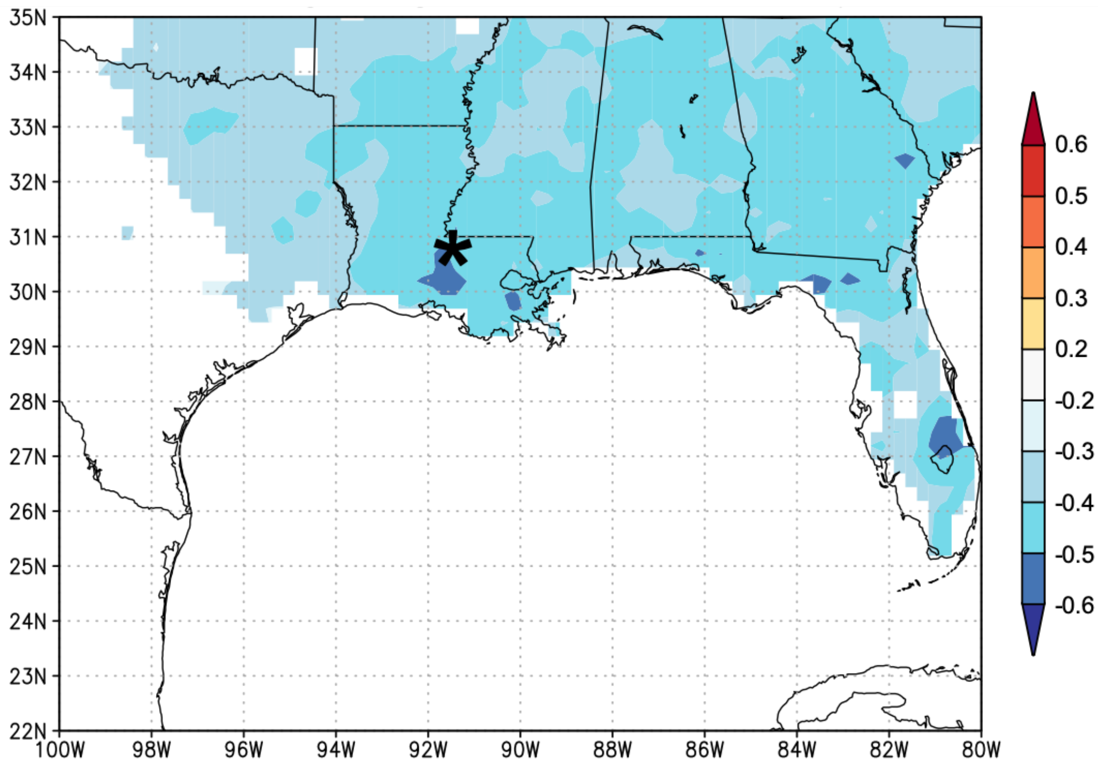

FIGURE 4.9: Spatial correlation of Doyle's Bayou ring-width index and TMAX. TMAX is averaged maximum monthly temperatures for months June–August (1973–2018). Blue colors indicate negative correlations. The location of the study site is indicated by the black asterisk.

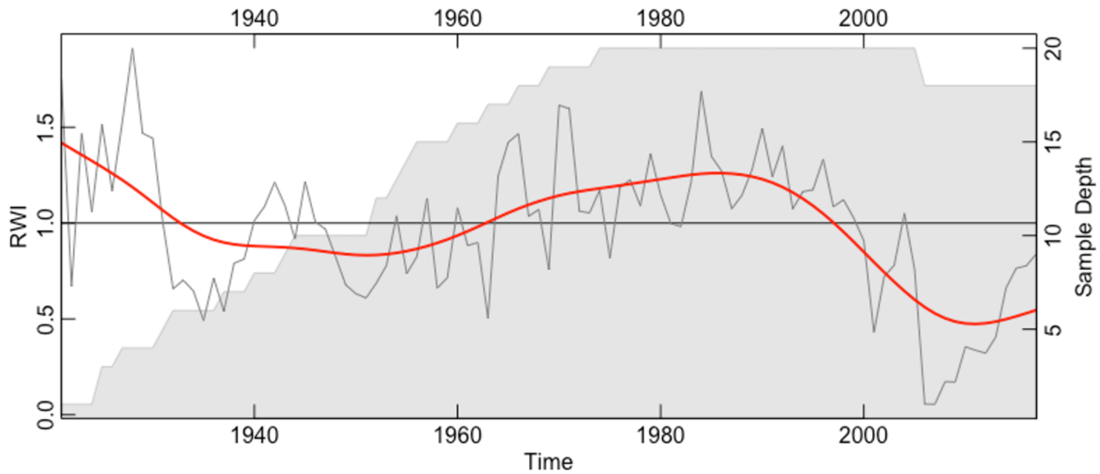

FIGURE 4.10: Ring-width index (RWI) of Gulf State Park *Pinus elliotti* 1921–2017 (gray line). Red line is the 50% spline of the ring-width data within a 10-year moving window. The gray polygon in the background represents the sample depth for that given year.

and growth drops to its lowest point after 2000. During the 2006 season, growth drops to its lowest point within the entire series and gradually increases until 2017. Years with lowest growth include 1935, 1937, 1963, 2001, 2006, and 2007, while highest-growth years include 1928, 1965, 1970–71, and 1984. Substantial TCs brought >2.0 m storm surge to the site during Hurricanes Betsy (1965), Camille (1969), Frederic (1979), Georges (1998), and Katrina-Dennis (2005). Some, but not all, of those TC years correspond with low growth in subsequent years. However, none of the TC years correspond with a dramatic increase in growth the following year.

Strongest moving window correlations show that GSP tree growth agrees with drought measurements, specifically the Palmer Drought Severity Index (PDSI; Figure 4.11). Significant correlations with PDSI are positive, showing that wetter periods correlate with higher growth. Longest interval of significant correlations with PDSI exist for the current year February, but stronger correlations exist for previous year summers (June, July, August). However, all correlations are significant only for moving windows within years 1951–2017. Additionally, the highest correlations exist when years 1998–2006 are included in the analysis.

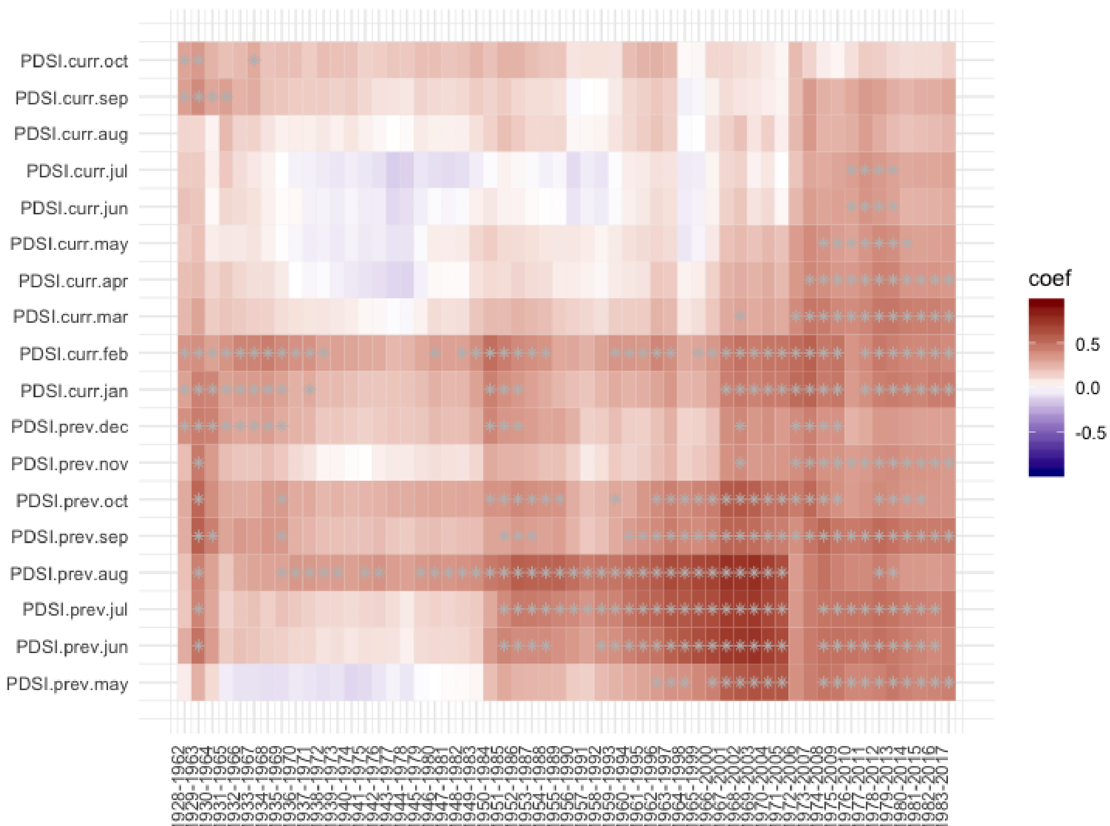

FIGURE 4.11: Moving correlation of Gulf State Park tree-ring width and PDSI 1928–2017. Each square represents the correlation coefficient for that window of time. The vertical axis represents the monthly window of correlation for PDSI. "prev" indicates that month for the previous year, and "curr" indicates that month for the current year. The horizontal axis shows the interval for the window through which the correlation analysis was conducted. Red colors indicate positive correlations, and blue colors indicate negative correlations. A white asterisk indicates statistical significance at $p<0.05$.

Drought indices are based on calculations of incoming and outgoing water availability, and these two factors are often controlled by precipitation and temperature, therefore the GSP tree-ring widths were also compared to precipitation (PCP) and maximum average monthly temperatures (TMAX; Figure 4.12). Correlations with PCP are largely positive, while correlations with TMAX are negative with the exception of positive correlations early in the period of record with current April. Correlations with TMAX are stronger and last through larger portions of the time interval than PCP.

The most stable relationships with PCP exist for winter months (previous December, January, and February). The stability in TMAX relationship exists for summer months for both previous and current year (June, July, and August). High summer temperatures correspond with lower growth for that given year. Earlier in the record, significant TMAX correlations exist for the month of August. Through the period of record the correlation with TMAX shifts earlier in the year. The strongest correlations with TMAX exist in the years 1977–2017 for June.

4.3.3 LaBranche Wetlands

Seventeen *Taxodium distichum* inland tree cores of the available 32 (53%), and nineteen of the available coastal cores (63%) were successfully crossdated for the LaBranche Wetlands for years 1895–2017 (Appendix H). Series intercorrelation and average mean sensitivity for inland trees are r=0.42 and r=0.57, respectively, and r=0.42 and r=0.51 for coastal trees. The two sites follow similar patterns, but the year-to-year variability is slightly lower in the coastal trees. Expressed population signal remains above 0.85 for years 1932–2017.

Tree-ring series for the LaBranche Wetlands do not show a typical negative exponential growth decrease as seen in many tree species in relation to a geometrically-caused age-related growth trend (Figure 4.13). Many individual tree-ring width series show growth increase in 1930s and 1940s. Older trees (established before 1930) show a trend that is not apparent in younger trees. Additionally, after 1994, all series show a decreased variability.

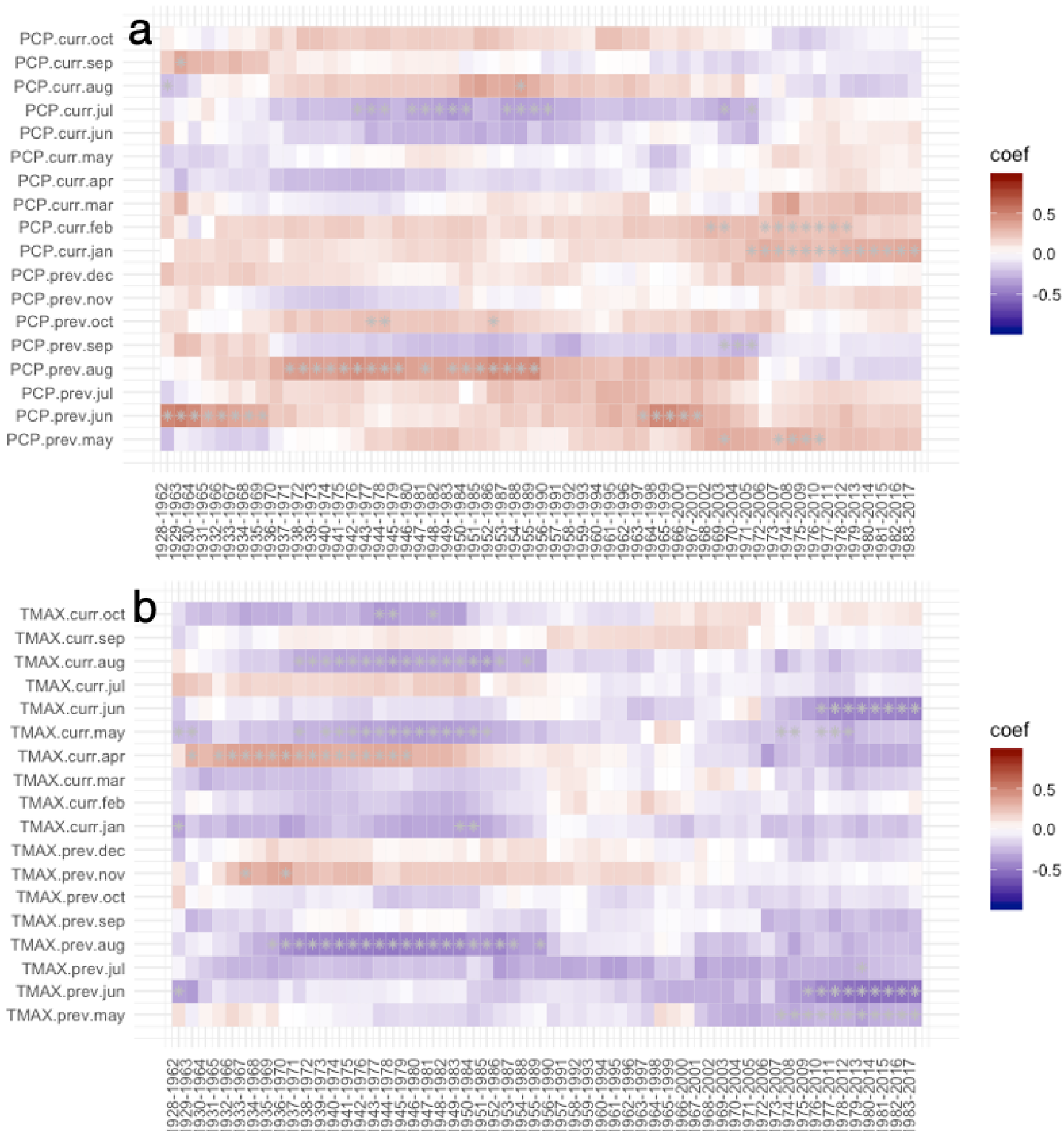

FIGURE 4.12: Moving correlation of Gulf State Park tree-ring width PCP and TMAX 1928–2017. (a) PCP is the monthly precipitation totals, and (b) TMAX is the averaged monthly maximum temperatures. Each square represents the correlation coefficient for that window of time. The vertical axis represents the monthly window of correlation for the climate variables. “prev” indicates that month for the previous year, and “curr” indicates that month for the current year. The horizontal axis shows the interval for the window through which the correlation analysis was conducted. Red colors indicate positive correlations, and blue colors indicate negative correlations. A white asterisk indicates statistical significance at $p<0.05$.

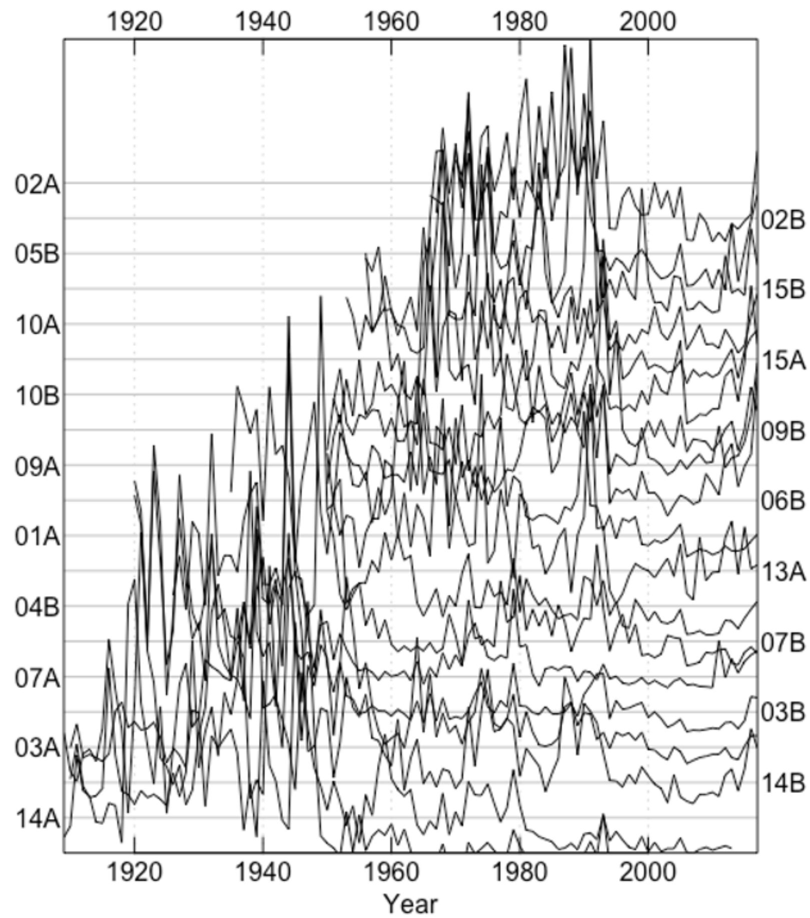

FIGURE 4.13: Raw ring-width index of inland *Taxodium distichum* at LaBranche Wetlands 1910–2018. Each black line represents a series from that site, and they are labelled on the vertical axis.

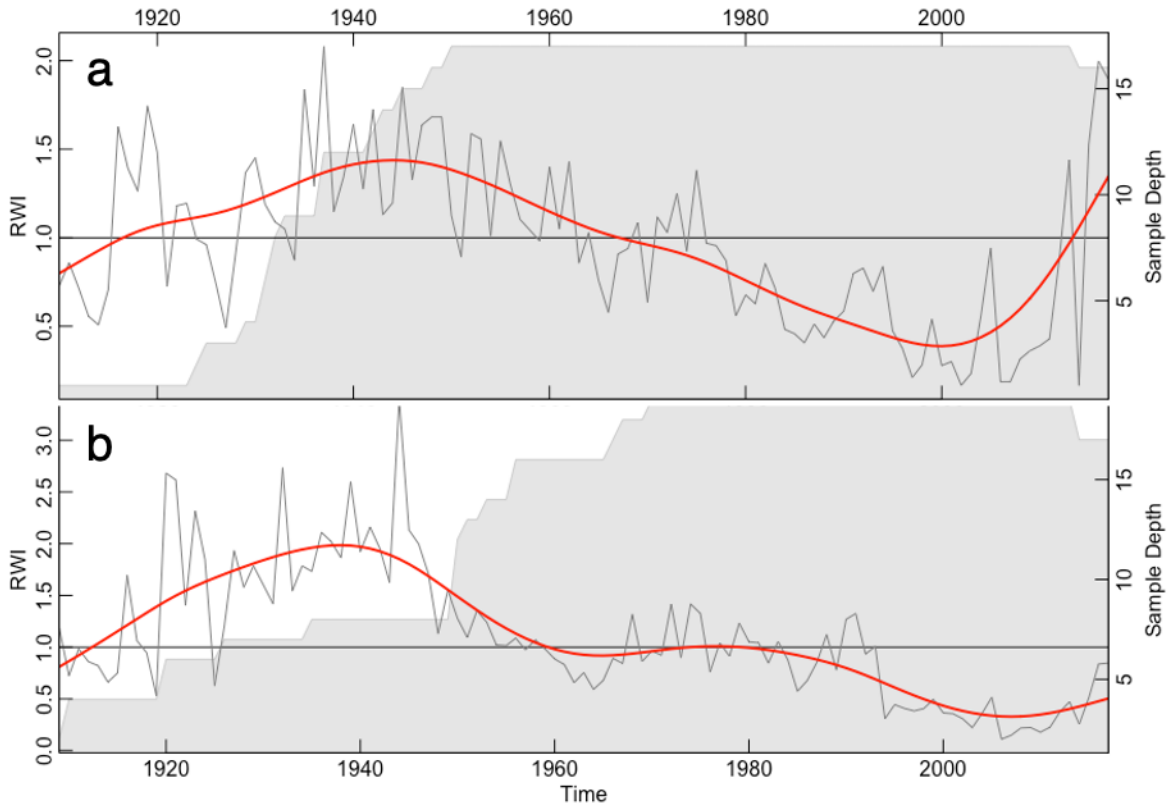

FIGURE 4.14: Ring-width index (RWI) of LaBranche Wetlands *Taxodium distichum* for (a) inland and (b) coastal trees 1973–2018 (gray line). Red line is the 50% spline of the ring-width data within a (a) 10-year and (b) 12-year moving window. The gray polygon in the background represents the sample depth for that given year.

The two sites at LaBranche Wetlands span a similar time interval (1911–2017). An abrupt increase in sample size for the inland site (Figure 4.14a) shows that tree sapling establishment occurred rapidly between 1930–1940, whereas the establishment in the coastal site occurred through a longer time interval. Growth does not follow a typical negative exponential age-related trend. Highest growth rates occur concurrently with highest establishment rates. However, many individual series show growth increases during that period as well, therefore it is assumed that the high growth concurrent with establishment is not due to age-related growth trends. Growth declines through the 1950s and 1960s and hits a low point in 1966 for both sites. Another rapid growth decline occurs through the 1990s with growth falling to its lowest levels in the late 2000s. For both series, growth increases after 2010.

Few correlations exist between LaBranche tree growth and environmental factors, but Mississippi River discharge near the site shows a strong relationship (Figure 4.15). In the early part of the record, the (b) inland trees show significant positive correlations to spring river flooding, but this relationship is not stable through time. However, the coastal site shows significant positive correlations to river flooding throughout the record. The correlation shifts from a summer (June/July) in the early part of the record to winter/spring (January/February) later in the record.

4.4 Discussion

Plant communities for study sites vary widely, but trees at each site correlate to environmental parameters important to coastal tree growth. At the site furthest from the coast (Doyle's Bayou), *Q. nigra* growth shows substantial decreases in growth following years of intense TCs. These trees are too far inland (>100 km) to experience any coastal storm surge flooding. However, wind damage likely affected these trees. In previous research, *Quercus* species show substantially more damage evidence from high wind events than coniferous species, and of those species, *Q. nigra* expresses the most damage Sharitz et al. [1993]; Shirakura et al. [2006]. More specifically, damage during wind events to *Quercus* species was largely the result of limb damage and removal, and largest trees sustained the most damage Gresham et al. [1991]. As limb damage occurs, the tree must first repair its wounds before resuming growth in the stem. At Doyle's Bayou, trees were selected based on their large size, so the trees used in this study were likely heavily affected by high wind speeds from TCs in 1992, 2005, and 2008.

Doyle's Bayou trees are also negatively correlated to summer maximum monthly temperatures, and the large spatial signal shows that weather patterns are likely similar throughout the region (Figure 4.9). Trees from every study site in this Dissertation show a similar relationship. Previous studies have discussed the importance of temperature to moisture stress Wilson and Luckman [2002]; Youngblut and Luckman [2008]; Williams et al. [2013], but few

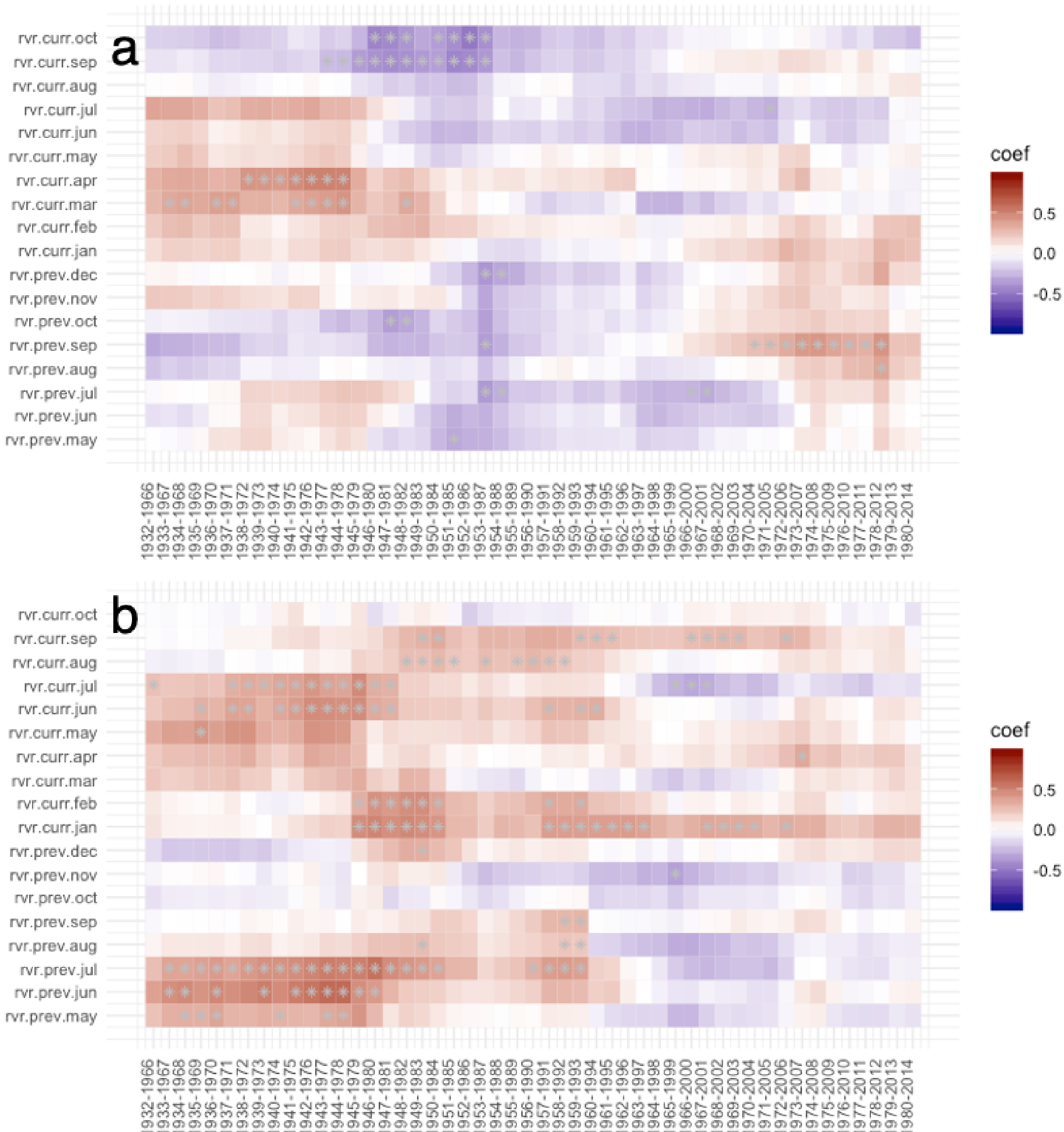

FIGURE 4.15: Moving correlation of *Taxodium distichum* and Mississippi River discharge at the Carrollton gauge for (a) inland and (b) coastal tree-ring width 1932–2017. Each square represents the correlation coefficient for that window of time. The vertical axis represents the monthly window of correlation for the climate variables. "prev" indicates that month for the previous year, and "curr" indicates that month for the current year. The horizontal axis shows the interval for the window through which the correlation analysis was conducted. Red colors indicate positive correlations, and blue colors indicate negative correlations. A white asterisk indicates statistical significance at $p<0.05$.

explored this relationship in the Southeast U.S. Results throughout this Dissertation show that maximum temperatures during the hottest part of the growing season are an important factor driving tree growth in the Southeast U.S.

Largest drops in growth for Gulf State Park *Pinus elliottii* are associated with periods of combined moisture stress and TC occurrences. Previous researchers showed that TCs cause tree growth suppressions in subsequent years Trouet et al. [2016]; Tucker et al. [2017]. After Hurricane Georges in 1998 and Hurricanes Katrina and Dennis in 2005, drought years of 1999–2000 and 2006 occurred. Unlike findings in Tucker et al. [2017], hurricane storm surge measurements alone do not describe other reductions in tree growth at Gulf State Park, but the drop in growth following 2005 is substantially larger than any other drops in growth during the record.

Gulf State Park tree growth shows strong agreement with PDSI in coastal Alabama ($r>0.75$; Figure 4.11). Correlations are only statistically significant for months of analysis in the previous year PDSI values. Studies have shown that tree growth is frequently correlated to precipitation in the previous fall because the precipitation of the previous year is stored in the ground until the trees need it in the following year's growing season Graumlich [1987]; Henderson and Grissino-Mayer [2009]; Martin-Benito et al. [2013].

Further exploring this relationship shows that both precipitation and temperature are important factors to tree growth at Gulf State Park (Figure 4.12). As postulated in previous studies, tree growth is low in soils with low water-holding capacities (*i.e.*, sandy), and those trees are most sensitive to moisture stress Palik and Pederson [1996]; Stephenson [1998]; Mitchell et al. [1999]; Ford and Brooks [2003]. Additionally, high summer temperatures are an important factor of *Pinus elliottii* at other sites in the Southeast U.S. as well Henderson and Grissino-Mayer [2009]; Harley et al. [2011].

LaBranche Wetlands *T. distichum* agree with previous studies that cypress trees are useful for dendrochronological analysis. However, *T. distichum* in this Dissertation show correlations with specific environmental parameters when other sites do not. The interseries correlation for trees in this study is near the range of previous tree-ring research on *T. distichum* ($r \simeq 0.47$) Stahle et al. [1985]. Many tree-ring series in this study show higher correlations during assessment of crossdating accuracy, though those proved to be spurious during visual reanalysis. Ultimately, non-quantitative measurements (*e.g.*, tree-ring color, false ring presence, density fluctuations) were helpful in final crossdating.

The ring-width series of the two different sites (coastal and inland) show similar patterns of growth, and most individual tree-ring series show high growth variability at a young age, but no age-related exponential growth trend emerged for these trees. Growth of *T. distichum* saplings frequently shows the presence of false-rings, and periodically flooded saplings show more growth variability Young et al. [1993]. Additionally, a common signal in the 1990s may also be responsible for a stabilization of tree growth as seen in Figure 4.13. Future dendrochronological analysis on *T. distichum* should focus on false-ring formation to determine if they correspond to specific environmental factors.

Logging evidence at both LaBranche Wetlands sites is prevalent. Large (>1.5 m diameter) snags and stumps are present, and few trees older than 120 years can be found at the sites. Additionally, the Louisiana cypress logging industry would have been active during the late 1800s when the oldest trees appear at LaBranche Wetlands Bull [1949]; Conner et al. [1986]. Growth peaks in the 1930s may indicate young trees that were rapidly taking advantage of low competition at the time. The slower establishment rate of trees at the coastal site may indicate stressful conditions caused by higher salinity levels similar to results of sapling *T. distichum* studies of the past Conner [1994]; Allen et al. [1997].

Unlike previous results, the tree growth at LaBranche Wetlands shows no correlations with TCs, but the coastal site shows strong correlations with Mississippi River discharge (Figure 4.15). Correlations exist most consistently with the months just before the growing season (current January–March) when Mississippi River levels are generally at their highest.

Correlations for the inland site are weaker and less consistent. Previous researchers show that the trees at a coastal site are likely more stressed by salinity than those further inland Raddi et al. [2009], thus the coastal trees may be responding to Mississippi River discharge more than the inland trees because they are more stressed.

Coastal trees at LaBranche Wetlands likely rely more on annual freshwater river flows to displace saltwater from Lake Pontchartrain. However, the Mississippi River has not been connected to coastal forests since the 1930s when its banks received levees. The LaBranche data support a hypothesis that the Mississippi River and its contents have widespread effects in Southern Louisiana. The massive amounts of freshwater, nutrients, and sediments within the Mississippi River get spread throughout the GOM, affecting all hydrology and landscape changes in the region Walker et al. [1994]; Rabalais et al. [2002]; Walker et al. [2005]. In other words, plant growth is not only affected directly by changes in the river, but also indirectly by changing GOM salinity, coastal sea level, and land loss/gain. The trees at LaBranche Wetlands are connected to this system through the estuarine Lake Pontchartrain.

The Mississippi River-Gulf Outlet Canal (MRGO) was built as an effort to create a more efficient pathway for ship traffic to travel from New Orleans to the GOM Freudenburg et al. [2009]. Construction of the MRGO was completed in 1968, and because of ship wake and wind-induced waves, by 2005 it was four times wider than it was constructed van Heerden et al. [2009]. Salinity levels increased dramatically during that time to nearby estuarine Lakes Pontchartrain and Borgne Tate et al. [2002]. Eventually, the MRGO would be blamed for increasing flood heights during Hurricane Katrina brought about by marsh degredation Day et al. [2007]. In 2009, the MRGO was closed to ship traffic, and salinity levels in Lake Pontchartrain decreased Poirrier [2013].

For the trees in this Dissertation, *T. distichum* begins a sharp decline in growth during the 1960s when the MRGO was being constructed and salinity levels began to rise in Lake Pontchartrain. Additionally, the results in this Dissertation show that after 2009 when the

MRGO was closed, tree growth increases, and tree growth reaches a maximum for the entire time interval in 2017 for the inland site (Figure 4.14). A previous study has shown similar effects to trees in nearby Bonnet Carré spillway Day et al. [2012], though that study does not extend to 2009 when recovery likely began.

4.5 Conclusions

Tree-ring chronologies in this Chapter show correlations with important coastal climatic processes. High winds from TCs affect *Quercus nigra* likely due to damage to the crown limbs of trees. Precipitation is an important factor to tree growth at all three sites, but high summer temperatures are equally important to controlling moisture stress at those sites. Freshwater resources are crucial to coastal wetland *Taxodium distichum* at LaBranche Wetlands. Nearby Mississippi River flow is an important part of the incoming freshwater, but anthropogenic modifications can also affect tree growth at the site by influencing salinity.

Conclusions

Results of this Dissertation show that wetland trees in coastal environments have important patterns of growth related to moisture stress, tropical cyclones, and saltwater inundation. The methods used in this Dissertation are generally traditional for tree-ring science, but their application is focused in new areas. Additionally, field methods in these studies have an important impact on analyses between coastal tree growth and environmental controls. The vulnerability of any system (at any scale) is a function of the exposure and sensitivity of that system to any hazardous condition, as well as the ability or capacity of the system to cope with and adapt from the effects of that condition Parry [2002]. Coastal trees are important sentinel species for determining the impact of climatic controls on vegetation and wildlife habitat. This final Chapter discusses major findings, offers suggestions for coastal/wetland land managers, and provides ideas for supplemental work to be completed in the future.

5.1 Research Summary

A wide variety of tree species are used for coastal dendrochronology in this study indicating that coastal tree-ring science relies on the influence of abiotic factors (*e.g.*, moisture stress, TCs). Additionally, year-to-year variability (*i.e.*, average mean sensitivity) for each master chronology is higher than most chronologies in the Southeast U.S. Visual crossdating frequently relied on non-quantitative measures (*e.g.*, ring color, intra-annual density fluctuations, earlywood-latewood fade). Therefore, series intercorrelations were low and crossdating verification aided in removing numerous cores whose growth did not match well with its sisters. However, those tree-ring width series used in final master chronologies showed strong correlation to logical environmental parameters (*e.g.*, precipitation, evaporative summer temperatures).

Coastal trees that are sensitive to their environment are often accompanied by mid- and understory plant species that are salt tolerant. On the Gulf of Mexico coastline, those plants frequently include *Spartina patens*, *Baccharis halimifolia*, and *Juncus roemarianus*. Identifying plants before choosing a study site location is crucial to finding locales that are affected by saltwater inundation. In locations where saltwater stress is high, new species (*e.g.*, *Taxodium ascendens*) may show their usefulness to dendrochronology.

At Grand Bay NERR, *T. ascendens* shows similar growth patters to previously published *Pinus elliottii* located nearby. Tropical cyclones are an important factor to tree growth at the site causing trees to suppress growth in years following intense storm surges (>2.0 m). The stressed *T. ascendens* also shows correlation with factors controlling moisture stress, especially during hottest summer months. Maximum July temperatures likely increase evapotranspiration and plant respiration, which reduces water availability at the site. In contrast, warm Septembers at the site are linked to higher growth, likely due to the fact that a warm autumnal season can extend the growing season.

The nearby *P. elliottii* at Grand Bay NERR added to their value by way of tree-ring carbon isotopic analysis. Tree-ring carbon isotopes at Grand Bay NERR show strong correlation with precipitation near the site, and the relationship extends throughout the region and into South Florida. Further exploring the data showed that both temperature and precipitation are likely responsible for moisture stress to these trees. Tree-ring Δ^{13}C values varied similarly to that of ENSO during the 20-year period. ^{13}C is enriched during strong La Niña events, and little relationship exists for neutral or El Niño conditions.

Finally, three different study sites show important implications for climate stress to tree species occupying different habitats. Doyle's Bayou *Quercus nigra* showed substantial decreases in growth following intense tropical cyclone wind speeds near the site. Gulf State Park *P. elliottii* correlated with PDSI, and LaBranche Wetlands *T. distichum* correlated with Mississippi River discharge. All three sites showed that maximum summer temperatures were equally as important as a lack of precipitation for moisture stress on the trees. LaBranche Wetlands also showed evidence of growth declines during increasing salinities near the site caused by anthropogenic modification, and they show evidence of recovery in the last decade during restoration activities.

5.2 Management Implications

Previous studies agree that hydrologic connectivity in anthropomorphized systems is an important abiotic factor for coastal vegetation growth Turner and Lewis [1996]; Penland et al. [1996]; Day et al. [2000]; Gosselink [2001]; Nyman [2014]. However, studies of coastal wetland vegetation changes suggest conflicting ideas for coastal restoration. Some studies argue that fragmentation is a large source of coastal wetland loss, and the introduction of surface freshwater diversions weaken belowground biomass of herbaceous vegetation and are detrimental to faunal production Turner and Lewis [1996]; Kearney et al. [2011]. Other researchers indicate that freshwater diversions are not detrimental to faunal production and promote a natural gradient of salinity in coastal waters Lane et al. [1999]; Das et al. [2012]; Nyman [2014]. An additional set of studies argue that coastal wetland loss is not sea-level-rise dependent and coastal marshes can keep up with changing sea level Nyman et al. [2006]; Fagherazzi et al. [2013]; Kirwan et al. [2016]. The results of this study show that freshwater resources (or lack thereof) are the most important drivers of growth to coastal trees, especially those stressed by saltwater inundation. During dry years, coastal forested wetlands suffer from increased salts in the soil. Dry years in the Southeast U.S. frequently occur during La Niña years when TC development is high in the region. Diverting surface waters during La Niña years into coastal forested wetlands impacted by saltwater storm surge may improve growing conditions for those trees.

Future management and projections of coastal forest change should concentrate efforts to provide freshwater resources to wetland trees. Management decisions that may increase freshwater resources in wetland areas include river diversions, marsh creation and restoration, and reduction of greenhouse gases. Additional measures should also be taken to reduce and prevent anthropogenic modifications that may increase the flux of saltwater to inland

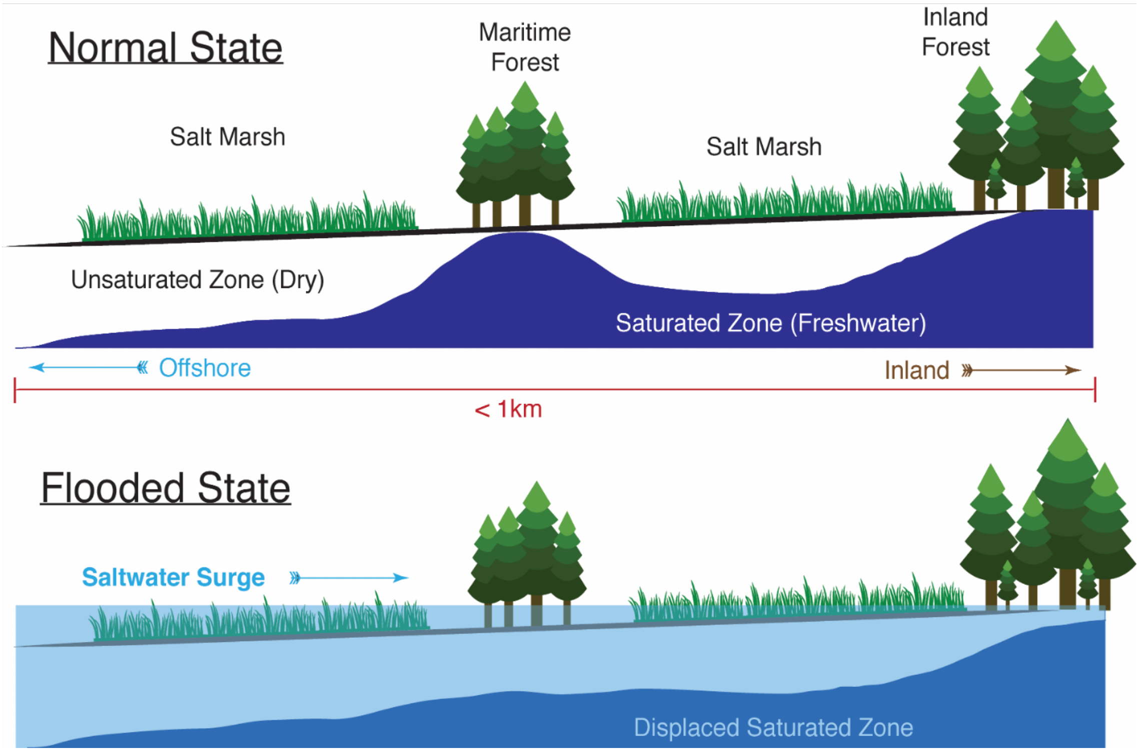

FIGURE 5.1: A hypothetical saltwater stress diagram that represents the stress undergone by a coastal tree in times of saltwater inundation. In the normal state (above), the saturated zone of freshwater undulates and can occasionally be pulled upward by large trees. However, in the flooded state (below), denser saltwater displaces the freshwater, and the trees are forced to exclude any salts left after the surge waters recede and/or evaporate.

locations. Canals that run perpendicular to the shoreline may increase saltwater intrusion to inland areas causing undue stress to coastal trees. Impoundments in one area may also cause trapping of saltwater fluxes in other areas.

5.3 Future Work

As a result of the studies within this Dissertation, I offer a hypothetical framework indicating the reason coastal trees are sensitive to their environment, and I suggest areas for future research. As noted in Fritts [1976] and Speer [2010], stressed trees are the most likely candidates useful for dendrochronological analysis. Throughout this Dissertation, the effects of saltwater inundation have proven to be stressful to tree growth, and a model of stress is described here (Figure 5.1).

In any forested area, trees may wick water to the surface causing undulation in the saturated zone. During storm surge and tidal flow inundation, a freshwater table may be displaced underneath the more dense, saline water. Before trees can wick water again, the displaced freshwater saturated zone needs time to recharge and salts must leach from the saturated zone. This hypothesis is directly related to the freshwater resources that will recharge and leach salts from the soil (*e.g.*, river flow, precipitation, groundwater fluxes). As sea-levels rise, this process will become more frequent and intense. Ultimately, salinity forces trees to be more sensitive to freshwater resources. Therefore, future coastal dendrochronology researchers should focus on areas where saltwater inundation occurs regularly.

Accelerating sea-level rise poses a threat to coastal forested wetlands that cannot withstand saltwater inundation. Maritime dendrochronology can assist projections of coastal vegetation and landscape change by analyzing changes of the past. By studying in areas where relative sea-level rise has been high in the past century, tree ring studies in those regions can provide an analog for other sites where sea-level rise rates will increase. For example, tree-ring data for Mississippi River backswamps can be compared to tree-ring data in Southeast Asia where people rely heavily on estuarine habitats. Additionally, research on coasts where sea-level rise rates are dissimilar to the northern Gulf of Mexico coast may hold insight to changes in different climate change scenarios. For example, trees in the colder Northeast U.S. may be responding to sea-level rise differently since growing seasons are shorter and summer maximum temperatures are lower.

Future work in coastal dendrochronology should also focus on responses to soil moisture. High temperatures during summer months are an important driver of growing season drought, and future climate change scenarios show that global temperatures will continue to warm. Care must also be taken to explain any effects caused by anthropogenic modification. Finding tree species and sites with older trees can provide information of coastal climate stress to pre-industrial levels and will be important for predicting the future effects of rising seas and global temperatures.

Appendix A. Format of Divisional Climate Data

NOAA divisional climate data (nCLIMDIV) used in this study are available through the online portal located at `https://www7.ncdc.noaa.gov/CDO/CDODivisionalSelect.jsp#`. The output indices include precipitation (PCP), average monthly temperature (TAVG), average minimum monthly temperature (TMIN), average maximum monthly temperature (TMAX), Palmer drought severity index (PDSI), Palmer hydrological drought index (PHDI), Palmer z-index (ZNDX), modified Palmer drought severity index (PMDI), cooling degree days (CDD), heating degree days (HDD), and standard precipitation indices averaged by months (SPnn).

Below is a two-year example (January 2017–December 2018) for Climate Division 08 (coastal) in the state of Alabama.

StateCode	Division	YearMonth	PCP	TAVG	PDSI	PHDI	ZNDX	PMDI	CDD	HDD	SP01	SP02	SP03	SP06	SP09	SP12	SP24	TMIN	TMAX
01	08	201701	12.29	58	2.38	2.38	5.6	2.38	71	288	2.28	2.51	1.54	.71	.19	.38	.76	48.1	67.8
01	08	201702	2.74	60.8	-.71	1.42	-2.14	.42	61	179	-.97	1.42	1.85	.24	.13	.31	.8	49.2	72.3
01	08	201703	3.02	63.4	-1.47	-1.47	-2.48	-1.47	84	133	-.94	-1.43	.57	.02	-.17	-.28	.66	52.6	74.3
01	08	201704	4.24	69.3	-1.52	-1.52	-.62	-1.52	150	21	.06	-.65	-1.13	.41	-.11	-.43	.23	57.6	81
01	08	201705	9.79	72.8	1.25	1.25	3.74	1.25	244	0	1.74	1.09	.4	1.28	.34	.28	.53	62.3	83.3
01	08	201706	15.42	78	3.53	3.53	7.23	3.53	390	0	2.27	2.6	2.15	1.89	1.4	1.19	1.18	70.5	85.4
01	08	201707	5.19	81.8	2.76	2.76	-1.2	2.23	521	0	-.63	1.45	1.9	.87	1.48	1.07	1.17	73.3	90.3
01	08	201708	12.14	81	4.02	4.02	4.63	4.02	496	0	2.02	.97	2.2	1.84	2.44	1.43	1.63	72.8	89.2
01	08	201709	1.78	77.1	2.97	2.97	-1.92	2.17	363	0	-1.35	.52	.05	1.88	1.73	1.28	1.44	67.4	86.9
01	08	201710	12.21	70	4.84	4.84	6.53	4.84	179	24	2.35	1.17	2.02	2.84	1.97	2.41	1.8	60.1	80
01	08	201711	.38	60.6	-.79	3.55	-2.36	2.61	41	173	-2.39	1.37	.41	2.14	1.74	2.4	1.49	48.8	72.4
01	08	201712	3.55	52.7	-1.11	2.78	-1.22	1.35	13	394	-.62	-2.11	.9	.62	2	1.93	1.14	43.4	62
01	08	201801	3.08	45.9	-1.29	2.2	-.87	.47	11	603	-.62	-.97	-1.67	.71	1.88	1.08	1.1	34.9	56.9
01	08	201802	6.98	64.2	-.94	2.19	.65	.71	104	126	.87	.19	-.24	.16	1.64	1.47	1.39	55.1	73.2
01	08	201803	3	60.6	-1.59	1.22	-2.25	-.95	48	185	-.94	-.19	-.49	.26	.2	1.44	.88	49.4	71.9
01	08	201804	4.25	63.3	-1.46	1.06	-.08	-1	47	98	.06	-.65	-.18	-1.1	.38	1.43	.72	51.1	75.6
01	08	201805	4.26	76.3	-1.51	.75	-.62	-1.35	350	0	.1	-.05	-.58	-.61	-.3	.99	.85	64.9	87.8
01	08	201806	5.67	81.1	-1.39	.64	-.1	-1.33	483	0	.21	.09	-.04	-.38	.15	.08	.85	72.2	90
01	08	201807	6.41	82.2	-1.51	-1.51	-.78	-1.51	533	0	-.06	-.03	-.05	-.3	-.96	.2	.85	73.4	91.1
01	08	201808	7.38	80.6	.3	-1.05	.9	-.5	484	0	.49	.12	.1	-.46	-.52	-.27	.83	71.8	89.4
01	08	201809	12.59	80.6	1.41	1.41	3.43	1.41	468	0	1.65	1.72	1.34	.83	.36	.71	1.33	72.2	89
01	08	201810	2.51	71.8	1.1	1.1	-.51	.73	225	14	-.12	1.37	1.4	.87	.44	-.21	1.44	61.7	82
01	08	201811	6.79	56.1	1.83	1.83	2.55	1.83	14	281	1.17	.69	1.57	1.33	.56	.4	1.85	45.8	66.5
01	08	201812	10.15	54.6	2.96	2.96	3.96	2.96	19	342	1.85	1.8	1.46	2.01	1.49	1.01	2.14	45.7	63.6

Appendix B. R Program Code for the *dplr* Package

The *dplr* (dendrochronology program library) package in R can perform similar functions to the COFECHA and ARSTAN programs. I have included an example from the Gulf State Park data used in Chapter 4 of this Dissertation. To begin, the user will need to install and require the *dplr* package.

```
> install.packages("dplR")
> require(dplR)
```

When tree-ring measurements have been compiled into the traditional 11-column "Tuscon" or "decadal" format, they can be read into R. For simplification in future analyses, I suggest naming the file, in this case `grow.rwl`.

```
> grow.rwl <- read.tucson(fname = "gsp.txt")
```

Summary data can be accessed for the data using the function `rwl.stats`, which will display first and last years, total years and general descriptive statistics for each ring-width series. A segment plot for all series and skeleton plot for each individual series can be displayed as well.

```
> rwl.stats(grow.rwl)
> seg.plot(grow.rwl)
> skel.plot(grow.rwl[1])
```

Similarly to the "Run Control Options" in COFECHA using the `corr.rwl.seg` function, *dplr* allows the user to (1) set the length and lag of the cubic smoothing spline (`seg.length` and `bin.floor`), (2) choose if the autoregressive model is applied (`prewhiten`), and (3) set a critical p-value (`pcrit`). Other options can be found in Bunn (2008). The function can also plot the series showing where problems might exist in the crossdating.

```
> corr.rwl.seg(rwl = grow.rwl, seg.length = 20,
+ bin.floor = 40, n = NULL, prewhiten = TRUE, pcrit = 0.05,
+ biweight = TRUE, method = c("spearman"), make.plot = TRUE,
+ label.cex = 1, floor.plus1 = FALSE, master = NULL)
```

Finally, the user can acquire the interseries correlations of individual series and mean sensitivity of the master chronology using the following functions. To obtain the interseries correlation for the master chronology, the user simply averages the individual correlations.

```
> interseries.cor(grow.rwl, n = NULL, prewhiten = TRUE,
+ biweight = TRUE, method = "spearman")
> sens1(grow.rwl)
```

The *dplr* package can also be used to detrend tree-ring data using the `detrend` function. The user can choose to detrend with six options for the `method`: “Spline”, “ModNegExp”, “Mean”, “Ar”, “Friedman”, “ModHugershoff”. Again, the user can find descriptive statistics of the detrended data as well.

```
> grow.rwi <- detrend(rwl = grow.rwl, method = c(``Spline"),
+ nyrs = NULL, f = 0.5, pos.slope = FALSE)
> rwi.stats(grow.rwi)
```

The user can also interactively detrend similarly to the function in ARSTAN using the function `i.detrend`. The raw ring widths of each series will be visually displayed along with the same six options for detrending. The user selects the option (1–6) for detrending, and a the next series appears. This process continues until all individual series are interactively detrended.

```
> grow.rwi.int <- i.detrend(rwl = grow.rwl, nyrs = NULL,
+ f = 0.5,pos.slope = FALSE)
```

The detrended data can be built to produce a residual chronology by choosing `prewhiten = TRUE` or a standardized chronology by choosing `prewhiten = FALSE`.

```
> grow.crn <- chron(x = grow.rwi, prefix = "GSP",
+ biweight = TRUE, prewhiten = TRUE)
```

Finally, the standardized chronology can be written to a .CSV file and/or plotted. The plots used in this Dissertation were all created using the presets selected in the following code:

```
> write.csv(grow.crn, file = `"GSPstd.csv")
> crn.plot(crn = grow.crn, add.spline = TRUE, nyrs = NULL,
+ f = 0.5, crn.line.col='grey50',spline.line.col='red',
+ samp.depth.col='grey90', samp.depth.border.col='grey80',
+ crn.lwd=1, spline.lwd=2.0, abline.pos=1, abline.col='black',
+ abline.lty=1,abline.lwd=1,xlab="Time", ylab="RWI")
```

Appendix C. R Program Code for the *TreeClim* Package

The *TreeClim* (tree-climate) package in R allows the user to test for tree growth-climate relationships. We will use the Gulf State Park chronology (`grow.crn`) from the previous *dplr* example. To begin, the user will need to install and require the *TreeClim* package.

```
> install.packages("treeclim")
> require(treeclim)
```

After acquiring the package and loading the tree-ring data, read in climate data. *TreeClim* works well with NOAA Climate Divisional Data available online. An example of the divisional data is available in Appendix G.

```
> climate <- read.csv("AL_Gulf8_Climate.csv", header = TRUE)
```

Using a favorite spreadsheet manager, format the climate data so that state and division columns are removed and the year/month category is split into separate columns. Create a dataframe with a year, month, and climate variable column. In this example, I use the 19^{th} column variable, which is TMAX.

```
> ym <- climate[,1:2]
> var1 <- climate[19]
> clim <- data.frame(c(ym, var1))
```

The final step uses the *TreeClim* `dcc` function to produce moving window correlations similar to Figure 4.12. The `dcc` function requires that the user input a tree-ring chronology and climate parameters. the `selection` option allows the user to set the monthly window of correlations between January (1) and December (12). Negative numbers indicate months of the previous year. The example below uses months previous May–current October. The `method` option allows the user to choose a calculation method: `"correlation"` or `"response"`, and the `dynamic` option allows the user to choose how the correlation is carried out `"static"`, `"moving"`, or `"evolving"`. All figures presented in this Dissertation use `"moving"`. The user can also select the size of the year window and how much to offset the window through the analysis `win_size` and `win_offset`. Finally, the `start_last` function allows the user to start from the earliest year and move forward as is the case of the example below, or to start from the oldest year and move backwards. Additional options are available in Zang and Biondi (2015). Plotting the function will reveal figures similar to Figure 4.12.

```
> resp <- dcc(chrono = grow.crn, climate = clim, selection = -5:10,
+ method = "correlation", dynamic = "moving", win_size = 35,
+ win_offset = 1, start_last = TRUE, ci = 0.05)
> plot(resp)
```

Appendix D. Tree-Ring Carbon Isotope Data

Sample	d13C..	Sample	d13C..	Sample	d13C..	Sample	d13C..
09GB15	-25.50	20GB15	n/a...	23GB15	-25.36	25GB15	-26.09
09GB14	-25.32	20GB14	-26.63	23GB14	-26.34	25GB14	-26.57
09GB13	-25.32	20GB13	-25.68	23GB13	-25.65	25GB13	-26.36
09GB12	-24.12	20GB12	-25.20	23GB12	-24.49	25GB12	-25.85
09GB11	-24.03	20GB11	-24.40	23GB11	-24.08	25GB11	-25.72
09GB10	-25.06	20GB10	-25.38	23GB10	-25.35	25GB10	-26.04
09GB09	-23.55	20GB09	-25.62	23GB09	-24.10	25GB09	-25.95
09GB08	-23.42	20GB08	-24.68	23GB08	-24.16	25GB08	-26.23
09GB07	n/a...	20GB07	-24.50	23GB07	-24.33	25GB07	-26.24
09GB06	n/a...	20GB06	-23.08	23GB06	-23.99	25GB06	-25.16
09GB05	-23.22	20GB05	-23.64	23GB05	-24.80	25GB05	-25.74
09GB04	-23.73	20GB04	-23.85	23GB04	-24.70	25GB04	-25.54
09GB03	-24.17	20GB03	-24.34	23GB03	-24.97	25GB03	-26.10
09GB02	-23.17	20GB02	-24.37	23GB02	-24.46	25GB02	-26.08
09GB01	-25.05	20GB01	-24.77	23GB01	-24.76	25GB01	-25.63
09GB00	-23.52	20GB00	-24.19	23GB00	-23.93	25GB00	-25.23
09GB99	-23.48	20GB99	-23.43	23GB99	-24.25	25GB99	-25.43
09GB98	-23.72	20GB98	-23.86	23GB98	-24.51	25GB98	-25.78
09GB97	-23.60	20GB97	-23.95	23GB97	-24.12	25GB97	-25.28
09GB96	-24.03	20GB96	-24.31	23GB96	-24.36	25GB96	-25.59

Appendix E. COFECHA Output for Doyle's Bayou *Quercus nigra*

```
P R O G R A M     C O F E C H A                                                                         Version 6.06P    30798
-----------------------------------------------------------------------------------------------------------------------------------

 QUALITY CONTROL AND DATING CHECK OF TREE-RING MEASUREMENTS                                                         COF12K.for

 File of DATED series:   DYL.txt

 CONTENTS:

    Part 1:  Title page, options selected, summary, absent rings by series
    Part 2:  Histogram of time spans
    Part 3:  Master series with sample depth and absent rings by year
    Part 4:  Bar plot of Master Dating Series
    Part 5:  Correlation by segment of each series with Master
    Part 6:  Potential problems: low correlation, divergent year-to-year changes, absent rings, outliers
    Part 7:  Descriptive statistics

 RUN CONTROL OPTIONS SELECTED                             VALUE

         1  Cubic smoothing spline 50% wavelength cutoff for filtering
                                                            32 years
         2  Segments examined are                           50 years lagged successively by  25 years
         3  Autoregressive model applied                     A  Residuals are used in master dating series and testing
         4  Series not transformed to logarithms             N
         5  CORRELATION is Pearson (parametric, quantitative)
            Critical correlation, 99% confidence level  0.3281
         6  Master dating series saved                       N
         7  Ring measurements listed                         N
         8  Parts printed                              1234567
         9  Absent rings are omitted from master series and segment correlations  (Y)

 Time span of Master dating series is  1973 to  2018    46 years
 Continuous time span is               1973 to  2018    46 years
 Portion with two or more series is    1975 to  2018    44 years


                                        ****************************************
                                        *C* Number of dated series        8 *C*
                                        *O* Master series 1973 2018   46 yrs *O*
                                        *F* Total rings in all series    309 *F*
                                        *E* Total dated rings checked    307 *E*
                                        *C* Series intercorrelation    0.520 *C*
                                        *H* Average mean sensitivity   0.274 *H*
                                        *A* Segments, possible problems    0 *A*
                                        *** Mean length of series      38.0 ***
                                        ****************************************

 ABSENT RINGS listed by SERIES:           (See Master Dating Series for absent rings listed by year)
```

```
              No ring measurements of zero value
PART 2:  TIME PLOT OF TREE-RING SERIES:                                                       17:58  Fri 26 Apr 2019  Page   2
------------------------------------------------------------------------------------------------------------------------------------
 1050 1100 1150 1200 1250 1300 1350 1400 1450 1500 1550 1600 1650 1700 1750 1800 1850 1900 1950 2000 2050 Ident   Seq Time-span  Yrs
   :    :    :    :    :    :    :    :    :    :    :    :    :    :    :    :    :    :    :    :    : -------- --- ---- ---- ----
   .    .    .    .    .    .    .    .    .    .    .    .    .    .    .    .    .    .    .  <==>   . 03A        1 1983 2018   36
   .    .    .    .    .    .    .    .    .    .    .    .    .    .    .    .    .    .    . <===>   . 05A        2 1975 2018   44
   .    .    .    .    .    .    .    .    .    .    .    .    .    .    .    .    .    .    .  <==>   . 05B        3 1987 2018   32
   .    .    .    .    .    .    .    .    .    .    .    .    .    .    .    .    .    .    . <===>   . 06A        4 1975 2018   44
   .    .    .    .    .    .    .    .    .    .    .    .    .    .    .    .    .    .    .  <==>   . 06B        5 1982 2018   37
   .    .    .    .    .    .    .    .    .    .    .    .    .    .    .    .    .    .    .  <==>   . 08A        6 1984 2018   35
   .    .    .    .    .    .    .    .    .    .    .    .    .    .    .    .    .    .    .  <==>   . 08B        7 1984 2018   35
   .    .    .    .    .    .    .    .    .    .    .    .    .    .    .    .    .    .    . <===>   . 09B        8 1973 2018   46
   :    :    :    :    :    :    :    :    :    :    :    :    :    :    :    :    :    :    :    :    :
 1050 1100 1150 1200 1250 1300 1350 1400 1450 1500 1550 1600 1650 1700 1750 1800 1850 1900 1950 2000 2050
PART 3:  Master Dating Series:                                                                17:58  Fri 26 Apr 2019  Page   3
------------------------------------------------------------------------------------------------------------------------------------
  Year  Value  No Ab    Year  Value  No Ab    Year  Value  No Ab    Year  Value  No Ab    Year  Value  No Ab    Year  Value  No Ab
  ------------------    ------------------    ------------------    ------------------    ------------------    ------------------
                        2000  0.950   8
                        2001  1.595   8
                        2002  1.795   8
                        2003  0.819   8
                        2004 -0.505   8
                        2005 -0.438   8
                        2006 -1.988   8
                        2007 -0.292   8
                        2008 -0.925   8
                        2009 -1.951   8

                        2010 -1.387   8
                        2011 -0.896   8
                        2012  0.602   8
                        2013  0.158   8
                        2014  1.067   8
                        2015  0.571   8
                        2016  0.658   8
                        2017  1.181   8
                        2018  0.434   8




  1973  1.614   1
  1974  1.291   1
  1975  1.282   3
  1976  0.113   3
  1977 -0.613   3
  1978 -0.288   3
```

```
  1979 -1.581   3

  1980 -1.130   3
  1981 -0.238   3
  1982  0.201   4
  1983 -1.136   5
  1984  0.715   7
  1985  0.540   7
  1986  0.463   7
  1987  0.197   8
  1988 -0.302   8
  1989  0.837   8

  1990  0.239   8
  1991 -0.180   8
  1992  0.351   8
  1993 -2.455   8
  1994  0.266   8
  1995 -0.765   8
  1996 -0.322   8
  1997  1.015   8
  1998 -1.146   8
  1999 -0.419   8
-------------------------------------------------------------------------------------------------------------------------------
PART 4:  Master Bar Plot:                                                                            17:58  Fri 26 Apr 2019  Page   4
-------------------------------------------------------------------------------------------------------------------------------
   Year Rel value  Year Rel value  Year Rel value  Year Rel value  Year Rel value  Year Rel value  Year Rel value  Year Rel value
                   2000--------D
                   2001----------F
                   2002----------G
                   2003--------C
                   2004---b
                   2005---b
                   2006h
                   2007---a
                   2008--d
                   2009h
                   2010-f
                   2011--d
                   2012-------B
                   2013-----A
                   2014---------D
                   2015-------B
                   2016-------C
                   2017---------E
                   2018------B



   1973----------F
```

```
1974---------E
1975---------E
1976-----@
1977--b
1978---a
1979f
1980-e
1981----a
1982-----A
1983-e
1984--------C
1985-------B
1986-------B
1987-----A
1988---a
1989--------C
1990-----A
1991----a
1992------A
1993j
1994-----A
1995--c
1996---a
1997---------D
1998-e
1999---b
```


PART 5: CORRELATION OF SERIES BY SEGMENTS: 17:58 Fri 26 Apr 2019 Page 5

Correlations of 50-year dated segments, lagged 25 years
Flags: A = correlation under 0.3281 but highest as dated; B = correlation higher at other than dated position

Seq	Series	Time_span	1975 2024
1	03A	1983 2018	.63
2	05A	1975 2018	.43
3	05B	1987 2018	.59
4	06A	1975 2018	.49
5	06B	1982 2018	.52
6	08A	1984 2018	.56
7	08B	1984 2018	.48
8	09B	1973 2018	.49
Av segment correlation			0.52

PART 6: POTENTIAL PROBLEMS: 17:58 Fri 26 Apr 2019 Page 5

For each series with potential problems the following diagnostics may appear:

[A] Correlations with master dating series of flagged 50-year segments of series filtered with 32-year spline, at every point from ten years earlier (-10) to ten years later (+10) than dated

```
[B] Effect of those data values which most lower or raise correlation with master series
    Symbol following year indicates value in series is greater (>) or lesser (<) than master series value

[C] Year-to-year changes very different from the mean change in other series

[D] Absent rings (zero values)

[E] Values which are statistical outliers from mean for the year
===================================================================================================================

03A      1983 to  2018     36 years                                                                    Series   1

[B] Entire series, effect on correlation ( 0.628) is:
      Lower   2017<-0.039   2012<-0.032   1997<-0.021   2000<-0.017   2016>-0.016   1986<-0.013  Higher   1993 0.075   2009 0.025

===================================================================================================================

05A      1975 to  2018     44 years                                                                    Series   2

[B] Entire series, effect on correlation ( 0.432) is:
      Lower   1977>-0.133   1983>-0.019   1990<-0.017   1988<-0.017   1981<-0.017   1984<-0.016  Higher   1993 0.080   1979 0.027

[E] Outliers     1   3.0 SD above or -4.5 SD below mean for year
      1977 +3.6 SD
===================================================================================================================

05B      1987 to  2018     32 years                                                                    Series   3

[B] Entire series, effect on correlation ( 0.595) is:
      Lower   1992>-0.059   2012<-0.050   2013>-0.037   1999<-0.020   2001<-0.018   1990>-0.014  Higher   1993 0.034   2006 0.033

[E] Outliers     1   3.0 SD above or -4.5 SD below mean for year
      1992 +3.2 SD
===================================================================================================================

06A      1975 to  2018     44 years                                                                    Series   4

[B] Entire series, effect on correlation ( 0.489) is:
      Lower   2017<-0.063   1977<-0.051   1976>-0.050   1990<-0.037   2003<-0.016   2018>-0.013  Higher   1993 0.044   2006 0.036

===================================================================================================================

06B      1982 to  2018     37 years                                                                    Series   5

[B] Entire series, effect on correlation ( 0.523) is:
      Lower   1990<-0.030   2016<-0.026   1982>-0.025   1986<-0.025   1999>-0.018   1988>-0.016  Higher   2006 0.040   2009 0.040

===================================================================================================================

08A      1984 to  2018     35 years                                                                    Series   6
```

```
 [B] Entire series, effect on correlation ( 0.558) is:
      Lower   2005>-0.047   1990>-0.044   1985<-0.036   1989<-0.025   2013<-0.021   2010>-0.018  Higher   2009 0.061   2006 0.041

=====================================================================================================================================

 08B       1984 to  2018      35 years                                                                                    Series   7

 [B] Entire series, effect on correlation ( 0.478) is:
      Lower   1990>-0.103   1984<-0.038   2002<-0.024   2000<-0.018   2013<-0.018   2015<-0.014  Higher   1993 0.097   2006 0.058

 [E] Outliers     2   3.0 SD above or -4.5 SD below mean for year
      1990 +3.9 SD;    2012 +3.0 SD
=====================================================================================================================================

 09B       1973 to  2018      46 years                                                                                    Series   8

 [*] Early part of series cannot be checked from 1973 to 1974 -- not matched by another series

 [B] Entire series, effect on correlation ( 0.493) is:
      Lower   1982<-0.070   2014<-0.050   2002<-0.047   1988>-0.021   1981>-0.016   1978>-0.010  Higher   2009 0.041   1993 0.034

=====================================================================================================================================

 [*] All segments correlate highest as dated with correlation with master series over  0.3281
PART 7:  DESCRIPTIVE STATISTICS:                                                                   17:58  Fri 26 Apr 2019  Page   6
-------------------------------------------------------------------------------------------------------------------------------------

                                                  Corr   //-------- Unfiltered --------\\  //---- Filtered -----\\
                          No.    No.    No.       with   Mean   Max     Std   Auto   Mean   Max     Std   Auto  AR
 Seq Series   Interval   Years  Segmt  Flags   Master  msmt   msmt     dev   corr   sens  value     dev   corr  ()
 --- -------- ---------  -----  -----  -----   ------ -----  -----   -----  -----  -----  -----   -----  -----  --
   1 03A      1983 2018     36      1      0    0.628  4.67  12.47  2.358  0.520  0.323   0.99  0.417 -0.022   1
   2 05A      1975 2018     44      1      0    0.432  5.07   9.04  1.836  0.696  0.232   0.62  0.317 -0.060   1
   3 05B      1987 2018     32      1      0    0.595  3.90   7.14  1.581  0.716  0.256   0.61  0.286  0.002   1
   4 06A      1975 2018     44      1      0    0.489  4.41   8.07  1.693  0.615  0.278   0.61  0.362 -0.010   1
   5 06B      1982 2018     37      1      0    0.523  3.93   8.87  1.934  0.648  0.391   1.25  0.456 -0.038   1
   6 08A      1984 2018     35      1      0    0.558  3.49  11.60  2.600  0.839  0.309   0.55  0.271 -0.101   3
   7 08B      1984 2018     35      1      0    0.478  6.51  15.67  4.096  0.909  0.228   0.65  0.264  0.018   1
   8 09B      1973 2018     46      1      0    0.493  4.09  11.10  2.423  0.932  0.197   0.46  0.211  0.029   1
 --- -------- ---------  -----  -----  -----   ------ -----  -----   -----  -----  -----  -----   -----  -----  --
 Total or mean:            309      8      0    0.520  4.51  15.67  2.292  0.736  0.274   1.25  0.321 -0.022

                                              - = [  COFECHA DYL COF  ] = -
```

Appendix F. COFECHA Output for Gulf State Park *Pinus elliottii*

```
P R O G R A M     C O F E C H A                                                                          Version 6.02P       0
---------------------------------------------------------------------------------------------------------------------------------

QUALITY CONTROL AND DATING CHECK OF TREE-RING MEASUREMENTS                                                    cofechaOSX_pjk2012.f

File of DATED series:   GSP.txt

CONTENTS:

   Part 1:  Title page, options selected, summary, absent rings by series
   Part 2:  Histogram of time spans
   Part 3:  Master series with sample depth and absent rings by year
   Part 4:  Bar plot of Master Dating Series
   Part 5:  Correlation by segment of each series with Master
   Part 6:  Potential problems: low correlation, divergent year-to-year changes, absent rings, outliers
   Part 7:  Descriptive statistics

RUN CONTROL OPTIONS SELECTED                             VALUE

        1  Cubic smoothing spline 50% wavelength cutoff for filtering
                                                           32 years
        2  Segments examined are                           50 years lagged successively by  25 years
        3  Autoregressive model applied                     A  Residuals are used in master dating series and testing
        4  Series not transformed to logarithms             N
        5  CORRELATION is Pearson (parametric, quantitative)
           Critical correlation, 99% confidence level  0.3281
        6  Master dating series saved                       N
        7  Ring measurements listed                         N
        8  Parts printed                              1234567
        9  Absent rings are omitted from master series and segment correlations  (Y)

Time span of Master dating series is  1921 to  2017    97 years
Continuous time span is               1921 to  2017    97 years
Portion with two or more series is    1925 to  2017    93 years

                                       ****************************************
                                       *C* Number of dated series        20 *C*
                                       *O* Master series 1921 2017   97 yrs *O*
                                       *F* Total rings in all series   1410 *F*
                                       *E* Total dated rings checked   1406 *E*
                                       *C* Series intercorrelation    0.554 *C*
                                       *H* Average mean sensitivity   0.383 *H*
                                       *A* Segments, possible problems    6 *A*
                                       *** Mean length of series      70.0 ***
                                       ****************************************

ABSENT RINGS listed by SERIES:           (See Master Dating Series for absent rings listed by year)
```

```
03A         3 absent rings:   2006  2007  2008
03B         3 absent rings:   2006  2007  2008
04B         2 absent rings:   2007  2008
05A         1 absent rings:   2006
05B         1 absent rings:   2006
07B         2 absent rings:   2006  2007
09A         1 absent rings:   2007
09B         2 absent rings:   2006  2007
11B         2 absent rings:   2006  2007
12A         3 absent rings:   2006  2007  2008
12B         1 absent rings:   2007
15A         1 absent rings:   2006

           22 absent rings   1.560%
PART 2:  TIME PLOT OF TREE-RING SERIES:                                                      Sun   Page   2
-----------------------------------------------------------------------------------------------------------------------------------
                                                                                                                 Beg  End
1000      1100      1200      1300      1400      1500      1600      1700      1800      1900      2000 Ident     Seq year year  Yrs
  :    :    :    :    :    :    :    :    :    :    :    :    :    :    :    :    :    :    :    :    : -------- --- ---- ---- ----
  .    .    .    .    .    .    .    .    .    .    .    .    .    .    .    .    .    .    . <======== 03A        1 1921 2017   97
  .    .    .    .    .    .    .    .    .    .    .    .    .    .    .    .    .    .    .  <======= 03B        2 1931 2017   87
  .    .    .    .    .    .    .    .    .    .    .    .    .    .    .    .    .    .    .    <===== 04A        3 1956 2017   62
  .    .    .    .    .    .    .    .    .    .    .    .    .    .    .    .    .    .    .    <===== 04B        4 1955 2017   63
  .    .    .    .    .    .    .    .    .    .    .    .    .    .    .    .    .    .    .   <====== 05A        5 1943 2017   75
  .    .    .    .    .    .    .    .    .    .    .    .    .    .    .    .    .    .    .    <===== 05B        6 1952 2017   66
  .    .    .    .    .    .    .    .    .    .    .    .    .    .    .    .    .    .    .    .<==== 07A        7 1963 2017   55
  .    .    .    .    .    .    .    .    .    .    .    .    .    .    .    .    .    .    .    <===== 07B        8 1954 2017   64
  .    .    .    .    .    .    .    .    .    .    .    .    .    .    .    .    .    .    .    <===== 09A        9 1952 2017   66
  .    .    .    .    .    .    .    .    .    .    .    .    .    .    .    .    .    .    .   <====== 09B       10 1944 2017   74
  .    .    .    .    .    .    .    .    .    .    .    .    .    .    .    .    .    .    .    .<==== 10A       11 1966 2017   52
  .    .    .    .    .    .    .    .    .    .    .    .    .    .    .    .    .    .    .    .<==== 10B       12 1969 2017   49
  .    .    .    .    .    .    .    .    .    .    .    .    .    .    .    .    .    .    .    .<==== 11A       13 1960 2017   58
  .    .    .    .    .    .    .    .    .    .    .    .    .    .    .    .    .    .    .    . <=== 11B       14 1974 2017   44
  .    .    .    .    .    .    .    .    .    .    .    .    .    .    .    .    .    .    .   <====== 12A       15 1940 2017   78
  .    .    .    .    .    .    .    .    .    .    .    .    .    .    .    .    .    .    .  <======= 12B       16 1932 2017   86
  .    .    .    .    .    .    .    .    .    .    .    .    .    .    .    .    .    .    . <======== 15A       17 1925 2017   93
  .    .    .    .    .    .    .    .    .    .    .    .    .    .    .    .    .    .    .  <======= 15B       18 1937 2017   81
  .    .    .    .    .    .    .    .    .    .    .    .    .    .    .    .    .    .    . <=======> 16A       19 1925 2005   81
  .    .    .    .    .    .    .    .    .    .    .    .    .    .    .    .    .    .    . <=======> 16B       20 1927 2005   79
PART 3:  Master Dating Series:                                                               Sun   Page   3
-----------------------------------------------------------------------------------------------------------------------------------
 Year  Value   No Ab    Year  Value   No Ab    Year  Value   No Ab    Year  Value   No Ab    Year  Value   No Ab    Year  Value   No Ab
 -------------------    -------------------    -------------------    -------------------    -------------------    -------------------
                                                                                                                    1950 -1.337*  10
                                                                                                                    1951 -1.600*  10
                                                                                                                    1952 -0.899   12
                                                                                                                    1953 -0.493   12
                                                                                                                    1954  1.012   13
                                                                                                                    1955 -0.394   14
                                                                                                                    1956 -0.115   15
```

PART 3: Master Dating Series: Sun Page 4

Year	Value	No Ab	Year	Value	No Ab	Year	Value	No Ab	Year	Value	No Ab	Year	Value	No Ab	Year	Value	No Ab
															1957	1.222	15
															1958	-1.111*	15
															1959	-0.870	15
															1960	0.746	16
															1961	-0.444	16
															1962	-0.283	16
															1963	-2.021*	17
															1964	0.804	17
															1965	1.369	17
															1966	1.373	18
															1967	-0.278	18
															1968	0.093	18
															1969	-1.205*	19
															1970	1.587	19
												1921	1.538	1	1971	1.340	19
												1922	-2.115*	1	1972	-0.278	19
												1923	0.873	1	1973	-0.799	19
												1924	-0.482	1	1974	0.122	20
												1925	0.339	3	1975	-1.410*	20
												1926	-0.448	3	1976	-0.076	20
												1927	0.355	4	1977	0.219	20
												1928	1.877	4	1978	-0.583	20
												1929	0.467	4	1979	0.577	20
												1930	0.945	4	1980	-0.247	20
												1931	-0.054	5	1981	-1.010*	20
												1932	-0.823	6	1982	-1.138*	20
												1933	-0.837	6	1983	-0.137	20
												1934	-1.072*	6	1984	1.937	20
												1935	-1.871*	6	1985	0.370	20
												1936	-0.714	6	1986	0.294	20
												1937	-1.721*	7	1987	-0.734	20
												1938	0.300	7	1988	-0.457	20
												1939	-0.193	7	1989	0.370	20
												1940	0.799	8	1990	1.340	20
												1941	0.998	8	1991	0.049	20
												1942	1.569	8	1992	0.959	20
												1943	0.879	9	1993	-0.536	20
												1944	-0.020	10	1994	0.191	20
												1945	1.455	10	1995	0.309	20
												1946	0.666	10	1996	1.284	20
												1947	0.458	10	1997	0.138	20
												1948	-0.045	10	1998	0.754	20
												1949	-0.617	10	1999	0.364	20

2000	0.112	20	
2001	-1.714*	20	
2002	-0.358	20	
2003	0.151	20	
2004	1.642	20	
2005	0.432	20	
2006	-1.186*	18	9
2007	-2.045*	18	9
2008	-1.721*	18	4
2009	-1.601*	18	
2010	-0.585	18	
2011	-0.515	18	
2012	-0.298	18	
2013	-0.129	18	
2014	0.643	18	
2015	1.092	18	
2016	1.143	18	
2017	2.062*	18	

```
------------------------------------------------------------------------------------------------------------------------------------
PART 5:  CORRELATION OF SERIES BY SEGMENTS:                                                                       Sun   Page   5
------------------------------------------------------------------------------------------------------------------------------------
Correlations of  50-year dated segments, lagged  25 years
Flags:  A = correlation under  0.3281 but highest as dated;  * = correlation higher at other than dated position

Seq Series  Time_span   1925 1950 1975
                        1974 1999 2024
--- -------- ---------  ---- ---- ---- ---- ---- ---- ---- ---- ---- ---- ---- ---- ---- ---- ---- ---- ---- ---- ---- ----
  1 03A      1921 2017   .70  .65  .55
  2 03B      1931 2017   .68  .56  .53
  3 04A      1956 2017        .56  .52
  4 04B      1955 2017        .56  .58
  5 05A      1943 2017   .79  .74  .67
  6 05B      1952 2017        .69  .65
  7 07A      1963 2017        .50  .48
  8 07B      1954 2017        .64  .59
  9 09A      1952 2017        .68  .68
 10 09B      1944 2017   .65  .73  .72
 11 10A      1966 2017        .34* .33*
 12 10B      1969 2017        .23*
 13 11A      1960 2017        .31* .36
 14 11B      1974 2017        .67
 15 12A      1940 2017   .50  .47  .44
 16 12B      1932 2017   .49  .54  .50
 17 15A      1925 2017   .25* .23A .34
 18 15B      1937 2017   .35  .47  .62
 19 16A      1925 2005   .70  .73  .71
 20 16B      1927 2005   .40  .71  .72
Av segment correlation  0.55 0.55 0.56
PART 6:  POTENTIAL PROBLEMS:                                                                                      Sun   Page   5
------------------------------------------------------------------------------------------------------------------------------------

For each series with potential problems the following diagnostics may appear:

[A] Correlations with master dating series of flagged  50-year segments of series filtered with  32-year spline,
    at every point from ten years earlier (-10) to ten years later (+10) than dated

[*] Early part of series cannot be checked from 1921 to 1924 -- not matched by another series

====================================================================================================================================

10A       1966 to  2017

[A] Segment    High   -10   -9   -8   -7   -6   -5   -4   -3   -2   -1    0   +1   +2   +3   +4   +5   +6   +7   +8   +9  +10
   ---------   ----   ---  ---  ---  ---  ---  ---  ---  ---  ---  ---  ---  ---  ---  ---  ---  ---  ---  ---  ---  ---  ---
   1966 2015    -1    .04 -.01 -.19  .22  .08 -.01 -.11 -.13  .00  .37* .34| .06  .02    -    -    -    -    -    -    -    -
   1968 2017    -1    .03 -.05 -.18  .22  .06  .00 -.12 -.10 -.01  .37* .33|   -    -    -    -    -    -    -    -    -    -
```

```
===================================================================================================
10B       1969 to  2017

[A] Segment   High   -10   -9   -8   -7   -6   -5   -4   -3   -2   -1    0   +1   +2   +3   +4   +5   +6   +7   +8   +9  +10
   ---------  ----   ---  ---  ---  ---  ---  ---  ---  ---  ---  ---  ---  ---  ---  ---  ---  ---  ---  ---  ---  ---  ---
   1969 2017   -7    .11 -.18  .04  .26*-.03 -.18 -.15 -.28  .02  .24  .23|   -    -    -    -    -    -    -    -    -    -
===================================================================================================
11A       1960 to  2017

[A] Segment   High   -10   -9   -8   -7   -6   -5   -4   -3   -2   -1    0   +1   +2   +3   +4   +5   +6   +7   +8   +9  +10
   ---------  ----   ---  ---  ---  ---  ---  ---  ---  ---  ---  ---  ---  ---  ---  ---  ---  ---  ---  ---  ---  ---  ---
   1960 2009    2    .17 -.25  .05 -.02  .30 -.14  .10 -.16  .05  .06  .31| .10  .42*-.13 -.17  .04  .02 -.01  .16    -    -
===================================================================================================
15A       1925 to  2017

[A] Segment   High   -10   -9   -8   -7   -6   -5   -4   -3   -2   -1    0   +1   +2   +3   +4   +5   +6   +7   +8   +9  +10
   ---------  ----   ---  ---  ---  ---  ---  ---  ---  ---  ---  ---  ---  ---  ---  ---  ---  ---  ---  ---  ---  ---  ---
   1925 1974   -1      -    -    -    -    -    - -.17 -.20 -.04  .35* .25| .08  .19  .01  .20  .10  .11 -.24 -.27 -.19 -.08
   1950 1999    0    .07 -.32  .08  .10  .18 -.09  .02 -.35  .19  .22  .23*-.20  .18 -.14  .19  .08  .22 -.13 -.05 -.05  .06
===================================================================================================
PART 7:  DESCRIPTIVE STATISTICS:                                                       Sun   Page   6
---------------------------------------------------------------------------------------------------

                                                Corr   //-------- Unfiltered --------\\  //---- Filtered -----\\
                          No.    No.    No.    with   Mean    Max     Std    Auto   Mean   Max     Std   Auto  AR
Seq Series   Interval   Years  Segmt  Flags   Master  msmt   msmt     dev    corr   sens  value    dev   corr  ()
--- -------- ---------  -----  -----  -----   ------ -----  -----  -----   -----  -----  -----  -----  -----  --
  1 03A      1921 2017     97      3      0    0.628  1.31   4.01  0.831   0.666  0.375   1.59  0.462 -0.031   1
  2 03B      1931 2017     87      3      0    0.613  1.51   3.53  0.782   0.607  0.365   1.44  0.520 -0.016   1
  3 04A      1956 2017     62      2      0    0.590  2.22   5.61  1.380   0.751  0.435   1.28  0.527  0.010   1
  4 04B      1955 2017     63      2      0    0.618  2.67   8.49  1.670   0.709  0.451   1.24  0.394  0.049   1
  5 05A      1943 2017     75      3      0    0.723  2.26   5.65  1.348   0.744  0.383   3.49  1.300  0.026   1
  6 05B      1952 2017     66      2      0    0.709  2.76   6.30  1.613   0.678  0.422   3.59  1.198  0.011   1
  7 07A      1963 2017     55      2      0    0.521  2.82   6.24  1.520   0.727  0.323   1.07  0.424 -0.001   1
  8 07B      1954 2017     64      2      0    0.656  2.41   5.93  1.373   0.716  0.364   1.28  0.491  0.008   1
  9 09A      1952 2017     66      2      0    0.725  2.40   5.65  1.275   0.679  0.382   1.10  0.465  0.049   1
 10 09B      1944 2017     74      3      0    0.658  2.20   4.78  1.153   0.709  0.337   0.91  0.394 -0.003   2
 11 10A      1966 2017     52      2      2    0.338  2.12   4.96  1.279   0.536  0.489   1.62  0.566  0.009   2
 12 10B      1969 2017     49      1      1    0.233  2.75   6.88  1.454   0.459  0.429   1.14  0.472  0.011   1
 13 11A      1960 2017     58      2      1    0.313  2.43   4.89  1.062   0.600  0.384   0.60  0.357 -0.022   2
 14 11B      1974 2017     44      1      0    0.702  2.13   4.15  1.006   0.668  0.402   0.71  0.404 -0.004   2
 15 12A      1940 2017     78      3      0    0.536  1.62   4.98  1.110   0.611  0.477   1.48  0.544  0.024   1
 16 12B      1932 2017     86      3      0    0.511  2.01   6.01  1.413   0.632  0.468   2.69  0.867  0.057   1
 17 15A      1925 2017     93      3      2    0.315  2.01   5.88  1.147   0.768  0.339   0.82  0.384  0.027   2
 18 15B      1937 2017     81      3      0    0.420  2.69   4.74  0.968   0.730  0.238   0.60  0.267 -0.007   3
```

19	16A	1925	2005	81	3	0	0.723	2.30	7.27	1.136	0.579	0.398	1.05	0.412	-0.017	2
20	16B	1927	2005	79	3	0	0.482	2.48	6.96	0.993	0.582	0.278	0.95	0.341	0.031	1
Total or mean:				1410	48	6	0.554	2.21	8.49	1.202	0.661	0.383	3.59	0.542	0.010	

- = [COFECHA GSP COF] = -

Appendix G. COFECHA Output for LaBranche Wetlands Inland and Coastal *Taxodium distichum*

```
P R O G R A M     C O F E C H A                                                                  Version 6.06P    30816
-----------------------------------------------------------------------------------------------------------------------

 QUALITY CONTROL AND DATING CHECK OF TREE-RING MEASUREMENTS                                          COF12K.for

 File of DATED series:   Inland.txt

 CONTENTS:

    Part 1:  Title page, options selected, summary, absent rings by series
    Part 2:  Histogram of time spans
    Part 3:  Master series with sample depth and absent rings by year
    Part 4:  Bar plot of Master Dating Series
    Part 5:  Correlation by segment of each series with Master
    Part 6:  Potential problems: low correlation, divergent year-to-year changes, absent rings, outliers
    Part 7:  Descriptive statistics

 RUN CONTROL OPTIONS SELECTED                             VALUE

         1  Cubic smoothing spline 50% wavelength cutoff for filtering
                                                           32 years
         2  Segments examined are                          50 years lagged successively by  25 years
         3  Autoregressive model applied                    A  Residuals are used in master dating series and testing
         4  Series not transformed to logarithms            N
         5  CORRELATION is Pearson (parametric, quantitative)
            Critical correlation, 99% confidence level  0.3281
         6  Master dating series saved                      N
         7  Ring measurements listed                        N
         8  Parts printed                             1234567
         9  Absent rings are omitted from master series and segment correlations  (Y)

 Time span of Master dating series is  1910 to  2017   108 years
 Continuous time span is               1910 to  2017   108 years
 Portion with two or more series is    1924 to  2017    94 years

                                       ****************************************
                                       *C* Number of dated series       17 *C*
                                       *O* Master series 1910 2017  108 yrs *O*
                                       *F* Total rings in all series   1416 *F*
                                       *E* Total dated rings checked   1402 *E*
                                       *C* Series intercorrelation    0.418 *C*
                                       *H* Average mean sensitivity   0.565 *H*
                                       *A* Segments, possible problems   19 *A*
                                       *** Mean length of series      83.0 ***
                                       ****************************************
```

```
 ABSENT RINGS listed by SERIES:            (See Master Dating Series for absent rings listed by year)

              No ring measurements of zero value
PART 2:  TIME PLOT OF TREE-RING SERIES:                                                                16:40  Tue 14 May 2019  Page   2
-------------------------------------------------------------------------------------------------------------------------------------
 1050 1100 1150 1200 1250 1300 1350 1400 1450 1500 1550 1600 1650 1700 1750 1800 1850 1900 1950 2000 2050 Ident    Seq Time-span  Yrs
   :    :    :    :    :    :    :    :    :    :    :    :    :    :    :    :    :    :    :    :    : -------- --- ---- ---- ----
   .    .    .    .    .    .    .    .    .    .    .    .    .    .    .    .    .    .  <======>   . 01A        1 1948 2017   70
   .    .    .    .    .    .    .    .    .    .    .    .    .    .    .    .    .    .   <=====>   . 02B        2 1950 2017   68
   .    .    .    .    .    .    .    .    .    .    .    .    .    .    .    .    .    .  <======>   . 04B        3 1945 2017   73
   .    .    .    .    .    .    .    .    .    .    .    .    .    .    .    .    .    . <=======>   . 05A        4 1933 2017   85
   .    .    .    .    .    .    .    .    .    .    .    .    .    .    .    .    .    . <=======>   . 05B        5 1932 2017   86
   .    .    .    .    .    .    .    .    .    .    .    .    .    .    .    .    .    . <========>  . 06A        6 1924 2017   94
   .    .    .    .    .    .    .    .    .    .    .    .    .    .    .    .    .    . <=======>   . 06B        7 1937 2013   77
   .    .    .    .    .    .    .    .    .    .    .    .    .    .    .    .    .    . <========>  . 07A        8 1929 2017   89
   .    .    .    .    .    .    .    .    .    .    .    .    .    .    .    .    .    . <=======>   . 07B        9 1931 2017   87
   .    .    .    .    .    .    .    .    .    .    .    .    .    .    .    .    .    .<=========>  . 09A       10 1910 2017  108
   .    .    .    .    .    .    .    .    .    .    .    .    .    .    .    .    .    . <=======>   . 09B       11 1937 2017   81
   .    .    .    .    .    .    .    .    .    .    .    .    .    .    .    .    .    . <=======>   . 12A       12 1932 2017   86
   .    .    .    .    .    .    .    .    .    .    .    .    .    .    .    .    .    . <========>  . 12B       13 1925 2017   93
   .    .    .    .    .    .    .    .    .    .    .    .    .    .    .    .    .    .  <======>   . 13A       14 1942 2017   76
   .    .    .    .    .    .    .    .    .    .    .    .    .    .    .    .    .    . <=======>   . 14A       15 1937 2017   81
   .    .    .    .    .    .    .    .    .    .    .    .    .    .    .    .    .    .  <======>   . 15B       16 1943 2017   75
   .    .    .    .    .    .    .    .    .    .    .    .    .    .    .    .    .    . <=======>   . 16A       17 1931 2017   87
   :    :    :    :    :    :    :    :    :    :    :    :    :    :    :    :    :    :    :    :    :
 1050 1100 1150 1200 1250 1300 1350 1400 1450 1500 1550 1600 1650 1700 1750 1800 1850 1900 1950 2000 2050
PART 3:  Master Dating Series:                                                                         16:40  Tue 14 May 2019  Page   3
-------------------------------------------------------------------------------------------------------------------------------------

  Year  Value  No Ab     Year  Value  No Ab     Year  Value  No Ab     Year  Value  No Ab     Year  Value  No Ab     Year  Value  No Ab
  ------------------     ------------------     ------------------     ------------------     ------------------     ------------------
                         1950 -0.528  17        2000 -0.508  17
                         1951 -1.268  17        2001 -0.343  17
                         1952  0.453  17        2002 -1.284  17
                         1953  0.640  17        2003 -0.527  17
                         1954 -0.679  17        2004  0.458  17
                         1955  0.775  17        2005  2.174  17
                         1956  0.138  17        2006 -1.429  17
                         1957 -0.356  17        2007 -1.199  17
                         1958 -0.182  17        2008 -1.192  17
                         1959 -0.370  17        2009 -1.006  17

  1910 -0.370   1        1960  0.613  17        2010 -0.449  17
  1911  0.300   1        1961 -0.053  17        2011 -0.869  17
  1912 -0.873   1        1962  1.052  17        2012  0.360  17
  1913 -1.935   1        1963 -0.792  17        2013  1.167  17
  1914 -2.254   1        1964 -0.237  17        2014 -2.146  16
  1915 -1.295   1        1965 -0.773  17        2015  0.664  16
  1916  3.000   1        1966 -1.267  17        2016  1.133  16
  1917  1.678   1        1967 -0.329  17        2017  0.800  16
  1918  0.940   1        1968 -0.028  17
```

```
 1919  2.967   1       1969  0.666  17

 1920  1.745   1       1970 -1.188  17
 1921 -1.640   1       1971  0.311  17
 1922  0.339   1       1972  0.143  17
 1923  0.378   1       1973  1.117  17
 1924  0.722   2       1974  0.190  17
 1925  0.667   3       1975  1.688  17
 1926 -0.667   3       1976  0.291  17
 1927 -2.198   3       1977  0.335  17
 1928 -0.955   3       1978  0.441  17
 1929 -0.169   4       1979 -0.689  17

 1930  0.387   4       1980 -0.192  17
 1931  0.239   6       1981 -0.500  17
 1932 -0.338   8       1982  0.419  17
 1933 -0.199   9       1983  0.102  17
 1934 -1.038   9       1984 -0.875  17
 1935  1.236   9       1985 -0.698  17
 1936 -0.394   9       1986 -1.215  17
 1937  1.183  12       1987 -0.260  17
 1938 -0.900  12       1988 -0.642  17
 1939 -0.338  12       1989  0.107  17

 1940  0.477  12       1990  0.255  17
 1941 -0.219  12       1991  1.692  17
 1942  0.830  13       1992  1.731  17
 1943 -0.620  14       1993  0.939  17
 1944 -0.215  14       1994  1.545  17
 1945  0.752  15       1995  0.173  17
 1946 -0.460  15       1996 -0.630  17
 1947  0.599  15       1997 -0.923  17
 1948  0.521  16       1998 -0.409  17
 1949  0.548  16       1999  1.025  17
-------------------------------------------------------------------------------------------------------------------------------------
PART 4:  Master Bar Plot:                                                                             16:40  Tue 14 May 2019  Page   4
-------------------------------------------------------------------------------------------------------------------------------------
   Year Rel value  Year Rel value  Year Rel value  Year Rel value  Year Rel value  Year Rel value  Year Rel value  Year Rel value
                   1950---b        2000---b
                   1951e           2001----a
                   1952-------B    2002e
                   1953--------C   2003---b
                   1954--c         2004-------B
                   1955--------C   2005----------I
                   1956------A     2006f
                   1957----a       2007-e
                   1958-----a      2008-e
                   1959----a       2009-d
   1910----a       1960--------B   2010---b
   1911------A     1961-----@      2011-c
   1912-c          1962---------D  2012------A
```

```
  1913h           1963--c         2013---------E
  1914i           1964----a       2014i
  1915e           1965--c         2015--------C
  1916----------L 1966e           2016---------E
  1917----------G 1967----a       2017--------C
  1918---------D  1968-----@
  1919----------L 1969--------C
  1920----------G 1970-e
  1921g           1971------A
  1922------A     1972------A
  1923-------B    1973---------D
  1924--------C   1974------A
  1925--------C   1975----------G
  1926--c         1976------A
  1927i           1977------A
  1928-d          1978-------B
  1929-----a      1979--c
  1930-------B    1980-----a
  1931------A     1981---b
  1932----a       1982-------B
  1933----a       1983-----@
  1934-d          1984-c
  1935---------E  1985--c
  1936----b       1986-e
  1937---------E  1987----a
  1938-d          1988--c
  1939----a       1989-----@
  1940-------B    1990------A
  1941----a       1991----------G
  1942--------C   1992----------G
  1943--b         1993---------D
  1944----a       1994----------F
  1945--------C   1995------A
  1946---b        1996--c
  1947--------B   1997-d
  1948-------B    1998----b
  1949-------B    1999---------D
PART 5:  CORRELATION OF SERIES BY SEGMENTS:                                                    16:40  Tue 14 May 2019  Page   5
-------------------------------------------------------------------------------------------------------------------------------
 Correlations of  50-year dated segments, lagged  25 years
 Flags:  A = correlation under  0.3281 but highest as dated;  B = correlation higher at other than dated position

 Seq Series  Time_span   1900 1925 1950 1975
                         1949 1974 1999 2024
 --- -------- ---------  ---- ---- ---- ---- ---- ---- ---- ---- ---- ---- ---- ---- ---- ---- ---- ---- ---- ---- ---- ----
   1 01A      1948 2017        .39  .34  .43
   2 02B      1950 2017             .25B .45
   3 04B      1945 2017        .17B .21B .53
   4 05A      1933 2017        .44B .62  .63
   5 05B      1932 2017        .47  .60  .61
   6 06A      1924 2017   .34  .32A .45  .48
```

```
  7 06B      1937 2013        .41  .35  .40
  8 07A      1929 2017        .12B .37  .48
  9 07B      1931 2017        .61  .59  .55
 10 09A      1910 2017   .07B .07B .38  .52
 11 09B      1937 2017        .21B .37  .48
 12 12A      1932 2017        .29B .43  .68
 13 12B      1925 2017        .49  .45  .57
 14 13A      1942 2017        .19B .19A .39
 15 14A      1937 2017        .04B .22A .38
 16 15B      1943 2017        .24A .30A .45
 17 16A      1931 2017        .25B .00B .27A
 Av segment correlation  0.20 0.29 0.36 0.49
PART 6:  POTENTIAL PROBLEMS:                                                                          16:40  Tue 14 May 2019  Page   5
-------------------------------------------------------------------------------------------------------------------------------------

 For each series with potential problems the following diagnostics may appear:

 [A] Correlations with master dating series of flagged  50-year segments of series filtered with  32-year spline,
     at every point from ten years earlier (-10) to ten years later (+10) than dated

 [B] Effect of those data values which most lower or raise correlation with master series
     Symbol following year indicates value in series is greater (>) or lesser (<) than master series value

 [C] Year-to-year changes very different from the mean change in other series

 [D] Absent rings (zero values)

 [E] Values which are statistical outliers from mean for the year
=====================================================================================================================================

 01A       1948 to  2017      70 years                                                                                    Series   1

 [B] Entire series, effect on correlation ( 0.419) is:
       Lower   1975<-0.048   1999<-0.033   1969>-0.032   2000>-0.020   2006>-0.018   1956>-0.017  Higher   2005 0.033   1994 0.030

 [E] Outliers     1   3.0 SD above or -4.5 SD below mean for year
       1969 +5.5 SD
=====================================================================================================================================

 02B       1950 to  2017      68 years                                                                                    Series   2

 [A] Segment   High   -10   -9   -8   -7   -6   -5   -4   -3   -2   -1    0   +1   +2   +3   +4   +5   +6   +7   +8   +9  +10
    ---------  ----   ---  ---  ---  ---  ---  ---  ---  ---  ---  ---  ---  ---  ---  ---  ---  ---  ---  ---  ---  ---  ---
    1950 1999    2    .01  .17 -.06 -.10 -.11 -.01 -.18  .06 -.08 -.04  .25|-.04  .35* .11  .23  .08  .09 -.27 -.19 -.26 -.02

 [B] Entire series, effect on correlation ( 0.361) is:
       Lower   1994<-0.035   1950>-0.030   1958>-0.029   1975<-0.026   1962<-0.019   2013<-0.016  Higher   2005 0.056   1991 0.038
     1950 to 1999 segment:
       Lower   1994<-0.049   1950>-0.044   1958>-0.039   1975<-0.036   1962<-0.026   1997>-0.019  Higher   1991 0.067   1999 0.042

 [E] Outliers     1   3.0 SD above or -4.5 SD below mean for year
```

```
      1971 +3.2 SD
====================================================================================================

 04B       1945 to  2017      73 years                                                    Series   3

 [A] Segment   High   -10    -9    -8    -7    -6    -5    -4    -3    -2    -1     0    +1    +2    +3    +4    +5    +6    +7    +8    +9   +10
    ---------  ----   ---   ---   ---   ---   ---   ---   ---   ---   ---   ---   ---   ---   ---   ---   ---   ---   ---   ---   ---   ---   ---
    1945 1994    3    -.15  .00   .02 -.06   .10  .00   .28 -.08 -.01   .14   .17| .15 -.15  .30*-.23 -.14 -.24   .16 -.03   .05 -.12
    1950 1999   -1    -.17 -.07 -.05 -.10   .05 -.09   .21 -.09  .03   .24*  .21| .20 -.20  .21 -.20 -.06 -.22   .04 -.05   .14  .01

 [B] Entire series, effect on correlation ( 0.350) is:
      Lower   1966>-0.076   1947<-0.030   1962<-0.022   2011>-0.022   1994<-0.020   1960<-0.019  Higher   2005 0.037   1991 0.036
    1945 to 1994 segment:
      Lower   1966>-0.116   1947<-0.041   1962<-0.031   1994<-0.029   1960<-0.026   1973<-0.025  Higher   1991 0.073   1970 0.043
    1950 to 1999 segment:
      Lower   1966>-0.116   1962<-0.034   1994<-0.031   1960<-0.028   1973<-0.027   1964>-0.019  Higher   1991 0.072   1975 0.038

 [E] Outliers     1   3.0 SD above or -4.5 SD below mean for year
      1966 +4.2 SD
====================================================================================================

 05A       1933 to  2017      85 years                                                    Series   4

 [A] Segment   High   -10    -9    -8    -7    -6    -5    -4    -3    -2    -1     0    +1    +2    +3    +4    +5    +6    +7    +8    +9   +10
    ---------  ----   ---   ---   ---   ---   ---   ---   ---   ---   ---   ---   ---   ---   ---   ---   ---   ---   ---   ---   ---   ---   ---
    1933 1982    7     .00 -.06   .07  .09 -.14   .03 -.14 -.12 -.02 -.14   .44|-.24   .05 -.09  .10   .27 -.07   .48*-.16 -.12 -.18

 [B] Entire series, effect on correlation ( 0.552) is:
      Lower   1937<-0.035   1968>-0.029   2011>-0.023   1933>-0.020   1978<-0.013   1939<-0.012  Higher   2014 0.029   1975 0.019
    1933 to 1982 segment:
      Lower   1937<-0.069   1968>-0.045   1933>-0.036   1978<-0.024   1957>-0.020   1939<-0.015  Higher   1975 0.046   1951 0.038

 [E] Outliers     1   3.0 SD above or -4.5 SD below mean for year
      1968 +3.7 SD
====================================================================================================

 05B       1932 to  2017      86 years                                                    Series   5

 [B] Entire series, effect on correlation ( 0.567) is:
      Lower   1968>-0.034   1937<-0.025   1942<-0.024   1936>-0.019   1978<-0.017   1996>-0.016  Higher   1994 0.018   1975 0.015

 [E] Outliers     2   3.0 SD above or -4.5 SD below mean for year
      1947 +3.3 SD;    1968 +3.9 SD
====================================================================================================

 06A       1924 to  2017      94 years                                                    Series   6

 [A] Segment   High   -10    -9    -8    -7    -6    -5    -4    -3    -2    -1     0    +1    +2    +3    +4    +5    +6    +7    +8    +9   +10
    ---------  ----   ---   ---   ---   ---   ---   ---   ---   ---   ---   ---   ---   ---   ---   ---   ---   ---   ---   ---   ---   ---   ---
    1925 1974    0    -.25  .06 -.06   .26 -.06   .05 -.23   .04  .09   .02   .32*-.41 -.10 -.04   .18   .11   .15   .02 -.17 -.14   .04
```

```
[B] Entire series, effect on correlation ( 0.402) is:
      Lower   2000>-0.027   1965>-0.020   1999<-0.019   1942>-0.017   1992<-0.016   1930<-0.014  Higher   1994 0.027   1927 0.018
    1925 to 1974 segment:
      Lower   1965>-0.040   1930<-0.027   1974<-0.023   1940<-0.020   1947<-0.017   1929<-0.017  Higher   1927 0.042   1970 0.030

[E] Outliers     2   3.0 SD above or -4.5 SD below mean for year
      1942 +5.4 SD;    1994 +3.0 SD
=====================================================================================================================================

06B       1937 to  2013      77 years                                                                                    Series   7

[B] Entire series, effect on correlation ( 0.388) is:
      Lower   1992<-0.036   1965>-0.033   1942<-0.031   1999<-0.026   1998>-0.025   1991<-0.024  Higher   1994 0.036   2013 0.022

[E] Outliers     2   3.0 SD above or -4.5 SD below mean for year
      1945 +3.9 SD;    1994 +3.4 SD
=====================================================================================================================================

07A       1929 to  2017      89 years                                                                                    Series   8

[A] Segment   High   -10   -9   -8   -7   -6   -5   -4   -3   -2   -1    0   +1   +2   +3   +4   +5   +6   +7   +8   +9  +10
   ---------  ----   ---  ---  ---  ---  ---  ---  ---  ---  ---  ---  ---  ---  ---  ---  ---  ---  ---  ---  ---  ---  ---
   1929 1978    7   -.03 -.25  .13 -.06  .07  .11 -.02  .07 -.03  .17  .12|-.13  .26 -.38 -.15 -.05 -.15  .36*-.14  .16 -.07

[B] Entire series, effect on correlation ( 0.345) is:
      Lower   1946>-0.022   1963>-0.021   1949<-0.016   1933>-0.016   1931<-0.015   1952<-0.015  Higher   2014 0.030   1992 0.029
    1929 to 1978 segment:
      Lower   1946>-0.041   1963>-0.039   1933>-0.028   1949<-0.027   1952<-0.027   1931<-0.026  Higher   1975 0.068   1966 0.033

[E] Outliers     3   3.0 SD above or -4.5 SD below mean for year
      1976 +3.0 SD;    1992 +4.1 SD;    2012 +3.3 SD
=====================================================================================================================================

07B       1931 to  2017      87 years                                                                                    Series   9

[B] Entire series, effect on correlation ( 0.586) is:
      Lower   2013<-0.021   1945<-0.018   2015<-0.013   1974>-0.011   1990>-0.011   1969<-0.009  Higher   2006 0.017   1951 0.012

[E] Outliers     1   3.0 SD above or -4.5 SD below mean for year
      1974 +3.1 SD
=====================================================================================================================================

09A       1910 to  2017     108 years                                                                                    Series  10

[*] Early part of series cannot be checked from 1910 to 1923 -- not matched by another series

[A] Segment   High   -10   -9   -8   -7   -6   -5   -4   -3   -2   -1    0   +1   +2   +3   +4   +5   +6   +7   +8   +9  +10
   ---------  ----   ---  ---  ---  ---  ---  ---  ---  ---  ---  ---  ---  ---  ---  ---  ---  ---  ---  ---  ---  ---  ---
   1924 1973   -4   -.37  .09 -.05  .12  .00 -.03  .18*-.32  .14 -.16  .07|-.09  .02  .12 -.16 -.06 -.02 -.11  .06  .12 -.12
   1925 1974   -4   -.38  .07 -.09  .11  .00 -.01  .15*-.32  .15 -.13  .07|-.06  .02  .14 -.14 -.08 -.02 -.12  .07  .12 -.15
```

```
[B] Entire series, effect on correlation ( 0.326) is:
      Lower   1939>-0.033   1948<-0.023   1935<-0.021   1925<-0.020   1993<-0.019   1947<-0.014  Higher   1975 0.034   2005 0.034
    1924 to 1973 segment:
      Lower   1939>-0.054   1948<-0.037   1935<-0.031   1925<-0.030   1947<-0.023   1946>-0.022  Higher   1937 0.064   1927 0.048
    1925 to 1974 segment:
      Lower   1939>-0.052   1948<-0.039   1935<-0.033   1925<-0.032   1947<-0.025   1946>-0.021  Higher   1937 0.067   1927 0.049

[E] Outliers     2   3.0 SD above or -4.5 SD below mean for year
      1939 +4.2 SD;    1975 +3.1 SD
====================================================================================================================================

09B       1937 to  2017      81 years                                                                                    Series  11

[A] Segment   High   -10    -9    -8    -7    -6    -5    -4    -3    -2    -1     0    +1    +2    +3    +4    +5    +6    +7    +8    +9   +10
   ---------  ----   ---   ---   ---   ---   ---   ---   ---   ---   ---   ---   ---   ---   ---   ---   ---   ---   ---   ---   ---   ---   ---
   1937 1986    2    .01   .06 -.31   .20   .22   .04 -.05 -.27   .24 -.02   .21| .03   .28*-.05 -.36 -.12 -.05   .07   .01   .04 -.02

[B] Entire series, effect on correlation ( 0.364) is:
      Lower   1946>-0.039   1948<-0.027   1984>-0.025   1954>-0.022   1951>-0.019   1995>-0.016  Higher   1975 0.039   1992 0.021
    1937 to 1986 segment:
      Lower   1946>-0.061   1948<-0.046   1984>-0.042   1954>-0.036   1951>-0.031   1970>-0.025  Higher   1975 0.108   1962 0.038

[E] Outliers     3   3.0 SD above or -4.5 SD below mean for year
      1946 +3.5 SD;    1995 +3.2 SD;    2012 +3.4 SD
====================================================================================================================================

12A       1932 to  2017      86 years                                                                                    Series  12

[A] Segment   High   -10    -9    -8    -7    -6    -5    -4    -3    -2    -1     0    +1    +2    +3    +4    +5    +6    +7    +8    +9   +10
   ---------  ----   ---   ---   ---   ---   ---   ---   ---   ---   ---   ---   ---   ---   ---   ---   ---   ---   ---   ---   ---   ---   ---
   1932 1981    4   -.17 -.07 -.19   .02   .10   .05   .15 -.01   .00 -.20   .29| .02   .20 -.16   .32*-.10 -.18 -.08 -.20   .10 -.04

[B] Entire series, effect on correlation ( 0.497) is:
      Lower   1943>-0.036   2009>-0.022   1958>-0.021   1962<-0.019   1955<-0.017   1944>-0.017  Higher   2014 0.032   2006 0.018
    1932 to 1981 segment:
      Lower   1943>-0.063   1962<-0.033   1958>-0.032   1955<-0.030   1944>-0.026   1953<-0.022  Higher   1970 0.045   1973 0.035

[E] Outliers     1   3.0 SD above or -4.5 SD below mean for year
      1943 +3.0 SD
====================================================================================================================================

12B       1925 to  2017      93 years                                                                                    Series  13

[B] Entire series, effect on correlation ( 0.534) is:
      Lower   1951>-0.020   2013<-0.020   1994<-0.019   1954>-0.015   1972<-0.015   2010>-0.014  Higher   2005 0.025   1991 0.024

====================================================================================================================================

13A       1942 to  2017      76 years                                                                                    Series  14

[A] Segment   High   -10    -9    -8    -7    -6    -5    -4    -3    -2    -1     0    +1    +2    +3    +4    +5    +6    +7    +8    +9   +10
```

```
   --------- ----   ---  ---  ---  ---  ---  ---  ---  ---  ---  ---  ---  ---  ---  ---  ---  ---  ---  ---  ---  ---  ---
   1942 1991   -3   -.03 -.03 -.08  .20  .03  .06  .03  .22* .07 -.14  .19|-.08  .19 -.09  .10 -.30 -.15 -.23 -.20 -.02 -.14
   1950 1999    0    .01  .03 -.10  .11 -.07 -.08  .08  .12  .12 -.02  .19* .01  .16 -.04  .13 -.38 -.12 -.28 -.15  .06 -.15

[B] Entire series, effect on correlation ( 0.349) is:
      Lower   1979>-0.083   1975<-0.056   1994<-0.033   1951>-0.025   1949<-0.020   1945<-0.014  Higher   1991 0.039   2014 0.030
    1942 to 1991 segment:
      Lower   1979>-0.123   1975<-0.092   1951>-0.040   1949<-0.031   1945<-0.022   1968<-0.015  Higher   1991 0.091   1970 0.052
    1950 to 1999 segment:
      Lower   1979>-0.117   1975<-0.085   1994<-0.050   1951>-0.035   1968<-0.014   1999<-0.014  Higher   1991 0.082   1970 0.050

[E] Outliers     1   3.0 SD above or -4.5 SD below mean for year
      1979 +5.1 SD
=====================================================================================================================================

14A       1937 to  2017      81 years                                                                                    Series  15

[A] Segment   High   -10   -9   -8   -7   -6   -5   -4   -3   -2   -1    0   +1   +2   +3   +4   +5   +6   +7   +8   +9  +10
   --------- ----   ---  ---  ---  ---  ---  ---  ---  ---  ---  ---  ---  ---  ---  ---  ---  ---  ---  ---  ---  ---  ---
   1937 1986    3   -.20  .03  .04  .01  .08 -.01  .27 -.05  .16 -.11  .04| .03 -.14  .28*-.23 -.21 -.14 -.20 -.05 -.15  .09
   1950 1999    0   -.15  .03 -.09 -.04  .00  .05  .03  .10 -.03  .12  .22* .18  .15  .07 -.30 -.22 -.29  .13 -.13 -.17 -.09

[B] Entire series, effect on correlation ( 0.275) is:
      Lower   1961>-0.055   2016<-0.029   1939>-0.022   1940<-0.020   1969<-0.016   1999<-0.016  Higher   1992 0.038   2006 0.029
    1937 to 1986 segment:
      Lower   1961>-0.075   1939>-0.034   1940<-0.032   1969<-0.027   1942<-0.024   1981>-0.020  Higher   1951 0.045   1962 0.043
    1950 to 1999 segment:
      Lower   1961>-0.095   1969<-0.028   1999<-0.028   1981>-0.022   1993<-0.020   1982<-0.019  Higher   1992 0.086   1951 0.035

[E] Outliers     2   3.0 SD above or -4.5 SD below mean for year
      1961 +4.9 SD;    1992 +3.8 SD
=====================================================================================================================================

15B       1943 to  2017      75 years                                                                                    Series  16

[A] Segment   High   -10   -9   -8   -7   -6   -5   -4   -3   -2   -1    0   +1   +2   +3   +4   +5   +6   +7   +8   +9  +10
   --------- ----   ---  ---  ---  ---  ---  ---  ---  ---  ---  ---  ---  ---  ---  ---  ---  ---  ---  ---  ---  ---  ---
   1943 1992    0    .08 -.25  .10 -.02 -.04  .06 -.02  .08  .15 -.19  .24* .02 -.11  .00 -.13  .12 -.12  .12  .19 -.03  .01
   1950 1999    0   -.04 -.25 -.02 -.09 -.12  .02  .08  .22  .29 -.01  .30*-.04 -.18 -.01 -.08  .16 -.14 -.01 -.02  .02  .11

[B] Entire series, effect on correlation ( 0.440) is:
      Lower   1991<-0.026   1992<-0.022   1969<-0.020   1956<-0.017   1968<-0.016   1986>-0.014  Higher   1975 0.036   2014 0.031
    1943 to 1992 segment:
      Lower   1991<-0.036   1969<-0.030   1992<-0.030   1986>-0.023   1956<-0.020   1968<-0.019  Higher   1975 0.101   1951 0.021
    1950 to 1999 segment:
      Lower   1991<-0.040   1992<-0.033   1969<-0.030   1956<-0.020   1968<-0.020   1986>-0.019  Higher   1975 0.077   1994 0.076

[E] Outliers     2   3.0 SD above or -4.5 SD below mean for year
      1952 +3.3 SD;    1994 +3.8 SD
=====================================================================================================================================
```

```
16A       1931 to  2017      87 years                                                                                    Series  17

[A] Segment   High   -10   -9   -8   -7   -6   -5   -4   -3   -2   -1    0   +1   +2   +3   +4   +5   +6   +7   +8   +9  +10
   ---------  ----   ---  ---  ---  ---  ---  ---  ---  ---  ---  ---  ---  ---  ---  ---  ---  ---  ---  ---  ---  ---  ---
   1931 1980    5    .31 -.07 -.15 -.09 -.22  .07 -.10 -.01 -.10 -.11  .25| .07  .10  .25 -.11  .33*-.22  .23  .02 -.25 -.14
   1950 1999    3    .16 -.08  .17  .07  .08 -.04 -.20 -.14 -.29 -.23  .00| .18  .18  .25* .11  .23  .11 -.01 -.03 -.14 -.17
   1968 2017    0    .00 -.15  .13 -.10  .09 -.02 -.09 -.15 -.27 -.14  .27*   -    -    -    -    -    -    -    -    -    -

[B] Entire series, effect on correlation ( 0.312) is:
      Lower   1992<-0.051   1970>-0.046   1994<-0.036   1997>-0.025   1931<-0.019   1985>-0.017  Higher   2005 0.052   2014 0.038
    1931 to 1980 segment:
      Lower   1970>-0.098   1959>-0.035   1931<-0.035   1932>-0.034   1975<-0.031   1957>-0.021  Higher   1935 0.047   1966 0.029
    1950 to 1999 segment:
      Lower   1992<-0.080   1970>-0.073   1994<-0.054   1997>-0.039   1985>-0.027   1959>-0.025  Higher   1991 0.041   1966 0.038
    1968 to 2017 segment:
      Lower   1992<-0.082   1970>-0.071   1994<-0.058   1997>-0.038   1985>-0.027   1975<-0.025  Higher   2005 0.087   2014 0.071

[E] Outliers     1   3.0 SD above or -4.5 SD below mean for year
      1970 +3.8 SD
==================================================================================================================================
PART 7:  DESCRIPTIVE STATISTICS:                                                                    16:40  Tue 14 May 2019  Page   6
----------------------------------------------------------------------------------------------------------------------------------
```

Seq	Series	Interval	No. Years	No. Segmt	No. Flags	Corr with Master	//-------- Unfiltered --------\\ Mean msmt	Max msmt	Std dev	Auto corr	Mean sens	//---- Filtered -----\\ Max value	Std dev	Auto corr	AR ()
1	01A	1948 2017	70	3	0	0.419	1.63	9.38	1.576	0.158	0.577	3.60	0.865	0.000	1
2	02B	1950 2017	68	2	1	0.361	2.42	24.45	3.589	0.461	0.569	2.02	0.780	-0.010	1
3	04B	1945 2017	73	3	2	0.350	2.87	8.72	1.537	0.478	0.418	1.01	0.432	0.003	3
4	05A	1933 2017	85	3	1	0.552	2.06	4.91	1.104	0.187	0.726	1.55	0.620	0.000	1
5	05B	1932 2017	86	3	0	0.567	2.40	7.99	1.708	0.471	0.667	1.80	0.666	-0.007	1
6	06A	1924 2017	94	4	1	0.402	1.91	6.97	1.392	0.363	0.615	2.97	0.728	-0.003	1
7	06B	1937 2013	77	3	0	0.388	1.98	6.39	1.306	0.463	0.590	2.38	0.741	0.002	1
8	07A	1929 2017	89	3	1	0.345	1.72	5.38	1.288	0.519	0.536	2.34	0.615	0.007	1
9	07B	1931 2017	87	3	0	0.586	1.91	10.25	1.757	0.559	0.528	1.95	0.680	-0.040	1
10	09A	1910 2017	108	4	2	0.326	1.46	7.07	0.971	0.490	0.477	1.79	0.594	0.029	1
11	09B	1937 2017	81	3	1	0.364	1.21	7.51	1.181	0.342	0.632	2.36	0.792	0.018	1
12	12A	1932 2017	86	3	1	0.497	1.92	9.28	2.104	0.798	0.536	1.31	0.560	-0.010	1
13	12B	1925 2017	93	3	0	0.534	1.77	6.63	1.456	0.731	0.462	1.51	0.490	-0.001	1
14	13A	1942 2017	76	3	2	0.349	2.27	7.92	1.904	0.522	0.658	2.68	0.887	-0.003	1
15	14A	1937 2017	81	3	2	0.275	1.98	8.24	1.798	0.497	0.576	2.99	0.838	0.002	1
16	15B	1943 2017	75	3	2	0.440	1.98	11.20	1.728	0.447	0.612	2.55	0.725	0.001	2
17	16A	1931 2017	87	3	3	0.312	2.56	8.28	1.621	0.471	0.465	1.55	0.563	-0.024	1
Total or mean:			1416	52	19	0.418	1.98	24.45	1.613	0.473	0.565	3.60	0.675	-0.002	

- = [COFECHA Inland COF] = -

```
P R O G R A M     C O F E C H A                                                                     Version 6.06P    30815
----------------------------------------------------------------------------------------------------------------------------------
```

```
QUALITY CONTROL AND DATING CHECK OF TREE-RING MEASUREMENTS                                             COF12K.for

File of DATED series:   Coastal.txt

CONTENTS:

   Part 1:  Title page, options selected, summary, absent rings by series
   Part 2:  Histogram of time spans
   Part 3:  Master series with sample depth and absent rings by year
   Part 4:  Bar plot of Master Dating Series
   Part 5:  Correlation by segment of each series with Master
   Part 6:  Potential problems: low correlation, divergent year-to-year changes, absent rings, outliers
   Part 7:  Descriptive statistics

RUN CONTROL OPTIONS SELECTED                            VALUE

        1  Cubic smoothing spline 50% wavelength cutoff for filtering
                                                          50 years
        2  Segments examined are                          50 years lagged successively by  25 years
        3  Autoregressive model applied                    A  Residuals are used in master dating series and testing
        4  Series not transformed to logarithms            N
        5  CORRELATION is Pearson (parametric, quantitative)
           Critical correlation, 99% confidence level  0.3281
        6  Master dating series saved                      N
        7  Ring measurements listed                        N
        8  Parts printed                             1234567
        9  Absent rings are omitted from master series and segment correlations  (Y)

Time span of Master dating series is  1895 to  2017   123 years
Continuous time span is               1895 to  2017   123 years
Portion with two or more series is    1897 to  2017   121 years

                                       ****************************************
                                       *C* Number of dated series       19 *C*
                                       *O* Master series 1895 2017  123 yrs *O*
                                       *F* Total rings in all series   1504 *F*
                                       *E* Total dated rings checked   1502 *E*
                                       *C* Series intercorrelation    0.418 *C*
                                       *H* Average mean sensitivity   0.511 *H*
                                       *A* Segments, possible problems   20 *A*
                                       *** Mean length of series      79.0 ***
                                       ****************************************

ABSENT RINGS listed by SERIES:            (See Master Dating Series for absent rings listed by year)

              No ring measurements of zero value
PART 2:  TIME PLOT OF TREE-RING SERIES:                                                            17:07  Mon 13 May 2019  Page   2
-------------------------------------------------------------------------------------------------------------------------------------
 1050 1100 1150 1200 1250 1300 1350 1400 1450 1500 1550 1600 1650 1700 1750 1800 1850 1900 1950 2000 2050 Ident   Seq Time-span  Yrs
```

```
  :    :    :    :    :    :    :    :    :    :    :    :    :    :    :    :    :    :    :    :    : -------- --- ---- ---- ----
  .    .    .    .    .    .    .    .    .    .    .    .    .    .    .    .    .    .    <=====>   . 01A        1 1950 2017   68
  .    .    .    .    .    .    .    .    .    .    .    .    .    .    .    .    .    .    . <===>   . 02A        2 1970 2017   48
  .    .    .    .    .    .    .    .    .    .    .    .    .    .    .    .    .    .    .<====>   . 02B        3 1967 2017   51
  .    .    .    .    .    .    .    .    .    .    .    .    .    .    .    .    .  <===========>   . 03A        4 1895 2017  123
  .    .    .    .    .    .    .    .    .    .    .    .    .    .    .    .    .  <===========>   . 03B        5 1897 2017  121
  .    .    .    .    .    .    .    .    .    .    .    .    .    .    .    .    .    . <========>   . 04B        6 1926 2017   92
  .    .    .    .    .    .    .    .    .    .    .    .    .    .    .    .    .    .    .<====>   . 05B        7 1966 2017   52
  .    .    .    .    .    .    .    .    .    .    .    .    .    .    .    .    .    .    <=====>   . 06B        8 1950 2017   68
  .    .    .    .    .    .    .    .    .    .    .    .    .    .    .    .    .    . <========>   . 07A        9 1920 2017   98
  .    .    .    .    .    .    .    .    .    .    .    .    .    .    .    .    .    . <========>   . 07B       10 1920 2017   98
  .    .    .    .    .    .    .    .    .    .    .    .    .    .    .    .    .    .    <=====>   . 09A       11 1950 2017   68
  .    .    .    .    .    .    .    .    .    .    .    .    .    .    .    .    .    .    <=====>   . 09B       12 1950 2017   68
  .    .    .    .    .    .    .    .    .    .    .    .    .    .    .    .    .    .    <=====>   . 10A       13 1956 2017   62
  .    .    .    .    .    .    .    .    .    .    .    .    .    .    .    .    .    .    <=====>   . 10B       14 1951 2017   67
  .    .    .    .    .    .    .    .    .    .    .    .    .    .    .    .    .    .  <=======>   . 13A       15 1935 2017   83
  .    .    .    .    .    .    .    .    .    .    .    .    .    .    .    .    .   <==========>   . 14A       16 1909 2013  105
  .    .    .    .    .    .    .    .    .    .    .    .    .    .    .    .    .   <==========>   . 14B       17 1909 2013  105
  .    .    .    .    .    .    .    .    .    .    .    .    .    .    .    .    .    .    <=====>   . 15A       18 1953 2017   65
  .    .    .    .    .    .    .    .    .    .    .    .    .    .    .    .    .    .    <=====>   . 15B       19 1956 2017   62
  :    :    :    :    :    :    :    :    :    :    :    :    :    :    :    :    :    :    :    :    :
1050 1100 1150 1200 1250 1300 1350 1400 1450 1500 1550 1600 1650 1700 1750 1800 1850 1900 1950 2000 2050
PART 3:  Master Dating Series:                                                                    17:07  Mon 13 May 2019  Page   3
------------------------------------------------------------------------------------------------------------------------------------
 Year  Value  No Ab    Year  Value  No Ab    Year  Value  No Ab    Year  Value  No Ab    Year  Value  No Ab    Year  Value  No Ab
 ------------------    ------------------    ------------------    ------------------    ------------------    ------------------
                       1900 -1.578   2       1950 -0.324  12       2000 -1.057  19
                       1901 -0.420   2       1951 -0.335  13       2001 -0.403  19
                       1902 -0.183   2       1952  0.267  13       2002 -1.079  19
                       1903 -1.399   2       1953  0.213  14       2003 -1.242  19
                       1904 -1.157   2       1954 -0.533  14       2004 -0.347  19
                       1905 -1.002   2       1955 -0.775  14       2005  0.886  19
                       1906 -1.256   2       1956 -0.306  16       2006 -2.101  19
                       1907 -1.060   2       1957 -0.459  16       2007 -1.639  19
                       1908 -1.139   2       1958 -0.162  16       2008 -0.876  19
                       1909 -0.678   4       1959 -0.146  16       2009 -0.826  19

                       1910 -0.974   4       1960 -0.531  16       2010 -1.115  19
                       1911  0.821   4       1961 -0.546  16       2011 -0.305  19
                       1912 -0.873   4       1962 -0.744  16       2012  0.540  19
                       1913 -1.018   4       1963 -0.764  16       2013  0.774  19
                       1914 -1.416   4       1964 -0.656  16       2014 -0.703  17
                       1915 -1.135   4       1965 -0.418  16       2015  0.662  17
                       1916  1.598   4       1966  0.079  17       2016  2.073  17
                       1917  0.801   4       1967 -0.593  18       2017  2.440  17
                       1918 -0.114   4       1968  0.840  18
                       1919  0.092   4       1969 -0.728  18

                       1920  1.027   6       1970 -0.241  19
                       1921  0.990   6       1971 -0.633  19
                       1922 -0.559   6       1972  1.137  19
```

```
                                  1923  0.467   6       1973 -0.312  19
                                  1924 -0.261   6       1974  1.165  19
                                  1925 -2.155   6       1975  1.028  19
                                  1926 -1.252   7       1976 -0.444  19
                                  1927  0.295   7       1977  0.329  19
                                  1928 -0.466   7       1978  0.236  19
                                  1929  0.130   7       1979  1.607  19

                                  1930 -0.402   7       1980  0.371  19
                                  1931 -0.698   7       1981  0.479  19
                                  1932  1.605   7       1982 -0.178  19
                                  1933 -0.081   7       1983  0.101  19
                                  1934  0.171   7       1984  0.012  19
                                  1935 -0.541   8       1985 -0.792  19
                                  1936  0.357   8       1986 -0.684  19
                                  1937  0.090   8       1987  0.234  19
                                  1938  0.404   8       1988  0.816  19
                                  1939  1.298   8       1989 -0.334  19

                                  1940 -0.003   8       1990  1.890  19
                                  1941  0.873   8       1991  2.383  19
                                  1942  0.301   8       1992  0.791  19
                                  1943 -0.048   8       1993  2.262  19
                                  1944  2.853   8       1994 -1.101  19
  1895  2.341   1                 1945  0.694   8       1995 -0.243  19
  1896  1.100   1                 1946  0.622   8       1996 -0.828  19
  1897  2.027   2                 1947  0.511   8       1997 -0.976  19
  1898  2.063   2                 1948 -0.107   8       1998 -0.624  19
  1899  0.713   2                 1949  0.991   8       1999  0.220  19
------------------------------------------------------------------------------------------------------------------------------------
PART 4:  Master Bar Plot:                                                                        17:07  Mon 13 May 2019  Page   4
------------------------------------------------------------------------------------------------------------------------------------
   Year Rel value  Year Rel value  Year Rel value  Year Rel value  Year Rel value  Year Rel value  Year Rel value  Year Rel value
                   1900f           1950----a       2000-d
                   1901----b       1951----a       2001----b
                   1902-----a      1952-------A    2002-d
                   1903f           1953------A     2003e
                   1904e           1954---b        2004----a
                   1905-d          1955--c         2005--------D
                   1906e           1956----a       2006h
                   1907-d          1957---b        2007g
                   1908e           1958-----a      2008--d
                   1909--c         1959-----a      2009--c
                   1910-d          1960---b        2010-d
                   1911--------C   1961---b        2011----a
                   1912--c         1962--c         2012-------B
                   1913-d          1963--c         2013--------C
                   1914f           1964--c         2014--c
                   1915-e          1965----b       2015--------C
                   1916----------F 1966------@     2016----------H
                   1917--------C   1967---b        2017----------J
```

```
                    1918-----@      1968--------C
                    1919------@     1969--c
                    1920---------D  1970-----a
                    1921---------D  1971---c
                    1922---b        1972---------E
                    1923-------B    1973----a
                    1924-----a      1974---------E
                    1925i           1975---------D
                    1926e           1976----b
                    1927-------A    1977-------A
                    1928---b        1978-------A
                    1929------A     1979----------F
                    1930----b       1980-------A
                    1931--c         1981-------B
                    1932----------F 1982-----a
                    1933-----@      1983------@
                    1934------A     1984------@
                    1935---b        1985--c
                    1936-------A    1986--c
                    1937------@     1987-------A
                    1938-------B    1988--------C
                    1939---------E  1989----a
                    1940------@     1990----------H
                    1941--------C   1991----------J
                    1942-------A    1992--------C
                    1943-----@      1993----------I
                    1944----------K 1994-d
  1895----------I 1945--------C     1995-----a
  1896---------D  1946--------B     1996--c
  1897----------H 1947-------B      1997-d
  1898----------H 1948-----@        1998---b
  1899--------C   1949---------D    1999------A
PART 5:  CORRELATION OF SERIES BY SEGMENTS:                                                  17:07  Mon 13 May 2019  Page   5
------------------------------------------------------------------------------------------------------------------------------------
 Correlations of  50-year dated segments, lagged  25 years
 Flags:  A = correlation under  0.3281 but highest as dated;  B = correlation higher at other than dated position

 Seq Series  Time_span   1875 1900 1925 1950 1975
                         1924 1949 1974 1999 2024
 --- -------- ---------  ---- ---- ---- ---- ---- ---- ---- ---- ---- ---- ---- ---- ---- ---- ---- ---- ---- ---- ---- ----
   1 01A      1950 2017                     .24B .40
   2 02A      1970 2017                     .45
   3 02B      1967 2017                     .55  .57
   4 03A      1895 2017   .30B .26B .31B .47  .60
   5 03B      1897 2017   .15B .13B .19B .42  .64
   6 04B      1926 2017             .40B .04B .21B
   7 05B      1966 2017                  .39  .45
   8 06B      1950 2017                  .11B .40
   9 07A      1920 2017        .66  .62  .62  .69
  10 07B      1920 2017        .58  .57  .57  .53
  11 09A      1950 2017                  .15B .43
```

```
 12 09B      1950 2017                  .22B .44
 13 10A      1956 2017                  .42B .58
 14 10B      1951 2017                  .24B .46
 15 13A      1935 2017             .09B .43  .65
 16 14A      1909 2013       -.12B .04B .65  .72
 17 14B      1909 2013        .04B .13B .53  .64
 18 15A      1953 2017                  .56  .67
 19 15B      1956 2017                  .55  .64
 Av segment correlation  0.22 0.26 0.30 0.40 0.54
PART 6:  POTENTIAL PROBLEMS:                                                                     17:07  Mon 13 May 2019  Page   5
------------------------------------------------------------------------------------------------------------------------------------

 For each series with potential problems the following diagnostics may appear:

 [A] Correlations with master dating series of flagged  50-year segments of series filtered with  50-year spline,
     at every point from ten years earlier (-10) to ten years later (+10) than dated

 [B] Effect of those data values which most lower or raise correlation with master series
     Symbol following year indicates value in series is greater (>) or lesser (<) than master series value

 [C] Year-to-year changes very different from the mean change in other series

 [D] Absent rings (zero values)

 [E] Values which are statistical outliers from mean for the year
====================================================================================================================================

 01A       1950 to  2017      68 years                                                                                    Series   1

 [A] Segment   High   -10   -9   -8   -7   -6   -5   -4   -3   -2   -1    0   +1   +2   +3   +4   +5   +6   +7   +8   +9  +10
    ---------  ----   ---  ---  ---  ---  ---  ---  ---  ---  ---  ---  ---  ---  ---  ---  ---  ---  ---  ---  ---  ---  ---
    1950 1999    1    .00 -.05 -.08 -.13 -.06 -.27 -.18 -.07  .19  .16  .24| .26* .13 -.22  .03 -.01 -.03  .09  .05 -.14  .14

 [B] Entire series, effect on correlation ( 0.283) is:
       Lower   1979<-0.046   1967>-0.036   2016<-0.027   1988<-0.025   1972<-0.021   1975<-0.021  Higher   1991 0.089   2006 0.030
     1950 to 1999 segment:
       Lower   1979<-0.067   1967>-0.054   1988<-0.035   1972<-0.030   1975<-0.029   1960>-0.025  Higher   1991 0.153   1974 0.046

 [E] Outliers     1   3.0 SD above or -4.5 SD below mean for year
       1991 +3.2 SD
====================================================================================================================================

 02A       1970 to  2017      48 years                                                                                    Series   2

 [B] Entire series, effect on correlation ( 0.454) is:
       Lower   1974<-0.063   1979<-0.045   1985>-0.044   2003>-0.026   1987>-0.021   2012<-0.018  Higher   2017 0.058   2006 0.037

 [E] Outliers     1   3.0 SD above or -4.5 SD below mean for year
       1987 +3.0 SD
====================================================================================================================================
```

```
02B       1967 to  2017      51 years                                                                                    Series   3

[B] Entire series, effect on correlation ( 0.574) is:
      Lower   1993<-0.082   1992<-0.033   1988>-0.029   1977<-0.013   2012<-0.013   1984>-0.010  Higher   2017 0.024   1990 0.023

[E] Outliers     1   3.0 SD above or -4.5 SD below mean for year
      1988 +3.6 SD
====================================================================================================================================

03A       1895 to  2017     123 years                                                                                    Series   4

[*] Early part of series cannot be checked from 1895 to 1896 -- not matched by another series

[A] Segment   High   -10   -9   -8   -7   -6   -5   -4   -3   -2   -1    0   +1   +2   +3   +4   +5   +6   +7   +8   +9  +10
   ---------  ----   ---  ---  ---  ---  ---  ---  ---  ---  ---  ---  ---  ---  ---  ---  ---  ---  ---  ---  ---  ---  ---
   1897 1946    5      -    -    -    -    -    -    -    -  .03 -.04  .30| .12  .06  .15  .14  .37*-.08  .17  .13 -.20  .12
   1900 1949    5      -    -    -    -    -  .09 -.18 -.12  .04 -.07  .26| .04  .03  .21  .12  .38*-.07  .18  .16 -.17  .17
   1925 1974    5   -.15  .11  .02  .02  .08  .10 -.06 -.08  .20  .08  .31|-.14  .01  .25 -.04  .34*-.20  .11  .06 -.12  .07

[B] Entire series, effect on correlation ( 0.386) is:
      Lower   1929>-0.022   2005<-0.018   1920<-0.015   1916>-0.013   1927<-0.013   1947<-0.012  Higher   1944 0.037   2016 0.020
    1897 to 1946 segment:
      Lower   1929>-0.037   1920<-0.031   1927<-0.026   1899<-0.023   1945>-0.015   1904<-0.013  Higher   1944 0.087   1900 0.023
    1900 to 1949 segment:
      Lower   1929>-0.035   1920<-0.033   1927<-0.027   1947<-0.026   1904<-0.014   1945>-0.013  Higher   1944 0.103   1900 0.024
    1925 to 1974 segment:
      Lower   1929>-0.051   1927<-0.034   1947<-0.031   1945>-0.020   1961>-0.016   1968<-0.011  Higher   1944 0.118   1972 0.032

[E] Outliers     3   3.0 SD above or -4.5 SD below mean for year
      1916 +4.7 SD;    1929 +3.1 SD;    1939 +3.7 SD
====================================================================================================================================

03B       1897 to  2017     121 years                                                                                    Series   5

[A] Segment   High   -10   -9   -8   -7   -6   -5   -4   -3   -2   -1    0   +1   +2   +3   +4   +5   +6   +7   +8   +9  +10
   ---------  ----   ---  ---  ---  ---  ---  ---  ---  ---  ---  ---  ---  ---  ---  ---  ---  ---  ---  ---  ---  ---  ---
   1897 1946    1      -    -    -    -    -    -    -    -  .10  .18  .15| .25*-.09  .14  .00  .06  .21 -.31 -.02  .05  .01
   1900 1949    6      -    -    -    -    - -.18  .19 -.07  .02  .14  .13| .25 -.04  .18  .01  .13  .31*-.25  .01  .09  .03
   1925 1974    6   -.26 -.04  .12 -.03  .15 -.12  .24 -.08 -.07  .02  .19| .25 -.05 -.01  .11  .09  .36*-.32  .24  .04 -.17

[B] Entire series, effect on correlation ( 0.340) is:
      Lower   1938>-0.041   1916<-0.035   1964>-0.020   1918>-0.016   1946<-0.011   1917>-0.011  Higher   1944 0.023   2006 0.022
    1897 to 1946 segment:
      Lower   1938>-0.064   1916<-0.053   1918>-0.029   1917>-0.019   1946<-0.019   1899>-0.018  Higher   1944 0.073   1925 0.055
    1900 to 1949 segment:
      Lower   1938>-0.064   1916<-0.052   1918>-0.031   1917>-0.020   1931>-0.019   1946<-0.019  Higher   1944 0.084   1925 0.058
    1925 to 1974 segment:
      Lower   1938>-0.070   1964>-0.041   1939<-0.029   1946<-0.024   1931>-0.021   1943>-0.021  Higher   1944 0.074   1925 0.070

[C] Year-to-year changes diverging by over 4.0 std deviations:
      1937 1938   4.3 SD    1938 1939  -4.1 SD
```

```
[E] Outliers     2   3.0 SD above or -4.5 SD below mean for year
      1938 +5.0 SD;    1964 +3.2 SD
====================================================================================================================================

 04B       1926 to  2017      92 years                                                                                  Series   6

 [A] Segment   High   -10   -9   -8   -7   -6   -5   -4   -3   -2   -1    0   +1   +2   +3   +4   +5   +6   +7   +8   +9  +10
   ---------  ----   ---  ---  ---  ---  ---  ---  ---  ---  ---  ---  ---  ---  ---  ---  ---  ---  ---  ---  ---  ---  ---
   1926 1975   -5    .10 -.03  .15 -.09  .13  .46*-.06  .17  .05  .06  .40|-.16  .18  .10 -.04  .01 -.06  .07 -.15  .19 -.10
   1950 1999   -5   -.01 -.03  .09  .04 -.06  .50*-.03  .21  .28  .28  .04| .28  .00 -.07 -.05 -.19  .02  .09 -.14  .09 -.07
   1968 2017   -5   -.11 -.21  .01 -.01 -.05  .41* .06  .15  .16  .21  .21|   -    -    -    -    -    -    -    -    -    -

 [B] Entire series, effect on correlation ( 0.326) is:
       Lower   1992>-0.029   1980>-0.018   1988<-0.016   1974<-0.015   1969>-0.014   1996>-0.014  Higher   1944 0.069   1932 0.028
     1926 to 1975 segment:
       Lower   1949>-0.048   1969>-0.044   1974<-0.034   1968<-0.025   1955>-0.017   1973>-0.017  Higher   1944 0.177   1932 0.066
     1950 to 1999 segment:
       Lower   1988<-0.028   1974<-0.024   1969>-0.024   1996>-0.024   1986>-0.021   1968<-0.019  Higher   1994 0.041   1990 0.023
     1968 to 2017 segment:
       Lower   1992>-0.042   1988<-0.027   1980>-0.026   1974<-0.024   1969>-0.019   1968<-0.019  Higher   2006 0.062   2016 0.041

 [C] Year-to-year changes diverging by over 4.0 std deviations:
       1991 1992   4.3 SD

 [E] Outliers     2   3.0 SD above or -4.5 SD below mean for year
       1949 +4.4 SD;    1992 +4.1 SD
====================================================================================================================================

 05B       1966 to  2017      52 years                                                                                  Series   7

 [B] Entire series, effect on correlation ( 0.449) is:
       Lower   1993<-0.063   1970>-0.050   1999>-0.024   1989>-0.019   1979<-0.015   1983>-0.013  Higher   2016 0.049   1990 0.035

 [E] Outliers     1   3.0 SD above or -4.5 SD below mean for year
       1999 +3.2 SD
====================================================================================================================================

 06B       1950 to  2017      68 years                                                                                  Series   8

 [A] Segment   High   -10   -9   -8   -7   -6   -5   -4   -3   -2   -1    0   +1   +2   +3   +4   +5   +6   +7   +8   +9  +10
   ---------  ----   ---  ---  ---  ---  ---  ---  ---  ---  ---  ---  ---  ---  ---  ---  ---  ---  ---  ---  ---  ---  ---
   1950 1999    1   -.12  .04 -.09 -.21 -.10  .02 -.20  .02  .04 -.13  .11| .29* .15  .19  .02 -.15 -.18  .00 -.08 -.06 -.09

 [B] Entire series, effect on correlation ( 0.332) is:
       Lower   1993<-0.055   1962>-0.034   1964>-0.025   1991<-0.023   1999<-0.023   1975<-0.017  Higher   1990 0.068   2017 0.050
     1950 to 1999 segment:
       Lower   1993<-0.064   1962>-0.042   1964>-0.031   1999<-0.025   1975<-0.019   1991<-0.019  Higher   1990 0.181   1968 0.027

 [C] Year-to-year changes diverging by over 4.0 std deviations:
       1990 1991  -4.1 SD    1993 1994   4.3 SD
```

```
[E] Outliers     2   3.0 SD above or -4.5 SD below mean for year
      1962 +3.1 SD;    1990 +4.7 SD
=======================================================================================================================================

07A       1920 to  2017      98 years                                                                                    Series   9

[B] Entire series, effect on correlation ( 0.664) is:
      Lower   1973>-0.021   1992>-0.013   1975<-0.009   1936<-0.009   1964>-0.008   1942>-0.007  Higher   1944 0.027   1925 0.016

[E] Outliers     1   3.0 SD above or -4.5 SD below mean for year
      1979 +3.7 SD
=======================================================================================================================================

07B       1920 to  2017      98 years                                                                                    Series  10

[B] Entire series, effect on correlation ( 0.543) is:
      Lower   2011>-0.035   1940>-0.012   1941<-0.010   1991<-0.009   1983<-0.009   1938<-0.007  Higher   1944 0.037   1993 0.020

[E] Outliers     3   3.0 SD above or -4.5 SD below mean for year
      1944 +4.7 SD;    1979 +3.6 SD;    2011 +3.4 SD
=======================================================================================================================================

09A       1950 to  2017      68 years                                                                                    Series  11

[A] Segment   High   -10   -9   -8   -7   -6   -5   -4   -3   -2   -1    0   +1   +2   +3   +4   +5   +6   +7   +8   +9  +10
    ---------  ----   ---  ---  ---  ---  ---  ---  ---  ---  ---  ---  ---  ---  ---  ---  ---  ---  ---  ---  ---  ---  ---
    1950 1999   -9    .04  .21* .19  .06 -.13  .01 -.14  .12 -.12  .08  .15| .08  .00  .09 -.09 -.07 -.01 -.02  .00  .18  .09

[B] Entire series, effect on correlation ( 0.297) is:
      Lower   1965>-0.058   1972<-0.045   1974<-0.031   1990<-0.021   1963>-0.018   1957>-0.017  Higher   2017 0.059   1991 0.042
    1950 to 1999 segment:
      Lower   1965>-0.070   1972<-0.060   1974<-0.042   1990<-0.026   1963>-0.023   1957>-0.022  Higher   1991 0.075   1993 0.072

[E] Outliers     1   3.0 SD above or -4.5 SD below mean for year
      1965 +4.5 SD
=======================================================================================================================================

09B       1950 to  2017      68 years                                                                                    Series  12

[A] Segment   High   -10   -9   -8   -7   -6   -5   -4   -3   -2   -1    0   +1   +2   +3   +4   +5   +6   +7   +8   +9  +10
    ---------  ----   ---  ---  ---  ---  ---  ---  ---  ---  ---  ---  ---  ---  ---  ---  ---  ---  ---  ---  ---  ---  ---
    1950 1999    1    .08  .08  .14  .09 -.13  .00 -.13  .21 -.11  .06  .22| .33*-.04  .18 -.07 -.05 -.05 -.21 -.07  .05  .02

[B] Entire series, effect on correlation ( 0.324) is:
      Lower   1972<-0.085   1965>-0.040   1968<-0.024   2012<-0.020   1971>-0.018   1974<-0.017  Higher   2017 0.048   1991 0.041
    1950 to 1999 segment:
      Lower   1972<-0.121   1965>-0.048   1968<-0.034   1974<-0.025   1971>-0.023   1966<-0.019  Higher   1991 0.066   1994 0.052

[C] Year-to-year changes diverging by over 4.0 std deviations:
      1971 1972  -4.3 SD
```

```
[E] Outliers     2   3.0 SD above or -4.5 SD below mean for year
      1965 +3.4 SD;    1978 +3.4 SD
====================================================================================================================================

 10A       1956 to  2017      62 years                                                                                    Series  13

[A] Segment   High   -10   -9   -8   -7   -6   -5   -4   -3   -2   -1    0   +1   +2   +3   +4   +5   +6   +7   +8   +9  +10
   ---------  ----   ---  ---  ---  ---  ---  ---  ---  ---  ---  ---  ---  ---  ---  ---  ---  ---  ---  ---  ---  ---  ---
   1956 2005   -2   -.20  .08 -.11 -.15 -.02 -.10 -.11  .07  .55*-.06  .42|-.07 -.04  .02 -.04  .12  .08  .13 -.13 -.08  .06

[B] Entire series, effect on correlation ( 0.511) is:
      Lower   1979<-0.057   1967>-0.055   1991<-0.044   1987<-0.017   1956>-0.011   1975<-0.011  Higher   1993 0.051   2006 0.026
    1956 to 2005 segment:
      Lower   1979<-0.074   1967>-0.067   1991<-0.059   1987<-0.021   1975<-0.014   1956>-0.013  Higher   1993 0.100   1974 0.026

[E] Outliers     2   3.0 SD above or -4.5 SD below mean for year
      1967 +3.4 SD;    1993 +3.4 SD
====================================================================================================================================

 10B       1951 to  2017      67 years                                                                                    Series  14

[A] Segment   High   -10   -9   -8   -7   -6   -5   -4   -3   -2   -1    0   +1   +2   +3   +4   +5   +6   +7   +8   +9  +10
   ---------  ----   ---  ---  ---  ---  ---  ---  ---  ---  ---  ---  ---  ---  ---  ---  ---  ---  ---  ---  ---  ---  ---
   1951 2000   -2   -.27  .09 -.25 -.21 -.07 -.08 -.03  .08  .53*-.03  .24|-.20 -.16  .04 -.02 -.12  .08  .07 -.10  .06  .07

[B] Entire series, effect on correlation ( 0.381) is:
      Lower   1979<-0.041   1991<-0.035   1965>-0.031   1976>-0.025   1952<-0.025   1955>-0.022  Higher   1993 0.071   2016 0.048
    1951 to 2000 segment:
      Lower   1979<-0.052   1991<-0.043   1965>-0.036   1976>-0.032   1952<-0.031   1955>-0.029  Higher   1993 0.144   1968 0.031

[E] Outliers     2   3.0 SD above or -4.5 SD below mean for year
      1993 +3.2 SD;    1995 +3.0 SD
====================================================================================================================================

 13A       1935 to  2017      83 years                                                                                    Series  15

[A] Segment   High   -10   -9   -8   -7   -6   -5   -4   -3   -2   -1    0   +1   +2   +3   +4   +5   +6   +7   +8   +9  +10
   ---------  ----   ---  ---  ---  ---  ---  ---  ---  ---  ---  ---  ---  ---  ---  ---  ---  ---  ---  ---  ---  ---  ---
   1935 1984   -7    .00  .08 -.16  .36*-.18  .06  .23  .14  .17 -.22  .09| .07  .11  .23 -.27  .13  .01  .05  .12 -.01 -.13

[B] Entire series, effect on correlation ( 0.420) is:
      Lower   1944<-0.041   1948>-0.033   1968<-0.030   1953<-0.019   1945<-0.017   1998>-0.017  Higher   1993 0.030   1990 0.029
    1935 to 1984 segment:
      Lower   1948>-0.049   1968<-0.045   1944<-0.035   1974<-0.023   1971>-0.022   1953<-0.022  Higher   1979 0.089   1972 0.055

[E] Outliers     1   3.0 SD above or -4.5 SD below mean for year
      1948 +3.1 SD
====================================================================================================================================

 14A       1909 to  2013     105 years                                                                                    Series  16
```

```
[A] Segment   High   -10   -9   -8   -7   -6   -5   -4   -3   -2   -1    0   +1   +2   +3   +4   +5   +6   +7   +8   +9  +10
   ---------  ----   ---  ---  ---  ---  ---  ---  ---  ---  ---  ---  ---  ---  ---  ---  ---  ---  ---  ---  ---  ---  ---
   1909 1958   -3   -.18  .16  .13 -.26  .17 -.27  .14  .44* .03  .16 -.12|-.02 -.05  .03  .23 -.11 -.14 -.13  .04  .10  .02
   1925 1974   -6   -.20  .17  .10 -.13  .31*-.30  .09  .19  .16  .19  .04|-.13  .08  .02  .25 -.06  .14 -.06 -.21  .18 -.13

[B] Entire series, effect on correlation ( 0.289) is:
     Lower   1919>-0.052   1944<-0.042   1939<-0.025   1916<-0.024   1949<-0.018   1945>-0.016  Higher   1993 0.050   1979 0.028
    1909 to 1958 segment:
     Lower   1919>-0.075   1939<-0.033   1944<-0.028   1949<-0.023   1940>-0.020   1945>-0.014  Higher   1925 0.075   1920 0.034
    1925 to 1974 segment:
     Lower   1944<-0.052   1939<-0.043   1940>-0.033   1945>-0.030   1949<-0.029   1947>-0.019  Higher   1925 0.070   1972 0.055

[C] Year-to-year changes diverging by over 4.0 std deviations:
     1918 1919   4.2 SD    1944 1945   4.9 SD

[E] Outliers     4   3.0 SD above or -4.5 SD below mean for year
     1919 +3.8 SD;    1920 +3.1 SD;    1947 +3.2 SD;    1993 +3.6 SD
====================================================================================================================================

14B       1909 to  2013     105 years                                                                                    Series  17

[A] Segment   High   -10   -9   -8   -7   -6   -5   -4   -3   -2   -1    0   +1   +2   +3   +4   +5   +6   +7   +8   +9  +10
   ---------  ----   ---  ---  ---  ---  ---  ---  ---  ---  ---  ---  ---  ---  ---  ---  ---  ---  ---  ---  ---  ---  ---
   1909 1958    3    .06 -.05 -.36 -.03 -.25  .25  .07 -.04  .24  .00  .04|-.07  .07  .36*-.11 -.09  .08  .20  .18 -.20 -.06
   1925 1974   -2   -.06  .00 -.27  .03 -.23 -.01  .04  .01  .30*-.15  .13|-.12  .09  .25 -.07  .05  .10  .23  .11  .08 -.08

[B] Entire series, effect on correlation ( 0.318) is:
     Lower   1911<-0.036   1944<-0.029   1919<-0.021   1938<-0.017   1933>-0.013   1939<-0.012  Higher   1993 0.039   1979 0.025
    1909 to 1958 segment:
     Lower   1911<-0.051   1919<-0.031   1938<-0.025   1933>-0.024   1946>-0.017   1944<-0.016  Higher   1916 0.068   1932 0.048
    1925 to 1974 segment:
     Lower   1944<-0.039   1938<-0.034   1933>-0.029   1959>-0.024   1946>-0.022   1949<-0.021  Higher   1932 0.052   1972 0.051

[E] Outliers     1   3.0 SD above or -4.5 SD below mean for year
     1921 +3.2 SD
====================================================================================================================================

15A       1953 to  2017      65 years                                                                                    Series  18

[B] Entire series, effect on correlation ( 0.626) is:
     Lower   1993<-0.040   2017<-0.028   1969>-0.015   1981<-0.012   1953>-0.012   1987<-0.011  Higher   1991 0.036   2016 0.029

====================================================================================================================================

15B       1956 to  2017      62 years                                                                                    Series  19

[B] Entire series, effect on correlation ( 0.592) is:
     Lower   1993<-0.030   1992<-0.016   1967>-0.012   1977<-0.012   1969>-0.010   2008>-0.010  Higher   1991 0.030   2017 0.028

[E] Outliers     1   3.0 SD above or -4.5 SD below mean for year
```

1991 +4.1 SD

PART 7: DESCRIPTIVE STATISTICS: 17:07 Mon 13 May 2019 Page 6

							Unfiltered					Filtered			
Seq	Series	Interval	No. Years	No. Segmt	No. Flags	Corr with Master	Mean msmt	Max msmt	Std dev	Auto corr	Mean sens	Max value	Std dev	Auto corr	AR ()
1	01A	1950 2017	68	2	1	0.283	2.13	6.69	1.304	0.263	0.514	2.59	0.702	0.003	1
2	02A	1970 2017	48	1	0	0.454	1.78	5.69	1.338	0.299	0.675	2.45	0.909	0.002	1
3	02B	1967 2017	51	2	0	0.574	2.17	7.00	1.649	0.546	0.572	2.18	0.704	-0.003	2
4	03A	1895 2017	123	5	3	0.386	1.73	8.00	1.405	0.559	0.517	2.97	0.735	-0.010	1
5	03B	1897 2017	121	5	3	0.340	1.62	8.51	1.363	0.585	0.442	2.31	0.571	-0.003	1
6	04B	1926 2017	92	3	3	0.326	1.80	10.59	1.816	0.456	0.506	2.84	0.773	-0.004	1
7	05B	1966 2017	52	2	0	0.449	1.93	5.44	1.457	0.481	0.573	2.12	0.829	-0.008	1
8	06B	1950 2017	68	2	1	0.332	1.62	5.57	1.296	0.469	0.502	5.60	1.247	-0.009	1
9	07A	1920 2017	98	4	0	0.664	1.61	8.17	1.762	0.640	0.484	2.57	0.697	-0.002	2
10	07B	1920 2017	98	4	0	0.543	1.54	9.72	1.565	0.536	0.459	3.69	0.750	0.006	2
11	09A	1950 2017	68	2	1	0.297	1.54	4.04	0.924	0.443	0.481	1.87	0.601	0.013	2
12	09B	1950 2017	68	2	1	0.324	1.50	3.64	0.868	0.473	0.472	1.62	0.610	-0.029	1
13	10A	1956 2017	62	2	1	0.511	1.76	6.67	1.470	0.575	0.514	2.89	0.772	-0.022	1
14	10B	1951 2017	67	2	1	0.381	1.70	7.16	1.479	0.406	0.662	3.41	0.897	0.009	2
15	13A	1935 2017	83	3	1	0.420	1.98	7.21	1.859	0.818	0.408	1.33	0.521	-0.007	1
16	14A	1909 2013	105	4	2	0.289	1.81	8.55	1.860	0.693	0.517	2.84	0.714	-0.023	1
17	14B	1909 2013	105	4	2	0.318	2.05	9.14	1.989	0.758	0.502	1.78	0.633	-0.015	1
18	15A	1953 2017	65	2	0	0.626	1.86	4.83	1.215	0.420	0.528	1.62	0.652	0.006	1
19	15B	1956 2017	62	2	0	0.592	2.07	9.15	1.825	0.414	0.591	4.02	0.916	0.022	1
Total or mean:			1504	53	20	0.418	1.78	10.59	1.526	0.540	0.511	5.60	0.732	-0.005	

- = [COFECHA Coastal COF] = -

Bibliography

Allen, J. A., Chambers, J. L., and Pezeshki, S. R. (1997). Effects of salinity on baldcypress seedlings: Physiological responses and their relation to salinity tolerance. *Wetlands*, 17(2):310–320.

Allen, J. A., Chambers, J. L., and Stine, M. (1994). Prospects for increasing the salt tolerance of forest trees: A review. *Tree Physiology*, 14:843–853.

Allison, M. A. (1998). Historical changes in the Ganges-Brahmaputra delta front. *Journal of Coastal Research*, 14(4):1269–1275.

Anchukaitis, K. J., Evans, M. N., Lange, T., Smith, D. R., Leavitt, S. W., and Schrag, D. P. (2008). Consequences of a rapid cellulose extraction technique for oxygen isotope and radiocarbon analyses. *Analytical Chemistry*, 80(6):2035–2041.

Anderson, W. T., Sternberg, L., Pinzon, M., Gann-Troxler, T., Childers, D. L., and Duever, M. (2005). Carbon isotopic composition of cypress trees from South Florida and changing hydrologic conditions. *Dendrochronologia*, 23(1):1–10.

Andrade Jr, E. R. and Sellers, W. D. (1988). El Niño and its effect on precipitation in Arizona and western New Mexico. *Journal of Climatology*, 8(4):403–410.

Atwater, B. F. and Yamaguchi, D. K. (1991). Sudden, probably coseismic submergence of Holocene trees and grass in coastal Washington State. *Geology*, 19(7):706–709.

Baisan, C. H. and Swetnam, T. W. (1990). Fire history on a desert mountain range: Rincon Mountain Wilderness, Arizona, USA. *Canadian Journal of Forest Research*, 20(10):1559–1569.

Barnes, A. (2010). *Bibliography of Florence Hawley Ellis*. Maxwell Museum of Anthropology, University of New Mexico.

Berger, A. (1980). The Milankovitch astronomical theory of paleoclimates: A modern review. *Vistas in Astronomy*, 24:103–122.

Berger, A. (1988). Milankovitch theory and climate. *Reviews of Geophysics*, 26(4):624–657.

Berger, U., Rivera-Monroy, V. H., Doyle, T. W., Dahdouh-Guebas, F., Duke, N. C., Fontalvo-Herazo, M. L., Hildenbrandt, H., Koedam, N., Mehlig, U., Piou, C., et al. (2008). Advances and limitations of individual-based models to analyze and predict dynamics of mangrove forests: A review. *Aquatic Botany*, 89(2):260–274.

Blum, M. D. and Roberts, H. H. (2009). Drowning of the Mississippi Delta due to insufficient sediment supply and global sea-level rise. *Nature Geoscience*, 2(7):488.

Bocanegra-Ramírez, D. M., Li, H.-C., Vázquez, G. D., Israde-Alcántara, I., and Bischoff, J. L. (2019). Holocene climate change and sea level oscillations in the Pacific Coast of Mexico. *Quaternary International*, 528:100–108.

Bove, M. C., Elsner, J. B., Landsea, C. W., Niu, X., and O'Brien, J. J. (1998). Effect of El Niño on US landfalling hurricanes, revisited. *Bulletin of the American Meteorological Society*, 79(11):2477–2482.

Brendel, O., Iannetta, P., and Stewart, D. (2000). A rapid and simple method to isolate pure α-cellulose. *Phytochemical Analysis: An International Journal of Plant Chemical and Biochemical Techniques*, 11(1):7–10.

Brienen, R. J., Helle, G., Pons, T. L., Guyot, J.-L., and Gloor, M. (2012). Oxygen isotopes in tree rings are a good proxy for Amazon precipitation and El Niño-Southern Oscillation variability. *Proceedings of the National Academy of Sciences*, 109(42):16957–16962.

Brown, P. M. (1996). OLDLIST: A database of maximum tree ages. In *Tree rings, Environment, and Humanity. Radiocarbon 1996*, pages 727–731. University of Arizona.

Bull, H. (1949). Cypress planting in southern Louisiana. *Southern Lumberman Christmas*, page 1.

Bunn, A. G. (2008). A dendrochronology program library in R (dplR). *Dendrochronologia*, 26(2):115–124.

Cain, W. F. and Suess, H. E. (1976). Carbon 14 in tree rings. *Journal of Geophysical Research*, 81(21):3688–3694.

Castañeda-Moya, E., Rivera-Monroy, V. H., Chambers, R. M., Zhao, X., Lamb-Wotton, L., Gorsky, A., Gaiser, E. E., Troxler, T. G., Kominoski, J. S., and Hiatt, M. (2020). Hurricanes fertilize mangrove forests in the Gulf of Mexico (Florida Everglades, USA). *Proceedings of the National Academy of Sciences*, 117(9):4831–4841.

Church, J. A. and White, N. J. (2006). A 20th century acceleration in global sea-level rise. *Geophysical Research Letters*, 33(1).

Clark, P. U. and Mix, A. C. (2002). Ice sheets and sea level of the Last Glacial Maximum. *Quaternary Science Reviews*, 21(1-3):1–7.

Cleaveland, M. K., Stahle, D. W., Therrell, M. D., Villanueva-Diaz, J., and Burns, B. T. (2003). Tree-ring reconstructed winter precipitation and tropical teleconnections in Durango, Mexico. *Climatic Change*, 59(3):369–388.

Coker, C. E., Bachman, G., Boyd, C., Blanchard, P. B., Bush, E., and Gu, M. (2010). Coastal Roots: Connecting students with sustainability in Mississippi and Louisiana. *HortTechnology*, 20(3):499–502.

Coleman, J. M., Roberts, H. H., and Stone, G. W. (1998). Mississippi River delta: An overview. *Journal of Coastal Research*, 14(3):699–716.

Conner, W. H. (1994). The effect of salinity and waterlogging on growth and survival of baldcypress and Chinese tallow seedlings. *Journal of Coastal Research*, 10(4):1045–1049.

Conner, W. H. (1998). Impact of hurricanes on forests of the Atlantic and Gulf Coasts, USA. *Coastally Restricted Forests*, pages 271–277.

Conner, W. H. and Askew, G. R. (1992). Response of baldcypress and loblolly pine seedlings to short-term saltwater flooding. *Wetlands*, 12(3):230–233.

Conner, W. H., Toliver, J. R., and Sklar, F. H. (1986). Natural regeneration of baldcypress (*Taxodium distichum* (L.) Rich.) in a Louisiana swamp. *Forest Ecology and Management*, 14(4):305–317.

Cook, E. R. and Peters, K. (1981). The smoothing spline: A new approach to standardizing forest interior tree-ring width series for dendroclimatic studies. *Tree-Ring Bulletin*, 41:45–53.

Copenheaver, C. A., Pulice, M. J., Lawrence, N. J., Raso, C. H., Cankaya, E. C., Wan, H., and Poling, B. T. (2017). Dendroarchaeology reveals influence of early-European settlement on forest disturbance regimes in the Appalachian Mountains, USA. *Écoscience*, 24(1-2):33–40.

Cornejo-Oviedo, E. H., Voelker, S. L., Mainwaring, D. B., Maguire, D. A., Meinzer, F. C., and Brooks, J. R. (2017). Basal area growth, carbon isotope discrimination, and intrinsic water use efficiency after fertilization of Douglas-fir in the Oregon Coast Range. *Forest Ecology and Management*, 389:285–295.

Couvillion, B. R., Barras, J. A., Steyer, G. D., Sleavin, W., Fischer, M., Beck, H., Trahan, N., Griffin, B., and Heckman, D. (2011). Land area change in coastal Louisiana from 1932 to 2010: U.S. Geological Survey scientific investigations map 3164.

Couvillion, B. R. and Beck, H. (2013). Marsh collapse thresholds for coastal Louisiana estimated using elevation and vegetation index data. *Journal of Coastal Research*, 63(SI):58–67.

Csank, A. Z., Miller, A. E., Sherriff, R. L., Berg, E. E., and Welker, J. M. (2016). Tree-ring isotopes reveal drought sensitivity in trees killed by spruce beetle outbreaks in south-central Alaska. *Ecological Applications*, 26(7):2001–2020.

Daly, C., Taylor, G., and Gibson, W. (1997). The PRISM approach to mapping precipitation and temperature. In *Proceedings, 10th AMS Conference on Applied Climatology*, pages 20–23.

Das, A., Justic, D., Inoue, M., Hoda, A., Huang, H., and Park, D. (2012). Impacts of Mississippi River diversions on salinity gradients in a deltaic Louisiana estuary: Ecological and management implications. *Estuarine, Coastal and Shelf Science*, 111:17–26.

Day, J., Hunter, R., Keim, R. F., DeLaune, R., Shaffer, G., Evers, E., Reed, D., Brantley, C., Kemp, P., and Day, J. (2012). Ecological response of forested wetlands with and without large-scale Mississippi River input: Implications for management. *Ecological Engineering*, 46:57–67.

Day, J. W., Boesch, D. F., Clairain, E. J., Kemp, G. P., Laska, S. B., Mitsch, W. J., Orth, K., Mashriqui, H., Reed, D. J., Shabman, L., et al. (2007). Restoration of the Mississippi Delta: Lessons from Hurricanes Katrina and Rita. *Science*, 315(5819):1679–1684.

Day, J. W., Britsch, L. D., Hawes, S. R., Shaffer, G. P., Reed, D. J., and Cahoon, D. (2000). Pattern and process of land loss in the Mississippi Delta: A spatial and temporal analysis of wetland habitat change. *Estuaries*, 23(4):425–438.

Day Jr, J. and Templet, P. (1989). Consequences of sea level rise: Implications from the Mississippi Delta. *Coastal Management*, 17(3):241–257.

De Micco, V., Saurer, M., Aronne, G., Tognetti, R., and Cherubini, P. (2007). Variations of wood anatomy and δ^{13}C within-tree rings of coastal *Pinus pinaster* showing intra-annual density fluctuations. *Iawa Journal*, 28(1):61–74.

DeLaune, R. D., Nyman, J. A., and Patrick Jr, W. (1994). Peat collapse, ponding, and wetland loss in a rapidly submerging coastal marsh. *Journal of Coastal Research*, 10(4):1021–1030.

Delcourt, P. A., Delcourt, K. R., and Webb III, T. (1984). *Atlas of Mapped Distributions of Dominance and Modern Pollen Percentages for Important Tree Taxa of Eastern North America*. American Association of Stratigraphic Palynologists, Contributions Series, Number 14.

Donoghue, J. F. (2011). Sea level history of the northern Gulf of Mexico coast and sea level rise scenarios for the near future. *Climatic Change*, 107(1-2):17.

Doody, J. P. (2004). 'Coastal squeeze'—an historical perspective. *Journal of Coastal Conservation*, 10(1):129–138.

Douglass, A. E. (1909). Weather cycles in the growth of big trees. *Monthly Weather Review*, 37(6):225–237.

Douglass, A. E. (1914). A method of estimating rainfall by the growth of trees. *Bulletin of the American Geographical Society*, 46(5):321–335.

Doyle, T. and Gorham, L. (1996). Detecting hurricane impact and recovery from tree rings. *Tree Rings, Environment, and Humanity. Radiocarbon 1996*, pages 405–412.

Doyle, T. W., Conner, W. H., Ratard, M., and Inabinette, L. W. (2007). Assessing the impact of tidal flooding and salinity on long-term growth of baldcypress under changing climate and riverflow. In *Ecology of Tidal Freshwater Forested Wetlands of the Southeastern United States*, pages 411–445. Springer.

Doyle, T. W., Day, R. H., and Biagas, J. M. (2003). Predicting coastal retreat in the Florida Big Bend region of the Gulf Coast under climate change induced sea-level rise. In *Integrated Assessment of the Climate Change Impacts on the Gulf Coast Region*, pages 199–210. Gulf Coast Climate Change Assessment Council.

Doyle, T. W., Keeland, B. D., Gorham, L. E., and Johnson, D. J. (1995). Structural impact of Hurricane Andrew on the forested wetlands of the Atchafalaya Basin in south Louisiana. *Journal of Coastal Research*, 21(SI):354–364.

Doyle, T. W., Krauss, K. W., Conner, W. H., and From, A. S. (2010). Predicting the retreat and migration of tidal forests along the northern Gulf of Mexico under sea-level rise. *Forest Ecology and Management*, 259(4):770–777.

Drew, A. P. (1998). Growth rings, phenology, hurricane disturbance, and climate in *Cyrilla racemiflora* L., a rain forest tree of the Luquillo Mountains, Puerto Rico. *Biotropica*, 30(1):35–49.

Elsner, J. B., Jagger, T., and Niu, X.-F. (2000). Changes in the rates of North Atlantic major hurricane activity during the 20th century. *Geophysical Research Letters*, 27(12):1743–1746.

Elsner, J. B., Kossin, J. P., and Jagger, T. H. (2008). The increasing intensity of the strongest tropical cyclones. *Nature*, 455(7209):92.

Evans, M. N. and Schrag, D. P. (2004). A stable isotope-based approach to tropical dendroclimatology. *Geochimica et Cosmochimica Acta*, 68(16):3295–3305.

Ewe, S. M. and Sternberg, L. (2002). Seasonal water-use by the invasive exotic, *Schinus terebinthifolius*, in native and disturbed communities. *Oecologia*, 133:441–448.

Ewe, S. M. and Sternberg, L. d. S. L. (2003). Seasonal gas exchange characteristics of *Schinus terebinthifolius* in a native and disturbed upland community in Everglades National Park, Florida. *Forest Ecology and Management*, 179(1-3):27–36.

Ewel, K. C. (1995). Fire in cypress swamps in the southeastern United States. In *Fire in wetlands: A management perspective. Proceedings of the Tall Timbers Fire Ecology Conference*, number 19, pages 111–116.

Ewel, K. C. and Mitsch, W. J. (1978). The effects of fire on species composition in cypress dome ecosystems. *Florida Scientist*, pages 25–31.

Ewel, K. C. and Parendes, L. A. (1984). Usefulness of annual growth rings of cypress trees (*Taxodium distichum*) for impact analysis. *Tree-Ring Bulletin*, 44:39–43.

Fagherazzi, S., Mariotti, G., Wiberg, P. L., and McGlathery, K. J. (2013). Marsh collapse does not require sea level rise. *Oceanography*, 26(3):70–77.

Ford, C. R. and Brooks, J. R. (2003). Hydrological and climatic responses of *Pinus elliottii* var. *densa* in mesic pine flatwoods Florida, USA. *Annals of Forest Science*, 60(5):385–392.

Francey, R. and Farquhar, G. (1982). An explanation of $^{13}C/^{12}C$ variations in tree rings. *Nature*, 297(5861):28–31.

Freudenburg, W. R., Gramling, R., Laska, S., and Erikson, K. T. (2009). Disproportionality and disaster: Hurricane Katrina and the Mississippi River-Gulf Outlet. *Social Science Quarterly*, 90(3):497–515.

Fritts, H. (2012). *Tree Rings and Climate*. Elsevier.

George, S. S. and Esper, J. (2019). Concord and discord among Northern Hemisphere paleotemperature reconstructions from tree rings. *Quaternary Science Reviews*, 203:278–281.

Good, S. P., Mallia, D. V., Lin, J. C., and Bowen, G. J. (2014). Stable isotope analysis of precipitation samples obtained via crowdsourcing reveals the spatiotemporal evolution of Superstorm Sandy. *PloS one*, 9(3):e91117.

Gori, Y., Wehrens, R., Greule, M., Keppler, F., Ziller, L., La Porta, N., and Camin, F. (2013). Carbon, hydrogen, and oxygen stable isotope ratios of whole wood, cellulose, and lignin methoxyl groups of *Picea abies* as climate proxies. *Rapid Communications in Mass Spectrometry*, 27(1):265–275.

Gosselink, J. G. (2001). Comments on "Wetland loss in the northern Gulf of Mexico: Multiple working hypotheses" by RE Turner. 1997. *Estuaries* 20:1-13. *Estuaries*, 24(4):636–639.

Granato-Souza, D., Stahle, D. W., Barbosa, A. C., Feng, S., Torbenson, M. C., de Assis Pereira, G., Schöngart, J., Barbosa, J. P., and Griffin, D. (2018). Tree rings and rainfall in the equatorial Amazon. *Climate Dynamics*, pages 1–13.

Graumlich, L. J. (1987). Precipitation variation in the Pacific Northwest (1675–1975) as reconstructed from tree rings. *Annals of the Association of American Geographers*, 77(1):19–29.

Gresham, C. A., Williams, T. M., and Lipscomb, D. J. (1991). Hurricane Hugo wind damage to southeastern US coastal forest tree species. *Biotropica*, pages 420–426.

Grinsted, A., Ditlevsen, P., and Christensen, J. H. (2019). Normalized US hurricane damage estimates using area of total destruction, 1900–2018. *Proceedings of the National Academy of Sciences*, 116(48):23942–23946.

Grissino-Mayer, H. D., Miller, D. L., and Mora, C. I. (2010). Dendrotempestology and the isotopic record of tropical cyclones in tree rings of the southeastern United States. In *Tree Rings and Natural Hazards*, pages 291–303. Springer.

Harley, G. L., Grissino-Mayer, H. D., Franklin, J. A., Anderson, C., and Köse, N. (2012). Cambial activity of *Pinus elliottii* var. *densa* reveals influence of seasonal insolation on growth dynamics in the Florida Keys. *Trees*, 26(5):1449–1459.

Harley, G. L., Grissino-Mayer, H. D., and Horn, S. P. (2011). The dendrochronology of *Pinus elliottii* in the lower Florida Keys: Chronology development and climate response. *Tree-Ring Research*, 67(1):39–50.

Harley, G. L., Maxwell, J. T., Holt, D., and Speagle, C. B. (2017). Construction history of the Deason House, Jones County, Mississippi. *Dendrochronologia*, 43:50–58.

Harley, G. L., Maxwell, J. T., and Raber, G. T. (2015). Elevation promotes long-term survival of *Pinus elliottii* var. *densa*, a foundation species of the endangered pine rockland ecosystem in the Florida Keys. *Endangered Species Research*, 29(2):117–130.

Harris, I., Jones, P. D., Osborn, T. J., and Lister, D. H. (2014). Updated high-resolution grids of monthly climatic observations—the CRU TS3.10 dataset. *International Journal of Climatology*, 34(3):623–642.

Hawley, F. M. (1937). Relationship of southern cedar growth to precipitation and run off. *Ecology*, 18(3):398–405.

Hay, C. C., Morrow, E., Kopp, R. E., and Mitrovica, J. X. (2015). Probabilistic reanalysis of twentieth-century sea-level rise. *Nature*, 517(7535):481.

Hebert, P. J., Jarrell, J. D., and Mayfield, M. (1996). *The Deadliest, Costliest, and Most Intense United States Hurricanes of this Century (and Other Frequently Requested Hurricane Facts)*. National Hurricane Center Coral Gables, FL.

Henderson, J. P. and Grissino-Mayer, H. D. (2009). Climate–tree growth relationships of longleaf pine (*Pinus palustris* mill.) in the southeastern Coastal Plain, USA. *Dendrochronologia*, 27(1):31–43.

Hilbert, K. W. (2006). Land cover change within the Grand Bay National Estuarine Research Reserve: 1974–2001. *Journal of Coastal Research*, 22(6):1552–1557.

Holmes, R. L., Adams, R. K., and Fritts, H. C. (1986). *Tree-ring Chronologies of Western North America: California, Eastern Oregon and Northern Great Basin with Procedures Used in the Chronology Development Work Including Users Manuals for Computer Programs COFECHA and ARSTAN*. University of Arizona.

Huang, R., Zhu, H., Liang, E., Liu, B., Shi, J., Zhang, R., Yuan, Y., and Grießinger, J. (2019). A tree ring-based winter temperature reconstruction for the southeastern Tibetan Plateau since 1340 CE. *Climate Dynamics*, pages 1–13.

Jarvinen, B., Neumann, C., and Davis, M. (1984). A tropical cyclone data tape for the North Atlantic Basin, 1886–1983: Contents, limitations, and uses. Technical report, NWS NHC 22, National Oceanic and Atmospheric Administration.

Johnstone, J. A., Roden, J. S., and Dawson, T. E. (2013). Oxygen and carbon stable isotopes in coast redwood tree rings respond to spring and summer climate signals. *Journal of Geophysical Research: Biogeosciences*, 118(4):1438–1450.

Julian, P. R. and Chervin, R. M. (1978). A study of the Southern Oscillation and Walker Circulation phenomenon. *Monthly Weather Review*, 106(10):1433–1451.

Karsh, K., Bush, E., Hinson, J., and Blanchard, P. (2009). Integrating horticulture biology and environmental coastal issues into the middle school science curriculum. *HortTechnology*, 19(4):813–817.

Kearney, M. S., Riter, J. A., and Turner, R. E. (2011). Freshwater river diversions for marsh restoration in Louisiana: Twenty-six years of changing vegetative cover and marsh area. *Geophysical Research Letters*, 38(16).

Keddy, P. A. (2009). Thinking big: A conservation vision for the southeastern Coastal Plain of North America. *Southeastern Naturalist*, pages 213–226.

Keeling, C. D. (1979). The Suess effect: ^{13}Carbon-^{14}Carbon interrelations. *Environment International*, 2(4-6):229–300.

Keeling, R. F. and Keeling, C. D. (2017). Atmospheric monthly in situ CO_2 data-Mauna Loa Observatory, Hawaii. *Scripps CO_2 Program Data. UC San Diego Library Digital Collections.*

Keim, B., Muller, R., and Stone, G. (2007). Spatiotemporal patterns and return periods of tropical storm and hurricane strikes from Texas to Maine. *Journal of Climate*, 20:3498–3509.

Kindinger, J. L., Balson, P. S., and Flocks, J. G. (1994). Stratigraphy of the Mississippi-Alabama shelf and the Mobile River incised-valley system. In *Incised-valley Systems: Origin and Sedimentary Sequence*. Special Publications of SEPM.

Kirwan, M. L. and Gedan, K. B. (2019). Sea-level driven land conversion and the formation of ghost forests. *Nature Climate Change*, 9(6):450–457.

Kirwan, M. L., Kirwan, J. L., and Copenheaver, C. A. (2007). Dynamics of an estuarine forest and its response to rising sea level. *Journal of Coastal Research*, 23(2):457–463.

Kirwan, M. L., Temmerman, S., Skeehan, E. E., Guntenspergen, G. R., and Fagherazzi, S. (2016). Overestimation of marsh vulnerability to sea level rise. *Nature Climate Change*, 6(3):253–260.

Knapp, P. A., Maxwell, J. T., and Soulé, P. T. (2016). Tropical cyclone rainfall variability in coastal North Carolina derived from longleaf pine (*Pinus palustris* mill.): AD 1771–2014. *Climatic Change*, 135(2):311–323.

Knox, C. C. (2017). A football field lost every 45 minutes: Evaluating local capacity to implement Louisiana's Coastal Master Plan. *Coastal Management*, 45(3):233–252.

Kolker, A. S., Cable, J. E., Johannesson, K. H., Allison, M. A., and Inniss, L. V. (2013). Pathways and processes associated with the transport of groundwater in deltaic systems. *Journal of Hydrology*, 498:319–334.

Kramer, K. A. (1990). *Late Pleistocene to Holocene Geologic Evolution of the Grande Batture Headland Area, Jackson County, Mississippi*. PhD thesis, Mississippi State University. Department of Geology and Geography.

Krauss, K. W. and Duberstein, J. A. (2010). Sapflow and water use of freshwater wetland trees exposed to saltwater incursion in a tidally influenced South Carolina watershed. *Canadian Journal of Forest Research*, 40(3):525–535.

Kropf, U., Korošec, M., Bertoncelj, J., Ogrinc, N., Nečemer, M., Kump, P., and Golob, T. (2010). Determination of the geographical origin of Slovenian black locust, lime and chestnut honey. *Food Chemistry*, 121(3):839–846.

Kurz, H. and Wagner, K. A. (1953). Factors in cypress dome development. *Ecology*, 34(1):157–164.

Lafon, C. W. and Kutac, M. J. (2003). Effects of ice storms, southern pine beetle infestation, and fire on Table Mountain pine forests of southwestern Virginia. *Physical Geography*, 24(6):502–519.

Landsea, C., Franklin, J., and Beven, J. (2015). The revised Atlantic hurricane database (HURDAT2). *Available online at nhc.noaa.gov.*

Landsea, C. W., Anderson, C., Charles, N., Clark, G., Dunion, J., Fernandez-Partagas, J., Hungerford, P., Neumann, C., and Zimmer, M. (2004). The Atlantic hurricane database re-analysis project: Documentation for the 1851–1910 alterations and additions to the HURDAT database. In *Hurricanes and Typhoons: Past, Present, and Future*, pages 177–221. Columbia University Press New York.

Landsea, C. W. and Franklin, J. L. (2013). Atlantic hurricane database uncertainty and presentation of a new database format. *Monthly Weather Review*, 141(10):3576–3592.

Lane, R. R., Day, J. W., and Thibodeaux, B. (1999). Water quality analysis of a freshwater diversion at Caernarvon, Louisiana. *Estuaries*, 22(2):327–336.

Larsson, L. (2014). CooRecorder and Cdendro programs of the CooRecorder/Cdendro package version 7.7.

Latimer, S. D., Devall, M. S., Thomas, C., Ellgaard, E. G., Kumar, S. D., and Thien, L. B. (1996). Dendrochronology and heavy metal deposition in tree rings of baldcypress. *Journal of Environmental Quality*, 25(6):1411–1419.

Leavitt, S. W. (2010). Tree-ring C–H–O isotope variability and sampling. *Science of the Total Environment*, 408(22):5244–5253.

Leavitt, S. W. and Lone, A. (1991). Seasonal stable-carbon isotope variability in tree rings: Possible paleoenvironmental signals. *Chemical Geology: Isotope Geoscience Section*, 87(1):59–70.

Leavitt, S. W., Wright, W. E., and Long, A. (2002). Spatial expression of ENSO, drought, and summer monsoon in seasonal δ^{13}C of ponderosa pine tree rings in southern Arizona and New Mexico. *Journal of Geophysical Research: Atmospheres*, 107(D18):ACL–3–10.

Liang, S., Zhou, R., Dong, S., and Shi, S. (2008). Adaptation to salinity in mangroves: Implication on the evolution of salt-tolerance. *Chinese Science Bulletin*, 53(11):1708.

Liu, K.-b. and Fearn, M. L. (1993). Lake-sediment record of late Holocene hurricane activities from coastal Alabama. *Geology*, 21(9):793–796.

Lloyd, J. and Farquhar, G. D. (2008). Effects of rising temperatures and CO_2 on the physiology of tropical forest trees. *Philosophical Transactions of the Royal Society B: Biological Sciences*, 363(1498):1811–1817.

Loader, N., Robertson, I., and McCarroll, D. (2003). Comparison of stable carbon isotope ratios in the whole wood, cellulose and lignin of oak tree-rings. *Palaeogeography, Palaeoclimatology, Palaeoecology*, 196(3-4):395–407.

Loader, N., Young, G., McCarroll, D., and Wilson, R. (2013). Quantifying uncertainty in isotope dendroclimatology. *The Holocene*, 23(9):1221–1226.

Mann, M. E., Bradley, R. S., and Hughes, M. K. (1999). Northern hemisphere temperatures during the past millennium: Inferences, uncertainties, and limitations. *Geophysical Research Letters*, 26(6):759–762.

Martin-Benito, D., Beeckman, H., and Canellas, I. (2013). Influence of drought on tree rings and tracheid features of *Pinus nigra* and *Pinus sylvestris* in a mesic Mediterranean forest. *European Journal of Forest Research*, 132(1):33–45.

Maxwell, J., Ficklin, D. L., Harley, G., and Jones, G. V. (2016). Projecting future winegrape yields using a combination of *Vitis vinifera* L. growth rings and soil moisture simulations, northern California, USA. *Australian Journal of Grape and Wine Research*, 22(1):73–80.

McCaffrey, R. J. and Thomson, J. (1980). A record of the accumulation of sediment and trace metals in a Connecticut salt marsh. In *Advances in Geophysics*, volume 22, pages 165–236. Elsevier.

McCarroll, D. and Loader, N. J. (2004). Stable isotopes in tree rings. *Quaternary Science Reviews*, 23(7-8):771–801.

McCullough, I. M., Davis, F. W., and Williams, A. P. (2017). A range of possibilities: Assessing geographic variation in climate sensitivity of ponderosa pine using tree rings. *Forest Ecology and Management*, 402:223–233.

Milankovitch, M. (1920). *Théorie mathématique des phénomènes thermiques produits par la radiation solaire*. Paris Gauthier-Villars.

Miller, D. L., Mora, C. I., Grissino-Mayer, H. D., Mock, C. J., Uhle, M. E., and Sharp, Z. (2006). Tree-ring isotope records of tropical cyclone activity. *Proceedings of the National Academy of Sciences*, 103(39):14294–14297.

Milliken, K. T., Anderson, J. B., and Rodriguez, A. B. (2008). A new composite Holocene sea-level curve for the northern Gulf of Mexico. *Geological Society of America Special Papers*, 443:1–11.

Milliman, J. D., Broadus, J. M., and Gable, F. (1989). Environmental and economic implications of rising sea level and subsiding deltas: The Nile and Bengal examples. *Ambio*, pages 340–345.

Mitchell, R. J., Kirkman, L. K., Pecot, S. D., Wilson, C. A., Palik, B. J., and Boring, L. R. (1999). Patterns and controls of ecosystem function in longleaf pine-wiregrass savannas. I. Aboveground net primary productivity. *Canadian Journal of Forest Research*, 29(6):743–751.

Mitchell, T. J., Knapp, P. A., and Ortegren, J. T. (2019). Tropical cyclone frequency inferred from intra-annual density fluctuations in longleaf pine in Florida, USA. *Climate Research*, 78(3):249–259.

Mitsch, W. J. and Ewel, K. C. (1979). Comparative biomass and growth of cypress in Florida wetlands. *American Midland Naturalist*, pages 417–426.

Mo, K. C. and Schemm, J. E. (2008). Relationships between ENSO and drought over the southeastern United States. *Geophysical Research Letters*, 35(15).

Mora, C. I., Miller, D. L., and Grissino-Mayer, H. D. (2006). Tempest in a tree ring: Paleotempestology and the record of past hurricanes. *The Sediment Record*, 4:4–8.

Needham, H. F. and Keim, B. D. (2012). A storm surge database for the US Gulf Coast. *International Journal of Climatology*, 32(14):2108–2123.

Needham, H. F., Keim, B. D., Sathiaraj, D., and Shafer, M. (2013). Storm surge return periods for the United States Gulf Coast. In *Advances in Hurricane Engineering: Learning from Our Past*, pages 715–740.

Nelson, W. L. (2008). *Assessing the Tree-ring Oxygen Isotope Hurricane Proxy Along the Atlantic and Gulf Coastal Seaboards, USA*. PhD thesis.

Nicklen, E. F., Roland, C. A., Csank, A. Z., Wilmking, M., Ruess, R. W., and Muldoon, L. A. (2019). Stand basal area and solar radiation amplify white spruce climate sensitivity in interior Alaska: Evidence from carbon isotopes and tree rings. *Global Change Biology*, 25(3):911–926.

NOAA (2018). https://www.ncdc.noaa.gov/teleconnections/enso.

Noel, J. and Changnon, D. (1998). A pilot study examining US winter cyclone frequency patterns associated with three ENSO parameters. *Journal of Climate*, 11(8):2152–2159.

Noss, R. F., Platt, W. J., Sorrie, B. A., Weakley, A. S., Means, D. B., Costanza, J., and Peet, R. K. (2015). How global biodiversity hotspots may go unrecognized: Lessons from the North American Coastal Plain. *Diversity and Distributions*, 21(2):236–244.

Nyman, J. (2014). Integrating successional ecology and the delta lobe cycle in wetland research and restoration. *Estuaries and coasts*, 37(6):1490–1505.

Nyman, J. A., DeLaune, R. D., Roberts, H. H., and Patrick Jr, W. (1993). Relationship between vegetation and soil formation in a rapidly submerging coastal marsh. *Marine Ecology Progress Series*, pages 269–279.

Nyman, J. A., Walters, R. J., Delaune, R. D., and Patrick Jr, W. H. (2006). Marsh vertical accretion via vegetative growth. *Estuarine, Coastal and Shelf Science*, 69(3-4):370–380.

Palik, B. J. and Pederson, N. (1996). Overstory mortality and canopy disturbances in longleaf pine ecosystems. *Canadian Journal of Forest Research*, 26(11):2035–2047.

Palmer, W. C. (1965). *Meteorological drought*, volume 30. US Department of Commerce, Weather Bureau.

Parry, M. (2002). Scenarios for climate impact and adaptation assessment. *Global Environmental Change*, 12(3):149–153.

Patterson, T. and Knapp, P. (2018). Longleaf pine masting, northern bobwhite quail, and tick-borne diseases in the southeastern United States. *Applied Geography*, 98:1–8.

Patterson, T. W. and Knapp, P. A. (2016). Observations on a rare old-growth montane longleaf pine forest in central North Carolina, USA. *Natural Areas Journal*, 36(2):153–162.

Pearl, J. K., Anchukaitis, K. J., Pederson, N., and Donnelly, J. P. (2020). Multivariate climate field reconstructions using tree rings for the northeastern United States. *Journal of Geophysical Research: Atmospheres*, 125(1):e2019JD031619.

Penland, S., Mendelssohn, I., Wayne, L., and Britsch, D. (1996). Natural and human causes of coastal land loss in Louisiana-workshop summary. *Baton Rouge: Coastal Studies Institute, Wetland Biogeochemistry Institute, Louisiana State University. Baton Rouge, La.*

Penland, S. and Ramsey, K. E. (1990). Relative sea-level rise in Louisiana and the Gulf of Mexico: 1908-1988. *Journal of Coastal Research*, 6(2):323–342.

Peyronnin, N., Green, M., Richards, C. P., Owens, A., Reed, D., Chamberlain, J., Groves, D. G., Rhinehart, W. K., and Belhadjali, K. (2013). Louisiana's 2012 Coastal Master Plan: Overview of a science-based and publicly informed decision-making process. *Journal of Coastal Research*, 67(SI):1–15.

Pezeshki, S. (1990). A comparative study of the response of *Taxodium distichum* and *Nyssa aquatica* seedlings to soil anaerobiosis and salinity. *Forest Ecology and Management*, 33:531–541.

Pezeshki, S., DeLaune, R., and Patrick Jr, W. (1990). Flooding and saltwater intrusion: Potential effects on survival and productivity of wetland forests along the US Gulf Coast. *Forest Ecology and Management*, 33:287–301.

Platt, W. J., Doren, R. F., and Armentano, T. V. (2000). Effects of Hurricane Andrew on stands of slash pine (*Pinus elliottii* var. *densa*) in the everglades region of South Florida (USA). *Plant Ecology*, 146(1):43–60.

Poirrier, M. A. (2013). Effects of closure of the Mississippi River-Gulf Outlet on saltwater intrusion and bottom water hypoxia in Lake Pontchartrain. *Gulf and Caribbean Research*, 25(1):105–109.

Pontee, N. (2013). Defining coastal squeeze: A discussion. *Ocean & coastal management*, 84:204–207.

Powell, E. J. and Keim, B. D. (2015). Trends in daily temperature and precipitation extremes for the southeastern United States: 1948–2012. *Journal of Climate*, 28(4):1592–1612.

Preechamart, S., Pumijumnong, N., Payomrat, P., and Buajan, S. (2018). Variation in climate signals in teak tree-ring chronologies in two different growth areas. *Forests*, 9(12):772.

Rabalais, N. N., Turner, R. E., and Wiseman Jr, W. J. (2002). Gulf of Mexico hypoxia, aka "The dead zone". *Annual Review of Ecology and Systematics*, 33(1):235–263.

Raddi, S., Cherubini, P., Lauteri, M., and Magnani, F. (2009). The impact of sea erosion on coastal *Pinus pinea* stands: A diachronic analysis combining tree-rings and ecological markers. *Forest Ecology and Management*, 257(3):773–781.

Ragsdale, H. and Berish, C. (1988). The decline of lead in tree rings of *Carya* spp. in urban Atlanta, GA, USA. *Biogeochemistry*, 6(1):21–29.

Rakowski, A. Z., Nakamura, T., and Pazdur, A. (2008). Variations of anthropogenic CO_2 in urban area deduced by radiocarbon concentration in modern tree rings. *Journal of Environmental Radioactivity*, 99(10):1558–1565.

Razali, N. M., Wah, Y. B., et al. (2011). Power comparisons of shapiro-wilk, kolmogorov-smirnov, lilliefors and anderson-darling tests. *Journal of Statistical Modeling and Analytics*, 2(1):21–33.

Reese, C. A., Harley, G. L., DeLong, K. L., Bentley Sr, S. J., Xu, K., Gonzalez, S., Truong, J. T., Obelcz, J., and Caporaso, A. (2018). Stratigraphic pollen analysis performed on a late Pleistocene cypress forest preserved on the northern Gulf of Mexico continental shelf. *Journal of Quaternary Science*, 33(8):865–870.

Revelle, R. and Suess, H. E. (1957). Carbon dioxide exchange between atmosphere and ocean and the question of an increase of atmospheric CO_2 during the past decades. *Tellus*, 9(1):18–27.

Roberts, H. H. (1997). Dynamic changes of the Holocene Mississippi River delta plain: The delta cycle. *Journal of Coastal Research*, 13(3):605–627.

Roden, J. S., Bowling, D. R., McDowell, N. G., Bond, B. J., and Ehleringer, J. R. (2005). Carbon and oxygen isotope ratios of tree ring cellulose along a precipitation transect in Oregon, United States. *Journal of Geophysical Research: Biogeosciences*, 110(G2):1–11.

Roden, J. S., Johnstone, J. A., and Dawson, T. E. (2009). Intra-annual variation in the stable oxygen and carbon isotope ratios of cellulose in tree rings of coast redwood (*Sequoia sempervirens*). *The Holocene*, 19(2):189–197.

Rodgers III, J. C., Gamble, D. W., McCay, D. H., and Phipps, S. (2006). Tropical cyclone signals within tree-ring chronologies from Weeks Bay National Estuary and Research Reserve, Alabama. *Journal of Coastal Research*, 22(6):1320–1329.

Rohling, E. J., Grant, K., Bolshaw, M., Roberts, A., Siddall, M., Hemleben, C., and Kucera, M. (2009). Antarctic temperature and global sea level closely coupled over the past five glacial cycles. *Nature Geoscience*, 2(7):500–504.

Ross, M. S., O'Brien, J. J., and da Silveira Lobo Sternberg, L. (1994). Sea-level rise and the reduction in pine forests in the Florida Keys. *Ecological Applications*, 4(1):144–156.

Rother, M. T., Huffman, J. M., Harley, G. L., Platt, W. J., Jones, N., Robertson, K. M., and Orzell, S. L. (2018). Cambial phenology informs tree-ring analysis of fire seasonality in Coastal Plain pine savannas. *Fire Ecology*, 14(1):164–185.

Saladyga, T. and Maxwell, R. S. (2015). Temporal variability in climate response of eastern hemlock in the Central Appalachian Region. *Southeastern Geographer*, 55(2):143–163.

Salzer, M. W., Hughes, M. K., Bunn, A. G., and Kipfmueller, K. F. (2009). Recent unprecedented tree-ring growth in bristlecone pine at the highest elevations and possible causes. *Proceedings of the National Academy of Sciences*, 106(48):20348–20353.

Sánchez-Murillo, R., Durán-Quesada, A. M., Esquivel-Hernández, G., Rojas-Cantillano, D., Birkel, C., Welsh, K., Sánchez-Llull, M., Alonso-Hernández, C. M., Tetzlaff, D., Soulsby, C., et al. (2019). Deciphering key processes controlling rainfall isotopic variability during extreme tropical cyclones. *Nature Communications*, 10(1):1–10.

Saurer, M., Siegenthaler, U., and Schweingruber, F. (1995). The climate-carbon isotope relationship in tree rings and the significance of site conditions. *Tellus B*, 47(3):320–330.

Schmid, K. (2000). *Shoreline Erosion Analysis of Grand Bay Marsh*. Mississippi Department of Environmental Quality (Jackson, MS).

Schöngart, J., Junk, W. J., Piedade, M. T. F., Ayres, J. M., Hüttermann, A., and Worbes, M. (2004). Teleconnection between tree growth in the Amazonian floodplains and the El Niño-Southern Oscillation effect. *Global Change Biology*, 10(5):683–692.

Schwartz, Z., An, Y., Konstantynova, K. I., and Jackson, G. P. (2013). Analysis of household ignitable liquids and their post-combustion weathered residues using compound-specific gas chromatography-combustion-isotope ratio mass spectrometry. *Forensic Science International*, 233(1-3):365–373.

Senter, J. (2003). Live dunes and ghost forests: Stability and change in the history of North Carolina's Maritime Forests. *The North Carolina Historical Review*, 80(3):334–371.

Sharitz, R. R., Vaitkus, M., and Cook, A. (1993). Hurricane damage to an old growth floodplain forest in the Southeast. In *Hurricane Hugo: South Carolina Forest Land, Research, and Management Related to the Storm*.

Shirakura, F., Sasaki, K., Arévalo, J. R., and Palmer, M. W. (2006). Tornado damage of *Quercus stellata* and *Quercus marilandica* in the Cross Timbers, Oklahoma, USA. *Journal of Vegetation Science*, 17(3):347–352.

Simpson, R. H. and Saffir, H. (1974). The hurricane disaster potential scale. *Weatherwise*, 27(8):169.

Small, C. and Nicholls, R. J. (2003). A global analysis of human settlement in coastal zones. *Journal of Coastal Research*, 19(3):584–599.

Somers, R. L. (2005). *Putting Down Roots in Environmental Literacy: A Study of Middle School Students' Participation in Louisiana Sea Grant's Coastal Roots Project*. PhD thesis, Louisiana State University, Department of Human Education.

Sorrie, B. A. and Weakley, A. S. (2001). Coastal plain vascular plant endemics: Phytogeographic patterns. *Castanea*, 66(1/2):50–82.

Speer, J. H. (2010). *Fundamentals of Tree-Ring Research*. University of Arizona.

Spratt, R. M. and Lisiecki, L. E. (2016). A Late Pleistocene sea level stack. *Climate of the Past*, 12(4):1079–1092.

Stahle, D., Edmondson, J., Howard, I., Robbins, C., Griffin, R., Carl, A., Hall, C., Stahle, D., and Torbenson, M. (2019). Longevity, climate sensitivity, and conservation status of wetland trees at Black River, North Carolina. *Environmental Research Communications*, 1(4):041002.

Stahle, D. W., Burnette, D. J., Villanueva, J., Cerano, J., Fye, F. K., Griffin, R. D., Cleaveland, M. K., Stahle, D. K., Edmondson, J. R., and Wolff, K. P. (2012). Tree-ring analysis of ancient baldcypress trees and subfossil wood. *Quaternary Science Reviews*, 34:1–15.

Stahle, D. W. and Cleaveland, M. K. (1992). Reconstruction and analysis of spring rainfall over the southeastern US for the past 1000 years. *Bulletin of the American Meteorological Society*, 73(12):1947–1961.

Stahle, D. W., Cleaveland, M. K., Grissino-Mayer, H. D., Griffin, R. D., Fye, F. K., Therrell, M. D., Burnette, D. J., Meko, D. M., and Villanueva Diaz, J. (2009). Cool- and warm-season precipitation reconstructions over western New Mexico. *Journal of Climate*, 22(13):3729–3750.

Stahle, D. W., Cleaveland, M. K., and Hehr, J. G. (1988). North Carolina climate changes reconstructed from tree rings: AD 372 to 1985. *Science*, 240(4858):1517–1519.

Stahle, D. W., Cook, E. R., and White, J. W. (1985). Tree-ring dating of baldcypress and the potential for millennia-long chronologies in the Southeast. *American Antiquity*, 50(4):796–802.

Stahle, D. W., D'Arrigo, R. D., Krusic, P. J., Cleaveland, M. K., Cook, E. R., Allan, R. J., Cole, J. E., Dunbar, R. B., Therrell, M. D., Gay, D. A., et al. (1998). Experimental dendroclimatic reconstruction of the Southern Oscillation. *Bulletin of the American Meteorological Society*, 79(10):2137–2152.

Stanley, D. J. and Warne, A. G. (1994). Worldwide initiation of Holocene marine deltas by deceleration of sea-level rise. *Science*, 265(5169):228–231.

Stephenson, N. (1998). Actual evapotranspiration and deficit: Biologically meaningful correlates of vegetation distribution across spatial scales. *Journal of Biogeography*, 25(5):855–870.

Steyer, G. D. (2010). Coastwide Reference Monitoring System (CRMS). Technical report, US Geological Survey.

Steyer, G. D., Couvillion, B. R., and Barras, J. A. (2013). Monitoring vegetation response to episodic disturbance events by using multitemporal vegetation indices. *Journal of Coastal Research*, 63(SI):118–130.

Steyer, G. D., Sasser, C. E., Visser, J. M., Swenson, E. M., Nyman, J. A., and Raynie, R. C. (2003). A proposed coast-wide reference monitoring system for evaluating wetland restoration trajectories in Louisiana. In *Coastal Monitoring through Partnerships*, pages 107–117. Springer.

Stokes, M. A. and Smiley, T. L. (1968). *An Introduction to Tree-Ring Dating*. University of Arizona.

Stoneburner, D. L. (1978). Evidence of hurricane influence on barrier island slash pine forests in the northern Gulf of Mexico. *American Midland Naturalist*, pages 234–237.

Swetnam, T. W. (1993). Fire history and climate change in giant sequoia groves. *Science*, 262(5135):885–889.

Swift, D. J. (1973). Delaware Shelf Valley: Estuary retreat path, not drowned river valley. *Geological Society of America Bulletin*, 84(8):2743–2748.

Syvitski, J. P., Kettner, A. J., Overeem, I., Hutton, E. W., Hannon, M. T., Brakenridge, G. R., Day, J., Vörösmarty, C., Saito, Y., Giosan, L., et al. (2009). Sinking deltas due to human activities. *Nature Geoscience*, 2(10):681.

Taillie, P. J., Moorman, C. E., Smart, L. S., and Pacifici, K. (2019). Bird community shifts associated with saltwater exposure in coastal forests at the leading edge of rising sea level. *PloS one*, 14(5).

Tate, J., Carrillo, A., Berger, R., and Thibodeaux, B. (2002). Salinity changes in Pontchartrain Basin estuary, Louisiana, resulting from Mississippi River-Gulf Outlet partial closure plans with width reduction. Technical report, Engineer Research and Development Center, Vicksburg, MS Coastal and Hydraulics Lab.

Team, R. C. (2014). R: A language and environment for statistical computing. R Foundation for Statistical Computing, Vienna, Austria.

Torio, D. D. and Chmura, G. L. (2013). Assessing coastal squeeze of tidal wetlands. *Journal of Coastal Research*, 29(5):1049–1061.

Trepanier, J., Yuan, J., and Jagger, T. (2017). The combined risk of extreme tropical cyclone winds and storm surges along the US Gulf of Mexico Coast. *Journal of Geophysical Research: Atmospheres*, 122(6):3299–3316.

Trepanier, J. C., Ellis, K. N., and Tucker, C. S. (2015). Hurricane risk variability along the Gulf of Mexico coastline. *PLoS one*, 10:e0118196–e0118196.

Trepanier, J. C. and Scheitlin, K. N. (2014). Hurricane wind risk in Louisiana. *Natural Hazards*, 70:1181–1195.

Trouet, V., Harley, G. L., and Domínguez-Delmás, M. (2016). Shipwreck rates reveal Caribbean tropical cyclone response to past radiative forcing. *Proceedings of the National Academy of Sciences*, 113(12):3169–3174.

Trouet, V. and Van Oldenborgh, G. J. (2013). KNMI Climate Explorer: A web-based research tool for high-resolution paleoclimatology. *Tree-Ring Research*, 69(1):3–13.

Tucker, C. S., Trepanier, J. C., Harley, G. L., and DeLong, K. L. (2017). Recording tropical cyclone activity from 1909 to 2014 along the northern Gulf of Mexico using maritime slash pine trees (*Pinus elliottii* var. *elliottii* Engelm.). *Journal of Coastal Research*, 34(2):328–340.

Turner, R. and Lewis, R. (1996). Hydrologic restoration of coastal wetlands. *Wetlands Ecology and Management*, 4(2):65–72.

Turner, R. E., Baustian, J. J., Swenson, E. M., and Spicer, J. S. (2006). Wetland sedimentation from Hurricanes Katrina and Rita. *Science*, 314(5798):449–452.

Twilley, R. R., Bentley, S. J., Chen, Q., Edmonds, D. A., Hagen, S. C., Lam, N. S.-N., Willson, C. S., Xu, K., Braud, D., and Peele, R. H. (2016). Co-evolution of wetland landscapes, flooding, and human settlement in the Mississippi River Delta Plain. *Sustainability Science*, 11(4):711–731.

van Heerden, I. L., Kemp, G. P., Bea, R., Shaffer, G., Day, J., Morris, C., Fitzgerald, D., and Milanes, A. (2009). How a navigation channel contributed to most of the flooding of New Orleans during Hurricane Katrina. *Public Organization Review*, 9(4):291.

Villalba, R., Grau, H. R., Boninsegna, J. A., Jacoby, G. C., and Ripalta, A. (1998). Tree-ring evidence for long-term precipitation changes in subtropical South America. *International Journal of Climatology*, 18(13):1463–1478.

Vital, H. and Stattegger, K. (2000). Lowermost Amazon River: Evidence of late Quaternary sea-level fluctuations in a complex hydrodynamic system. *Quaternary International*, 72(1):53–60.

Walker, N. D., Rouse Jr, L. J., Fargion, G. S., and Biggs, D. C. (1994). The great flood of summer 1993: Mississippi river discharge studied. *Eos, Transactions American Geophysical Union*, 75(36):409–415.

Walker, N. D., Wiseman Jr, W. J., Rouse Jr, L. J., and Babin, A. (2005). Effects of river discharge, wind stress, and slope eddies on circulation and the satellite-observed structure of the Mississippi River plume. *Journal of Coastal Research*, 21(6):1228–1244.

Wang, S., Huang, J., He, Y., and Guan, Y. (2014). Combined effects of the Pacific Decadal Oscillation and El Niño-Southern Oscillation on global land dry-wet changes. *Scientific Reports*, 4:6651.

White, J., Vaughn, B., and Michel, S. (2011). Stable isotopic composition of atmospheric carbon dioxide (13c and 18o) from the NOAA ESRL carbon cycle cooperative global air sampling network, 1990–2012, version: 2013-04-05. University of Colorado, Institute of Arctic and Alpine Research (INSTAAR). *University of Colorado, Institute of Arctic and Alpine Research (INSTAAR).*

White, J. W., Winters, K., Peter, M., and Rossmann, A. (1998). Stable carbon isotope ratio analysis of honey: Validation of internal standard procedure for worldwide application. *Journal of AOAC International*, 81(3):610–619.

Wigley, T. M., Briffa, K. R., and Jones, P. D. (1984). On the average value of correlated time series, with applications in dendroclimatology and hydrometeorology. *Journal of Climate and Applied Meteorology*, 23(2):201–213.

Wilk, S. S. and Shapiro, S. (1965). An analysis of variance test for normality (complete samples). *Biometrika*, 52(3-4):591–611.

Williams, A. P., Allen, C. D., MacAlady, A. K., Griffin, D., Woodhouse, C. A., Meko, D. M., Swetnam, T. W., Rauscher, S. A., Seager, R., and Grissino-Mayer, H. D. (2013). Temperature as a potent driver of regional forest drought stress and tree mortality. *Nature Climate Change*, 3(3):292–297.

Wilson, R. J. and Luckman, B. H. (2002). Tree-ring reconstruction of maximum and minimum temperatures and the diurnal temperature range in British Columbia, Canada. *Dendrochronologia*, 20(3):257–268.

Woodruff, J. D., Irish, J. L., and Camargo, S. J. (2013). Coastal flooding by tropical cyclones and sea-level rise. *Nature*, 504(7478):44.

Yamaguchi, D. K. (1991). A simple method for cross-dating increment cores from living trees. *Canadian Journal of Forest Research*, 21(3):414–416.

Yanosky, T. M., Hupp, C. R., and Hackney, C. T. (1995). Chloride concentrations in growth rings of *Taxodium distichum* in a saltwater-intruded estuary. *Ecological Applications*, 5(3):785–792.

Young, P. J., Megonigal, J. P., Sharitz, R. R., and Day, F. P. (1993). False ring formation in baldcypress (*Taxodium distichum*) saplings under two flooding regimes. *Wetlands*, 13(4):293–298.

Youngblut, D. and Luckman, B. (2008). Maximum June–July temperatures in the southwest Yukon over the last 300 years reconstructed from tree rings. *Dendrochronologia*, 25(3):153–166.

Zang, C. and Biondi, F. (2015). treeclim: an R package for the numerical calibration of proxy-climate relationships. *Ecography*, 38(4):431–436.

Vita

Clay Stephens Tucker was born in November 1990 in Baton Rouge, Louisiana. He finished his undergraduate studies in the Department of Geography and Anthropology at Louisiana State University in May 2013. He earned a Master of Science degree in geography from Louisiana State University in December 2015. During his time at Louisiana State University, he served as a graduate teaching assistant in the Department of Geography and Anthropology and as a graduate research assistant for the South Central Climate Adaptation Science Center, the National Academies of Science Gulf Research Program, and Louisiana Sea Grant. He is currently a candidate for the degree of Doctor of Philosophy in geography that will be awarded in May 2020.